USE OF RATIONAL ENGINEERING AND COMBINATORIAL LIBRARY

SCREENING TO ENHANCE SYNTHETICALLY EVOLVED ANTIMICROBIAL

PEPTIDES.

AN ABSTRACT SUBMITTED ON THE NINTH DAY OF APRIL TWO THOUSAND

TWENTY-ONE TO THE DEPARTMENT OF BIOCHEMISTRY AND MOLECULAR

BIOLOGY IN PARTIAL FULFILLMENT OF THE REQUIREMENTS OF THE

GRADUATE SCHOOL OF TULANE UNIVERSITY FOR THE DEGREE OF

DOCTOR OF PHILOSOPHY BY

_____

JENISHA GHIMIRE

APPROVED:

_____

WILLIAM WIMLEY, Ph.D. ADVISOR

_____

DIANE BLAKE, Ph.D.

_____

SAMUEL LANDRY, Ph.D.

_____

JAMES JACKSON, Ph.D.

_____

LISA MORICI, Ph.D.

ABSTRACT

 Antimicrobial peptides (AMPs) have long been attractive drug candidates for the next

generation of clinical antibiotics due to their potent antimicrobial activity and low

propensity for inducing resistance in pathogens. However, due to toxicity, low solubility,

proteolysis, and activity loss *in vivo* because of host cell binding, AMPs have yet to have

much impact clinically. Here, we have identified antimicrobial peptides (AMPs) that

retain activity in the presence of eukaryotic cells by using a synthetic molecular evolution

(SME) based approach that we have developed. We have demonstrated that variation in

the sequence of AMPs selected from the primary screening of iterative peptide library

can lead to identification of peptides that have superior antimicrobial activity, solubility,

and lower cytotoxicity against red blood cells (RBCs) and mammalian cells. D-CONGA,

a variant obtained by rational modification of the consensus sequence of peptides selected

from the stringent screening of iterative, second-generation antimicrobial peptide library,

is highly effective *in vitro* against all ESKAPE pathogens in the presence of RBCs and

serum. The peptide also has anti-biofilm activity *in vitro* and shows potency against

gram-negative and gram-positive drug-resistant bacteria and their biofilms in relevant

infected wound model in mice. We have also designed and synthesized 13 variants of D-

CONGA and characterized them for their bactericidal activity in the presence and

absence of RBCs. Their cytotoxicity against mammalian fibroblast, WI-38, and

hemolysis in RBC was also measured. The most active D-CONGA variant, D-CONGA-

Q7, was then tested against 14 clinical isolates of drug-resistant bacteria. The

antimicrobial activity of the new peptide was compared with D-CONGA and eight

conventional antibiotics from four different classes and was found to be superior to all.

Following this, we designed and synthesized a third-generation peptide library based on D-CONGA-Q7. The library members were screened against gram-positive and gram-negative bacteria in the presence of RBCs. The selected peptides sterilize broad-spectrum bacteria at sub micromolar concentrations. Hence, we have shown that using rational design and SME, we can improve AMPs with each generation and discover evolved peptides that have increasingly potent and relevant activity against MDR bacteria, compared to conventional antibiotic or other known AMPs.

USE OF RATIONAL ENGINEERING AND COMBINATORIAL LIBRARY

SCREENING TO ENHANCE SYNTHETICALLY EVOLVED ANTIMICROBIAL

PEPTIDES.

A DISSERTATION SUBMITTED ON THE NINTH DAY OF APRIL TWO

THOUSAND TWENTY-ONE TO THE DEPARTMENT OF BIOCHEMISTRY AND

MOLECULAR BIOLOGY IN PARTIAL FULFILLMENT OF THE REQUIREMENTS

OF THE GRADUATE SCHOOL OF TULANE UNIVERSITY FOR THE DEGREE OF

DOCTOR OF PHILOSOPHY BY

_____

JENISHA GHIMIRE

APPROVED:

_____

WILLIAM WIMLEY, Ph.D. ADVISOR

_____
DIANE BLAKE, Ph.D.

_____
SAMUEL LANDRY, Ph.D.

_____
JAMES JACKSON, Ph.D.

_____
LISA MORICI, Ph.D.

DEDICATION

To my family, my parents Bishnu Bibhu and Sodha Ghimire, my sister Resha Ghimire,

and my partner, Gregory Mattson.

For always being my biggest cheerleaders.

ACKNOWLEDGMENT

First, I would like to thank my doctoral advisor, Dr. William Wimley. I did not initially start in your lab, but I consider it a stroke of luck that I ended up working with you. You are a great boss, mentor, and role model. I appreciate the guidance, advice, and support from you throughout the last four years that made my PhD an excellent learning and working experience. I would also like to thank my fellow lab mates for their friendship. Charlie, Berkeley, and Taylor showed me the way around the lab when I first joined. Shan, Eric, Leisheng, and Ryan were always there when I needed advice, support, and most times, someone to rant to or have a laugh with. Thank you for your patience and good faith. The work would not have been as fun or exciting without each of your presence.

Next, I would like to thank my committee members. Dr. Blake, Dr. Morici, Dr. Landry, and Dr. Jackson. They were excellent mentors and guides throughout this process. I would especially like to thank Dr. Morici and her lab members, including Joe, Yihui, and Josh, who were of massive help in the project presented here. A special shout out to my fellow students who joined the BMS PhD program with me in 2015. Joie, Shan, Dan, Joe, Lauren, Yihui, and Michelle are so much more than classmates. They have become close friends that I will cherish all my life. I would also like to take this opportunity to thank the faculty and staff working in Department of Biochemistry and Molecular Biology of Tulane Medical School, especially Gilbert and Marlene, in the front office. Thanks also to Zylkia in the BMS office, who was always happy to help me navigate all the paperwork.

people have contributed significantly to the person and professional I am. There are too many to list here but know that I appreciate each of you, and you guys make my life brighter and happier. A huge shout out to the city of New Orleans, which has become a second home. I have so many good memories here with the people I love the most. I have also achieved so much personally and professionally in this city. I had never imagined I will be leaving this life when I was growing up in Kathmandu. Thank you, universe, for all the blessings. I would like to end with my favorite quote by Douglas Adams, "I may not have gone where I intended to go, but I think I have ended up where I needed to be".

TABLE OF CONTENTS

LIST OF FIGURES

CHAPTER 1: Discovery of antibiotics, the emergence of antibiotic resistance, and antimicrobial peptides as promising alternatives to conventional antibiotics

1.1 The bacterial cell

Bacteria are a diverse kingdom of microscopic, single-celled organisms that occupy virtually every ecosystem. There are over 30,000 formally named bacterial species. However, a recent study reports that the number of distinct prokaryotic species that includes bacteria and archaea could be much higher, anywhere from 0.8 million to 1.6 million species[1,2]. Each bacterial species is distinguished by its structural and biochemical characteristics. However, they all share a basic cellular organization. Although the smallest of all the living cells, bacteria have a significant number of morphological variations. Common bacteria are simple cocci or rods (bacillus) or spirals, or curved forms. However, bacteria can also exist in complex forms. These morphological forms depend on environmental conditions. The shape, color, size, and motility of bacterial cells can differ with growth rate and the physical environment in which the cells exist. There are conditions where the cells may also differentiate and form structures like spores and aerial hyphae[3].

Prokaryotic cells, unlike eukaryotic cells, do not contain any membrane-bound organelles. The genetic material of bacteria is not organized into complex structures such as chromosomes. The bacterial cell is enclosed by an envelope that consists of a series of complex structures: the cell membrane, the cell wall, and, in some cases, an outer membrane. Some also have a well-defined region between the outer membrane and cytoplasmic membrane called the periplasm. The interior of the cells is called cytoplasm or cytosol and is packed with metabolites and macromolecules, including ribosomes and

nuclear material. Some bacteria have surface structures such as capsules, flagella, and pili primarily for protection or motility. The cell envelope protects bacterial cells against osmotic pressure, phages, enzymatic attack, organic poison, and even antibiotic action. It is also necessary for nutrient acquisition and as a buffer against changing environments. The cell membrane is similar in all bacteria. It is comprised of lipids and proteins, the latter taking up about 70% of the membrane weight. The membrane is mostly a two-dimensional fluid, which allows individual lipids to exchange positions with each other while still maintaining order, especially around proteins, which can also move or rotate within the membrane structure. The membrane also consists of complex transport systems and energy generation systems. Hence, disruption of the membrane can have catastrophic consequences for the bacterial cell.

Cell walls are responsible for the strength and resilience of a bacterial cell. They protect the cell from osmotic rupture and shield the cell membrane from external disruption. The composition of the cell envelope is different among bacterial species. The distinction in the structure of the cell wall is often used to differentiate between types of bacteria (figure 1-1)[3]. The Gram stain, named after Hans Christian Gram, who developed the method in 1884, distinguishes between two classes of bacteria, gram-positive and gram-negative, based on differential staining with crystal violet-iodide complex and a safranin counterstain[4]. The gram-positive cell wall consists of a thick layer of murein or peptidoglycan, which allows retention of the crystal violet-iodide complex even after the treatment with alcohol. The cell wall appears purple. This thick layer of peptidoglycan in gram-positive bacteria has scattered teichoic and teichuronic acid. It also has a sugar backbone with alternating N-acetylglucosamine and N-acetylmuramic acid that form very

long chains. The chains are cross-linked with small bridging tetra-peptides. Teichoic acid consists of repeating units of sugars, glycerol, and amino acids, linked together via phosphodiester bonds. The precise composition of the peptide bridge and the type of teichoic acid is primarily species-dependent and can be used to distinguish groups of gram-positive bacteria.

Gram-negative organisms have a more complex cell wall than gram-positive bacteria. They have a comparatively thin layer of peptidoglycan, which does not retain the color of crystal violet-iodide complex after treatment with alcohol and appears pink[4]. However, gram-negative bacteria have an additional outer membrane over the peptidoglycan layer. The outer membrane is connected to the rest of the cell by covalent bonding via outer membrane lipoprotein and weak bonds between proteins in the outer membrane and the cell wall. The outside of this outer membrane is comprised of lipopolysaccharide (LPS). LPS is made up of three distinct parts: Lipid A, Core carbohydrate, and O antigen. Lipid A anchors LPS to the membrane and consists of fatty acids[5]. Core carbohydrates, connected to lipid A, consist principally of ketodeoxytonic acid, octanoic acid, and heptose. O antigen is linked to the core carbohydrate and consists of up to 40 sugars that cover the surface of the cell. Hence, the gram-negative outer membrane is an effective barrier to both hydrophobic and hydrophilic materials. A small number of proteins, including porins, are embedded in the membrane to allow passive diffusion of low molecular-weight compounds. Some specific proteins on the membrane permit translocation of essential compounds. Gram-negative bacteria, due to the extra complex wall, are more resilient than gram-positive bacteria and have more resistance to antibiotics. LPS is also reported to initiate a larger immunological reaction in humans and

animals. The area between the cell membrane and the outer membrane of gram-negative

bacteria is called periplasm and can take up to 40% of the space in the membrane.

Periplasmic space is important for a variety of reasons. It contains a cell wall and proteins

that bind to essential compounds and hydrolyze them into usable forms. The periplasm

can also contain enzymes such as penicillinase to resist antibiotic attacks.

Some bacteria have atypical cell walls. Mycobacterium, for example, has mycolic

acid with a carbon backbone of up to 90 carbons. This results in waxy extensions from

the cell wall that forms the basis of the acid-fast tests, in which a dye that interacts with

the cells cannot be removed by hydrochloric acid as with most other bacteria. Thus, these

bacteria are called acid-fast[6,7]. Besides the waxy coat, the cell wall of these bacteria is

very similar to gram-positive bacteria. The waxy exterior protects these bacteria from

poisonous chemicals, the immune system, and antibiotics. There is also another class of

bacteria with a protein layer, in the form of crystal, outside their cell wall. These layers,

referred to as S-layer, are found in both gram-positive and gram-negative bacteria. The S-

layer consists of a single layer of a specific protein, sometimes with carbohydrates

attached to it. It is thought to protect against phagocytosis and phages and could aid in

adhesion to surfaces[3,8].

1.2 Antibiotics: a brief history

Salvarsan and Prontosil.

A biochemist, Selman A. Waksman, defined the word "antibiotics" for the first time

in 1947 as "a chemical substance, produced by microorganisms, which can inhibit the

growth of and even destroy bacteria and other microorganisms"[9]. However, before it was

even known as such, bioactive antimicrobial compounds have been used throughout human

history, as exemplified by the usage of cinchona tree bark, later discovered to have quinine against fever and malaria by indigenous people of South America in the late seventeenth century[10]. In 1893, antibiotics were reported for the first time when an Italian medical student, Bartolomeo Gosio, isolated and cultivated *Penicillium brevicompactum*, which demonstrated antibiotic activity against *Bacillus anthracis*, the causative agent of anthrax[11,12]. Later, Paul Ehrlich, Alfred Bertheim, and Sahachiro Hata discovered the first synthetic antibiotic called Arsphenamine, also known as Salvarsan or compound 606, in 1909 against *Treponema pallidum* and other spirochete bacteria[13,14]. Inspired by Ehrlich's success in combating syphilis, another German physician, Gerhard Domagk, led a large-scale *in vitro* and *in vivo* screen for antibacterial azo dyes. This led to the development of sulfamidochrysoidine, also known as Prontosil, a highly active antibiotic against gram-positive cocci. When introduced as a drug in 1935, Prontosil immediately decreased deaths due to pneumonia, childbed fever, and meningitis. Due to the profitability of Prontosil, the following years marked huge endeavors towards research and development of thousands of derivatives with sulfanilamide structure[15]. Despite these antibiotics against malaria, syphilis and gram-positive pathogens, there were still many infectious diseases caused by many bacteria that were untreatable until the accidental discovery of penicillin by Alexander Fleming and the subsequent decade long quest for the isolation and structure of the active compound in penicillin[16].

β-Lactam antibiotics

In 1929, Alexander Fleming, a bacteriologist at St. Mary's Hospital, London, described penicillin as an active compound in the mold that was able to lyse staphylococcus colonies[16]. Unfortunately, he was neither able to identify the structure of the compound nor

to produce an appreciable amount of it for further studies. As a result, no progress was made in the study of penicillin for another decade. Finally, in 1939, biochemists at Oxford University, Howard Walter Florey, and Ernst Boris Chain, in collaboration with microbiologist, Norman Heatley, were able to purify penicillin and elucidate its structure successfully. In 1940, they published their findings describing the production, purification, and experimental use of penicillin, which protected animals infected with *Streptococcus pyogenes*, *Staphylococcus aureus*, and *Clostridium septique* [17]. Due to the second world war commitments, the pharmaceutical companies in England could not mass-produce penicillin. Hence, Chain and Florey turned to the United States. Researchers in US drug companies developed techniques for the mass-production of penicillin as the United States entered the second world war. Penicillin was the first antibiotic against gram-positive bacteria and was vital in saving thousands of lives during the second world war that would have been otherwise lost due to rampant wound infections. It was used among the US military and civil population and resulted in an immediate decrease in deaths associated with gram-positive bacterial infections[18,19]. For this discovery of penicillin and its antimicrobial activity, Fleming, Chain, and Florey received the Nobel Prize in Physiology and Medicine in 1949.

The following years marked the discovery of many penicillin derived antibiotics. Ampicillin, a semi-synthetic penicillin-derivative, para-aminobenzyl penicillin, was discovered in 1953 by Brewer and Johnson[20]. In addition to gram-negative targets of penicillin, ampicillin could also sterilize some gram-negative pathogens like *Enterococcus faecalis, Escherichia coli, Haemophilus influenza,* and *Proteus mirabilis*. Next, another semi-synthetic penicillin derivative, methicillin, also called calbenin, was developed by

Beecham, a British pharmaceutical company[19]. Penicillin and derivatives belong to the class of β-lactam antibiotics, which is characterized by β-lactam rings in their molecular structure. β-lactam rings are potent inhibitors of cell-wall synthesis and are necessary for the activity of these antibiotics. With time and universal use of penicillin, many bacteria became able to produce β-lactamases, enzymes that destroy the β-lactam ring and therefore are resistant to β-lactam antibiotics. Hence, the discovery of methicillin was significant as it was the first β-lactamase resistant antibiotic of its class. In 1945, an Italian physician, Guiseppe Brotzu, isolated another β-lactam antibiotic, cephalosporin C, from fungus ascomycete *Acremonium chrysogenum*[21]. However, more and more bacterial strains developed resistance to most β-lactam antibiotics including penicillin, ampicillin, methicillin, and cephalosporin. Soon, research was directed towards discovery of compounds to circumvent the resistance mechanisms.

Carbapenems

In the search for β-lactamase inhibitors, thienamycin from *Streptomyces cattleya,* was discovered by J.S. Kahan and his collaborators at Merck Institute for Therapeutic Research in 1978[22]. Thienamycin was the first "carbapenem" and would eventually serve as the parent compound for a series of carbapenems. The hydroxyethyl side chain of thienamycin is different from penicillin and its derivatives and is necessary for the potent broad-spectrum antibacterial and β-lactamase activity of thienamycin[22,23]. Unfortunately, thienamycin was chemically unstable, which stimulated the search for analogous derivatives with increased stability. This resulted in the discovery of two closely related carbapenems, imipenem, and panipenem[23,24]. Imipenem became the first carbapenem available for the treatment of complex microbial infections. This was followed by the

development of broader spectrum carbapenems, such as meropenem, biapenem, ertapenem, and doripenem, which are still used as antibiotics [23]. Many novel carbapenems, with various modifications to increase their stability and antibacterial potency, were identified in the subsequent two decades, including antipseudomonal carbapenems, anti-methicillin-resistant *S. aureus* (MRSA) carbapenems, orally available carbapenems, trinem carbapenems, a dual quinolonyl-carbapenem, and others[23].

Tyrothricin and Gramicidin

As the research to find broad-spectrum, β-lactamase resistant, and chemically stable penicillin derivatives was ongoing, researchers were also looking at other avenues to discover natural and synthetic antibiotics. In 1939, American microbiologist René Dubos isolated tyrothricin from the soil bacterium *Bacillus brevis*, which showed antibacterial activity against Pneumococcus bacteria, the primary cause of pneumonia. Tyrothricin consists of a mixture of peptides, alkaline tyrocidine, and lipophilic gramicidins A, B, and C[25,26]. René Dubos and Rollin D. Hotchkiss were also able to isolate gramicidin D, a heterogeneous mixture of antibiotic gramicidin A, B, and C, from the same organism, *B. brevis*. Gramicidin D (D from Dubos) is active against gram-positive bacteria[27,28]. In 1944, two Russian scientists, Georgyi F. Gause and Mariya G. Brazhnikova, discovered antibacterial gramicidin S (Soviet Gramicidin) also in *B. brevi*s[29].

Actinomycin

Following multiples successes, a lot of effort was invested in the isolation and screening of microorganisms from the environment, primarily screening soil bacteria for antibacterial activity. This screening technique incorporated the method that investigated

growth inhibition zones surrounding single colonies of isolated soil microbe, previously

described by Alexander Fleming[19,30]. Alexander Waksman and H. Boyd Woodruff used

the technique to discover actinomycin, a polypeptide isolated from an actinobacterium,

Streptomyces antibioticus subsp. Antibioticus[31]. Actinomycin proved to be a broad-

spectrum antibiotic that even showed activity against a *Mycobacterium tuberculosis*

strain. However, actinomycin exhibited high toxicity against mammalian cells, making it

unfeasible for therapeutic purposes. It was later recognized for its anti-tumor activity and

is still used in cancer chemotherapy[32,33].

Bacitracin

In 1943, an important antibiotic, bacitracin, was discovered accidentally. Balbina

Johnson, a bacteriologist at Columbia University, noticed a compound present in a young

girl's leg wound that possessed antibacterial activity. She described this compound,

bacitracin, isolated from *Bacillus subtilis* and *Bacillus licheniformis*, as a broad-spectrum

polypeptide antibiotic complex that primarily has effects against gram-positive bacteria

like streptococci and staphylococci and the anaerobic pathogen *Clostridium difficile* [34].

Aminoglycosides

The next promising antibiotic discovered through screening was streptomycin, in

1944, from aminoglycoside class of antibiotics. Albert Schatz, Selman Waksman's

graduate student, isolated streptomycin from *Streptomyces anulatus subsp. griseus*[35].

Streptomycin showed high potency against both gram-positive and gram-negative

bacteria. It was the first antibiotic used against *Mycobacterium tuberculosis* and several

other pathogens that were not susceptible to penicillin and its derivatives. This promoted

research interest in aminoglycosides, and a series of antibiotics such as kanamycin,

gentamicin, and tobramycin from this class of antibiotics were subsequently discovered[19,36]. For the co-discovery of streptomycin, Waksman was awarded the Nobel Prize in 1952. In the following years, many broad-spectrum antibiotics were isolated from various species of the genus Streptomyces. Neomycin, a broad-spectrum aminoglycoside antibiotic active against streptomycin-resistant bacteria, including strains of *M. tuberculosis,* was isolated from *Streptomyces fradiae*[37]. Kanamycin was isolated from *Streptomyces kanamyceticus*, a strain from Japanese soil[38]. Gentamicin (genticin), a mixture of similar aminoglycosides, produced by *Micromonospora purpurea* was discovered in 1963 in the laboratories of the Schering Corporation, Bloomington, New Jersey[39]. While neomycin and kanamycin were broad-spectrum, exerting both bacteriostatic and bactericidal effects, gentamicin, had even greater activity in comparison. Gentamicin is most potent against gram-positive staphylococci but also has superior activity against all enterobacteria, including species of *Aerobacter, Escherichia, Klebsiella, Salmonella, Shigella, Proteus,* and some *Pseudomonas aeruginosa* strains.

Chloramphenicol

Chloramphenicol was isolated from another species of genus Streptomyces, *S. venezuelae*, by John Ehrlich and colleagues in 1947[40,41]. It had potency against gram-positive and gram-negative pathogens, anaerobes, spirochetes, rickettsiae, chlamydiae, and mycoplasma. At the time of its discovery, chloramphenicol was the only antibiotic that was active against Salmonella species, including *Salmonella typhi*[19,42,43].

Tetracyclines

Another important antibiotic class discovered from Streptomyces species is tetracyclines. Benjamin M. Duggar discovered the first tetracycline from broths of

Streptomyces aurefaciens in 1948, closely followed by the isolation of another

tetracycline, terramycin, from *S. rimosus*, by A.C. Finlay in 1950[44,45]. Tetracyclines are

broad-spectrum antibiotics and show activity against a wide range of gram-positive and

gram-negative pathogens such as chlamydiae, mycoplasmas, rickettsiae, and protozoan

parasites. Due to their superior activity and low toxicity, tetracyclines have been used

extensively, which has led to the emergence of microbial resistance, limiting their

effectiveness. Despite this, this class of antibiotics is still of great interest, and natural as

well as semi-synthetic tetracyclines continue to be discovered. The focus has been to

discover derivatives that can circumvent existing resistance mechanisms against

tetracyclines. This includes compounds like tetracycline efflux pump inhibitors that can

restore the activity of antibiotics when used in conjunction [46,47]. For example, researchers

have introduced carboxamido moiety of tetracyclines, necessary for its activity, into

chelocardins, a broad-spectrum but structurally atypical tetracycline with antibacterial

activity[48,49]. The mode of action of chelocardins is not well known but is presumed to be

different than conventional tetracyclines. This new compound had significantly

improved antibacterial activity against all gram-negative pathogens of the ESKAPE panel

(*Enterococcus faecium, S. aureus, Klebsiella pneumoniae, Acinetobacter baumannii, P.

aeruginosa, Enterobacter spp.*)[50]. This promising result demonstrates that tetracyclines

are still relevant antibiotics and more research needs to be done to discover newer

derivatives from this class of antibiotics.

Macrolides

In 1952, macrolides, another important class of antibiotics, was isolated by James

M. McGuire from *Strepromyces erythreus*. The first macrolide discovered was

erythromycin in the soil sample collected from a small Philippine island[51]. Macrolides are effective against gram-positive cocci and rods, gram-negative pathogens like *Legionella pneumophila, chlamydia, Bordetella pertussis, spirochaetes, Haemophilus influenza*, and also against cell wall lacking mycoplasmas. Erythromycin is still used against respiratory tract and throat-nose-ear infections. It is also used to treat pertussis and is a primary antibiotic for patients allergic to penicillin and derivatives. Over the years, many semi-synthetic macrolides, like clarithromycin and azithromycin, have been developed. When resistance against macrolides started emerging, enhanced macrolides, ketolides, were designed. Ketolides are semi-synthetic derivatives of the macrolide erythromycin A, and were first mentioned in literature by Griesgraber et al. [52–54]. With a similar mechanism of action to macrolides, ketolides exhibit good activity against gram-positive and some gram-negative aerobes. They also have excellent activity against drug-resistant *S. pneumoniae*, including some macrolide-resistant strains[53].

Glycopeptides

Concurrently, glycopeptides were also discovered from soil actinomycetes. The first glycopeptide, vancomycin, was isolated by McCormick et al. in 1955 from *Amycolatopsis orientalis*[55]. Vancomycin was used therapeutically from 1958[56]. The second glycopeptide antibiotic introduced for clinical use, teicoplanin, was isolated from a soil fermentation broth of *Actinoplanes teichomyceticus*[57]. Today, vancomycin and teicoplanin are used as last resort to treat infections caused by bacterial strains resistant to every other available antibiotic. In 1956, another glycopeptide antibiotic, ristocetin (ristomycin), was isolated by Grundy et al. from *Amycolatopsis lurida*. Ristocetin, however, was not clinically viable because of toxic side effects[19,58]. As of 2015, three

more lipoglycopeptides; telavancin, dalbavancin, and oritavancin, have been approved for

therapeutic use against *S. aureus,* including MRSA[59].

Streptogramins

Streptogramins, also isolated from streptomyces, was first described in 1953[60].

Streptogramins can be divided into two classes; group A consists of streptogramins with

polysaturated macrolactones, while group B streptogramins are cyclic

hexadepsipeptides[61]. Individually, each class of streptogramin act bacteriostatically, but

in combination, they have bactericidal effects[62]. Initially very promising, streptogramins,

showed high toxicity in vivo and thus were not clinically relevant.

Lincosamides

Lincosamides was first described in the 1960s. It consists of naturally occurring

lincomycin and semi-synthetic analogue clindamycin. It was isolated from *Streptomyces*

lincolnensis, from the soil in Lincoln, Nebraska, in 1962[63]. Lincomycin has similar

activities and modes of action as macrolides and erythromycin against gram-positive

pathogens[64]. Besides gram-positive cocci and bacilli, lincomycin is also effective against

gram-negative cocci and intracellular bacteria such as chlamydia and rickettsia species[65].

A semi-synthetic lincosamide, clindamycin, was reported in 1969, which is four to eight

times more active than lincomycin against most gram-positive organisms. It also acts

against anaerobic germs and toxoplasmas[66]. Currently, lincosamides are widely used in

clinical settings against infections caused by a large range of bacteria, including MRSA.

Rifamycin

In the late 1950s, another group of antibiotics, rifamycin, was isolated. The first

rifamycin, rifomycin, was discovered and isolated in Italy in 1957 from *Streptomyces*

mediterranei, now known as *Amycolatopsis rifamycinica*, by Sensi et al. [67]. Originally, there are five components of rifamycin, A, B, C, D, and E. Rifamycins O, S, and SV were derived from the inactive B component, and AG and X were obtained from the O component. The antibiotics clinically used against *Mycobacterium tuberculosis* and *Mycobacterium leprae* originated from rifamycin B. Rifamycin B was also used to develop semi-synthetic derivatives with higher potency, including rifamide, rifaximin, rifapentine, rifampicin, and rifabutin. In addition to mycobacteria, this group of antibiotics also shows activity against streptococci, enterococci, Neisseria, Legionella, and other bacteria, including resistant strains[19].

Quinolones

Quinolones are synthetic antibiotics discovered as a by-product while synthesizing the antimicrobial drug chloroquine. It was patented by the Sterling Drug company in 1963[68]. This accidental discovery of the quinolone, nalidixic acid, is probably one of the most significant serendipitous scientific discoveries in history. Based on nalidixic acid, fluoroquinolones were developed. Chemist K. Grohe from Bayer Company initiated a technique of cycloaracyclation that led to the synthesis of even superior derivative of naladixic acid, the broad-spectrum antibiotic, fluoroquinolone ciprofloxacin. Out of more than 20,000 tested bacterial strains, 98.2 % were sensitive to ciprofloxacin. It was patented in 1981 and clinically used since 1987[69]. Since its discovery, around 10,000 derivatives of quinolines have been synthesized, making it one of the most successful antibiotic classes, although resistance to quinolones is known.

Oxazolidonones

Oxazolidonones are a new class of synthetic compounds that are active against gram-positive bacteria. Although first described in 1978 in a patent by DuPont as antibiotics against only plant pathogens, Oxazolidonones were later introduced in 1987 for clinical trials in humans. Linezolid, the first antibiotic from this class, was available in the US market in 2000[19,70]. Linezolid is active against all gram-positive pathogens, including methicillin-resistant *S. aureus* and vancomycin-resistant enterococci. It is primarily bacteriostatic against gram-negative bacteria except for Pasteurella, which is resistant to the drug[71]. As of 2015, a second-generation oxazolidinone, tedizolid, is in the pipeline for therapy against acute bacterial skin infections by MRSA[59].

Antimicrobial Peptides (AMPs)

Antimicrobial peptides or AMPs are oligopeptides with a varying number of amino acids. They are broad-spectrum antibiotics with effects against parasites, bacteria, and viruses. AMPs have been identified in all domains of life, where they play an important role in the immune system. They are produced by insects and plants as a primary defense mechanism, against fungus and pathogens, to protect their environmental niche[72–74]. As mentioned above, gramicidin and bacitracin were the first AMPs discovered in 1939 and 1941, respectively[25,26,34]. However, the field of AMP research only started flourishing much later at the beginning of the 1980s, when the number of novel antimicrobial agents started dwindling. Due to their abundance in nature and broad-spectrum anti bactericidal activity, clinical interests in AMPs increased.

The cecropins from insects, the magainins from amphibians, and the mammalian defensins are a few of the novel AMPs that were discovered in the 1980s and early 1990s[75–77]. Since then, a plethora of AMPs has been identified from almost every

multicellular organism. Because they are made of amino acids, many synthetic AMPs have also been produced, either by chemical synthesis or by using a recombinant expression system. Synthetic AMPs can also be created through modification of existing peptides and also through *de novo* designs[72]. These peptides are mostly synthesized to potentially change the target of existing AMPs or to increase their stability and bioavailability.

Despite the promising bactericidal potential *in vitro*, most AMPs show low activity *in vivo* and high toxicity against eukaryotic cells. Hence, not many AMPs are clinically successful. In fact, there are only three AMPs that have been approved by the FDA for use in humans: daptomycin and two members of the same group, polymyxins. Daptomycin is a lipopeptide antimicrobial agent that was originally discovered and developed by Eli Lilly and Company in the early 1980s for treatment against bloodstream infections, endocarditis, and complicated skin and soft tissue infections[78]. Daptomycin is a potent AMP with rapid *in vitro* bactericidal activity against a broad range of multidrug-resistant gram-positive pathogens, including methicillin-resistant *S. aureus* (MRSA), glycopeptide-intermediate *S. aureus* (GISA), vancomycin resistant *S. Aureus* (VRSA), vancomycin resistant enterococci (VRE), and penicillin-resistant *Streptococcus pneumoniae*[78,79]. However, due to toxicity concerns, the clinical investigations for daptomycin was ceased in 1991. In 1997, Cubist pharmaceuticals licensed the drug with the intention of developing an antibiotic against serious gram-positive infections. The clinical trials for daptomycin started in 1999, and it was approved by FDA in September 2003[80].

Polymyxins is a group of polypeptide antibiotics that was discovered as fermentation products of the bacteria *Bacillus polymyxa*. They were first recognized for their antimicrobial activity in 1947[81,82]. Polymyxins consist of 5 chemically different compounds, polymyxins A to E, although only polymyxins B and E (colistin) are approved for clinical use. Colistin specifically was discovered in 1949 from *Bacillus polymyxa subspecies colistinus* Koyama[83,84]. It was first used therapeutically in Japan. Colistin reached the United States in 1959 and was approved for clinical use in the 1960s[85,86]. Polymyxins target the LPS of bacterial cells. Therefore, they show activity against most aerobic gram-negative bacteria. They also have bactericidal activity against many multidrug-resistant pathogens, including *Pseudomonas aeruginosa, Acinetobacter baumannii, Klebsiella pneumoniae,* and *Stenotrophomonas maltophilia*[87]. Polymyxin B and colistin were largely replaced by other antibiotics in the 1970s due to reports of high neurotoxicity and nephrotoxicity. However, the rise of antibiotic resistance and lack of treatment options against infections caused by multi-drug resistant gram-negative pathogens has led to the reconsideration of polymyxin B and colistin as a therapeutic option. They have re-emerged as important last-line agents against gram-negative bacteria that are resistant to nearly all other antimicrobial classes[88].

1.3 The emergence of antibiotic resistance

Prior to the discovery of antibiotics, bacterial infections were synonymous with death. The discovery, commercialization, and universal administration of antibiotics was a defining moment in the history of humanity that revolutionized medicine and saved countless lives. Antibiotics were also crucial for the advancement of many complex medical approaches, including surgery, that were paramount in decreasing human

mortality. Immediately after the discovery of penicillin, the US death rate was 220 per 100,000 people. Antimicrobials substantially reduced the risks associated with childbirth, injuries, and invasive medical procedures. Cutting-edge surgical procedures, organ transplantations, and management of patients with secondary diseases such as cancer, which only became possible due to the advent of antibiotics, brought the US death rate to 20 per 100,000 people over the following 45 years[89]. Unfortunately, the golden age of antibiotics discovery ended abruptly. The increasing use of antibiotics for human and non-therapeutic use in animals led to the development of antibiotic resistance.

Antibiotics exert bacteriostatic or bactericidal effects in a variety of ways (figure 1-2). Among the above-mentioned antibiotics, sulfonamides inhibit folate synthesis. The most commonly used antibiotics β-lactams; cephalosporins, carbapenems, penicillin, and their derivatives, primarily function by inhibiting cell wall synthesis. Glycopeptides like vancomycin are also cell wall synthesis inhibitors. Aminoglycosides, tetracyclines, chloramphenicols, macrolides, streptogramins, and oxazolidinones all work by inhibiting translation or protein synthesis. Rifamycins inhibit transcription, and quinolones bind to gyrase and prevent DNA synthesis[90,91]. Antibiotic resistance occurs when bacteria develop the ability to bypass these mechanisms and defeat the drugs that were designed to kill them. The infections caused by the resistant bacteria are difficult and sometimes impossible to treat[91].

Bacteria can be intrinsically resistant to antibiotics as *M. tuberculosis* is to β-lactams or can acquire the trait[92,93]. Antibiotics also function differently on gram-positive and gram-negative bacteria. Because of their intrinsic differences in the cell wall compositions, some antibiotics are effective against gram-positive bacteria and not gram-

18

negative or vice-versa. Antibiotics resistance can be genetically acquired in two major ways: chromosomal mutations and horizontal gene transfer from other resistant bacteria.

There are mainly three mechanisms that the bacteria can develop to bypass the effects of antibiotics (figure 1-3). One way bacteria protect themselves from antibiotics is by decreasing the influx and increasing the efflux of antibiotics. Bacteria can decrease the expression of porins or mutate the porin gene, leading to the reduced entry of antibiotics in the bacteria cells. Conversely, bacteria can mutate the gene sequence of multi-drug efflux pumps and overexpress them to increase the antibiotic efflux from the cells[92,93].

Next, bacterial cells can also modify the antibiotics themselves. Resistant bacteria can produce enzymes that can degrade or alter antibiotics. Such antibiotics cannot bind to their target and, thus, do not have activity against the bacterial cell. A prime example of such an enzyme is β-lactamase. Almost all pathogenic bacteria, such as *K. pneumoniae, E. coli, P. aeruginosa,* etc., have developed the ability to produce β-lactamase or its variants. Other enzymes that can transfer chemical groups like phosphate, acyl, nucleotidyl, etc., to the antibiotic molecules, to decrease their affinity to targets, have also emerged over the years. For example, aminoglycoside antibiotics can be modified by acetyltransferases, nucleotidyltransferases, and phosphotransferases[93].

Lastly, bacteria can also modify, mutate, or protect the cellular targets that antibiotics inhibit, leading to reduced antibiotic efficacy. For example, rifampicin-resistant *M. tuberculosis* strains contain mutations in the rpoB gene encoding B-subunit of RNA polymerase, which is the target for the antibiotic[92]. Similarly, methylation of 23S ribosomal RNA (rRNA) by Erm methyltransferase decreases antibiotic binding and

confers resistance to macrolides. Bacteria also can acquire genes encoding homologues for the drug target that does not bind the drug. MRSA has two copies of penicillin-binding protein (PBP), PBP2a, in addition to chromosomally encoded PBP. PBP binds with β-lactam antibiotics and their derivatives, but PBP2a does not. Hence, bacterial cells with PBP2a can continue to synthesize cell walls and are resistant to the effects of β-lactams[94]. Additionally, bacteria can also produce proteins that mimic the cellular target, as demonstrated by the MfpA protein produced by *M. tuberculosis* that mimics the size, shape, and electrostatic charge of B-form DNA. MfpA binds to DNA gyrase which is the target for antibiotic class quinolones. Its inhibitory effect on DNA gyrase results in quinolone resistance[91,95].

Antibiotics resistance is governed by a network of regulatory proteins, including sigma factors and transcription factors. In some bacteria, the stress created by the antibiotics can induce transcription factors that can regulate the expression of antibiotic resistance-associated genes, such as multi-drug transporters, efflux pumps, and ribosomal methyl transferase, which leads to increased antibiotic resistance. The genes responsible for antibiotic resistance acquired by a bacteria can also be transmitted to another. Since many antibiotics are produced by bacteria themselves, other bacteria in the environment often naturally encode genes that provide resistance. Such genes can also be acquired by pathogenic bacteria, making them resistant to the original antibiotic [91,92].

Bacterial infections are also able to persist in the host and become chronic infections even with antibiotic treatment. While antibiotic resistance and compromised immune systems may play a role, the presence of persister cells is thought to be the primary reason for the long and persistent infection. Persister cells were first described by

Joseph Bigger in 1944 after he discovered a culture of *S. aureus* could not be sterilized even with a very high dose of penicillin[96]. He theorized that some subpopulation of bacterial cells could survive antibiotic effects not due to inherent resistance but by growth arrest or very slow growth (figure 1-4). Once the antibiotic is removed, they start growing exponentially and re-establish the infection. His theory was confirmed almost 60 years later using microfluidics and live imaging that showed bacterial cells that persisted did not grow before the addition of antibiotics[97]. Persister cells can survive lethal stress and can potentially adapt to the changing environment. Persister cells may exist due to low patient compliance, poor pharmacokinetics of drugs in infected tissues, genetic adaptation, or development of increased tolerance to antibiotics[93,98–100]. They are responsible for recalcitrance and relapse of bacterial infections and have been linked to an increase in the emergence of antibiotic resistance. Hence, persister cells are a major public health concern, and yet not a lot is known about them. More research in understanding the mechanism by which they form and regrow is necessary.

1.4 Antibiotic resistance: a global crisis

Recent decades have seen a progressive decrease in the effectiveness of antibiotics against many bacteria that, in turn, have evolved into multidrug-resistant (MDR) strains. The rapid emergence and spread of MDR bacteria have become a source of global health concern. According to a national estimate published by CDC in 2019, over 2.8 million drug-resistant bacterial infections (DRBIs) occur every year in the US, causing more than 35,000 fatalities[101]. Worldwide, DRBIs kill an estimated 700,000 people per year, and mathematical models and experts alike predict that this number could rise to 10 million by 2050 if efforts are not made to curtail DRBIs or develop new

antimicrobial agents[102]. Along with substantial morbidity and mortality, DRBIs also have great financial implications as it causes serious illnesses with prolonged hospital admission and substantial increases in healthcare costs. In hospitals, DRBIs frequently begin in already immune-compromised patients with contaminating wounds, chronic skin ulcers, and medical devices such as catheters. This is demonstrated by the fact that 6% of hospitals in the US report an ongoing outbreak of drug-resistant bacteria at any given time[103]. In these nosocomial settings, ESKAPE organisms (*Enterococcus faecium, Staphylococcus aureus, Klebsiella pneumoniae, Acinetobacter baumannii, Pseudomonas aeruginosa, and Enterobacter spp.*), in particular, are emerging as important MDR pathogen.

Given the uprise in antibiotic resistance, there is an urgent need for alternative antimicrobial drugs against bacteria that are no longer susceptible to conventional antibiotics. Despite this, the once-robust drug development pipeline has seen a progressive decline in the production of viable antimicrobial agents. Hence, in 2017, World Health Organization (WHO) announced the first-ever list of antibiotic-resistant priority pathogens that consisted of 12 families of bacteria with the greatest threats to human health and required immediate therapeutic research and development attention. The critical category of the priority pathogens included three resistant gram-negative bacteria, *Klebsiella pneumoniae, Acinetobacter baumannii, Pseudomonas aeruginosa* [104]. In 2019, WHO published the third annual review to analyze how the clinical antimicrobial discovery pipeline is responding to this priority list. This review that describes all antibiotics and treatments in development against WHO priority pathogens demonstrates how the clinical pipeline remains insufficient to challenge antibiotic

resistance[105]. According to the report, 60 antibacterial products are in clinical trials, among which 32 are active against the priority pathogens. However, only eight antimicrobial agents have been approved since 2017, and even these have limited clinical benefits over existing treatments. Half of these agents target the same bacterial strain, carbapenem-resistant Enterobacteriaceae (CRE), while antibiotics against the other priority pathogens are still absent. Furthermore, six out of the eight approved antibiotics are from existing classes with established resistance mechanisms and are thus guaranteed to develop fast resistance[105–107]. Hence, the public health crisis created by the emergence of antibiotic resistance is bleak, and the only way to solve it is through the revitalization of the dwindling antibiotic development pipeline[101,102,104,108–111].

1.5 Antimicrobial peptides: a promising alternative to antibiotics

Antimicrobial peptides (AMPs) are ideal alternatives to conventional antibiotics as they are natural compounds that have broad-spectrum activity against gram-positive and gram-negative bacteria. Due to the diversity of available sequences, AMPs are versatile and can be screened against specific bacterial strains. AMPs usually function by targeting and disrupting the plasma membrane of bacteria. This mechanism of action also makes AMPs very efficient and attractive as antibiotics because, compared to conventional antibiotics that attack small, enzymatic targets that bacteria can modify to induce antibiotic resistance, the plasma membrane is costly for the bacteria to change. Thus, the emergence of resistance against AMPs is less likely.

However, despite promising features, not many AMPs have made it through clinical trials, and even fewer have been approved by the FDA[112–116]. This is, in part, because AMPs with high bactericidal effects display a significant reduction of their

antimicrobial activity in the presence of host cells, tissue and serum proteins. AMPs can also get deactivated through proteolytic degradation by the host or bacterial proteases during infection or through binding to host cells, tissue, and proteins, leading to loss of bioavailability[117,118]. This failure to function in the presence of biological specimens and bacteria has been a major roadblock in clinical trials of AMPs as therapeutics. Nevertheless, the AMP field continues to find ways to advance towards better activity *in vivo*.

To facilitate the discovery and synthesis of evolved AMPs, database-driven active peptides with low cationicity have been identified. Peptides with low cationicity are thought to have reduced host cell inhibition [119]. In silico optimization of AMPs also has shown some promise[120]. However, in the lack of extensive quantitative structure activity relationship (QSAR) rules that apply to rational design and engineering of AMPs, it is difficult to optimize AMPs to discover ones without impediments. As a result, most AMPs have been chosen from trial-and-error methods with modifications of known AMP sequences. Therefore, the presence and absence of impediments in the AMPs are not known and not tested until after the design, synthesis, and characterization of the peptide[117,118]. This process limits the flow of promising new AMP candidates into the drug development pipeline.

We use Synthetic molecular evolution (SME), an approach unique to our research, to identify potent AMPs (figure 1-5). SME involves design and orthogonal screening of iterative library. Through this process, we can design AMPs in the library to have higher selectivity for microbes over host cells. The selected antimicrobial peptides will also lack other impediments that prevent it from functioning *in vivo*. We achieve this

by screening the library under selective pressures for bactericidal activity with down-selection based on solubility, hemolysis, and host cell inhibition. We have been able to identify "host cell compatibility" before the characterization of the AMP by assessing the activity of the peptide in the presence of concentrated human red blood cells during screening. The selected AMPs are highly effective *in vitro* against bacterial cells even in the presence of concentrated host cells. These AMPs also have antibiofilm activity against gram-negative and gram-positive biofilms[121].

1.6 Goals of the research presented in this study.

Here, we implement SME based approach that uses iterative library design and orthogonal screening under selective pressures to specifically identify antimicrobial peptides with superior bactericidal activity *in vivo*. **In the first aim of this project, we seek to identify host cell-compatible, antimicrobial peptides effective against drug-resistant, biofilm-forming bacteria.** To fulfill this aim, a second-generation iterative library with 28,800 unique members, based on parent peptide ARVA and NATT, was synthesized (figure 1-5 A). The library was then screened in the presence of concentrated red blood cells for activity against *Pseudomonas aeruginosa* and *Escherichia coli*. Nine peptides were selected based on high solubility and antimicrobial activity as well as low hemolysis and host cell inhibition. Additionally, nine rational variants of the selected peptides were synthesized. One of the rational variants, D-CONGA, was obtained by removing the invariant glycine from the consensus sequence of the selected nine peptides (figure 1-5 B). Characterization of these selected and rational variant peptides showed D-CONGA has a superior antimicrobial activity against ESKAPE organisms (*Enterococcus faecium, Staphylococcus aureus, Klebsiella pneumoniae, Acinetobacter baumannii,*

Pseudomonas aeruginosa, and Enterobacter spp.) with minimum hemolysis. D-CONGA

demonstrated anti-biofilm activity in low concentrations against gram-negative

Pseudomonas aeruginosa and gram-positive *Streptococcus mutans*. Additionally, D-

CONGA did not induce resistance up to 10 passages of *Pseudomonas aeruginosa,* and

had low toxicity against the human fibroblast cell line, WI-38[121]. In a mouse model of a

deep surgical wound infected by *Pseudomonas aeruginosa* and MRSA, D-CONGA

inhibited the growth and formation of biofilm[121–123].

In the second aim of this project, we seek to use SME to identify D-CONGA

variants and to study how different alterations in the sequence and structure of D-

CONGA affect its activity. Through this process, we hoped to discover peptides that are

superior to D-CONGA with improved bactericidal activity and reduced cytotoxicity. We

synthesized 13 variants of D-CONGA and characterized them for their activity against

gram-positive *S. aureus* and gram-negative *E. coli* and *K. pneumoniae* in the presence

and absence of red blood cells (RBCs). Their cytotoxicity against mammalian fibroblast

cell line, WI-38, and hemolysis in RBCs were also measured. The best D-CONGA

variant, D-CONGA-Q7, was then tested against 14 clinical isolates that included resistant

strains of *K. pneumoniae*, pan drug-resistant (PDR) *A. baumannii*, methicillin-resistant *S.*

aureus, and *P. aeruginosa* from patients with cystic fibrosis. The antimicrobial activity of

the peptide was compared with D-CONGA and eight conventional antibiotics from four

different classes. D-CONGA-Q7 outperformed D-CONGA and major conventional

antibiotics *in vitro*. D-CONGA-Q7 was able to inhibit bacterial infection as well as their

biofilms on an animal wound model. Given this excellent bactericidal activity of D-

CONGA-Q7, we believe we successfully discovered a variant that outperforms the lead peptide D-CONGA.

In the third aim of this project, we seek to further improve D-CONGA-Q7 by synthesizing a combinatorial third-generation peptide library based on D-CONGA and D-CONGA-Q7 and screening it for peptides that are active against gram-positive *S. aureus* and gram-negative *K. pneumoniae* in sub micromolar concentrations. We designed and synthesized a library with 6,912 members using a solid-phase peptide synthesis (SPPS) method (figure 1-5 C). A "split and recombine" technique was used to synthesize the library on TentaGel mega beads. Prior to amino acid addition, the loading capacity of the beads was increased three times using glycine, lysine, and beta-alanine for branching. UV sensitive photolabile linker was added after the branching to allow each peptide to be cleaved, post-synthesis, by UV-light. These peptides in sub micromolar concentrations are used for screening. Individual library members were tested for microbicidal activity against gram-positive and gram-negative bacteria and for hemolytic effects against RBCs. Only the library members that sterilize both organisms in these low concentrations are selected. Hemolysis of each selected peptide is also calculated. Lastly, the selected peptides will be used for sequencing through MS/MS or by Edman degradation.

Figure 1-1
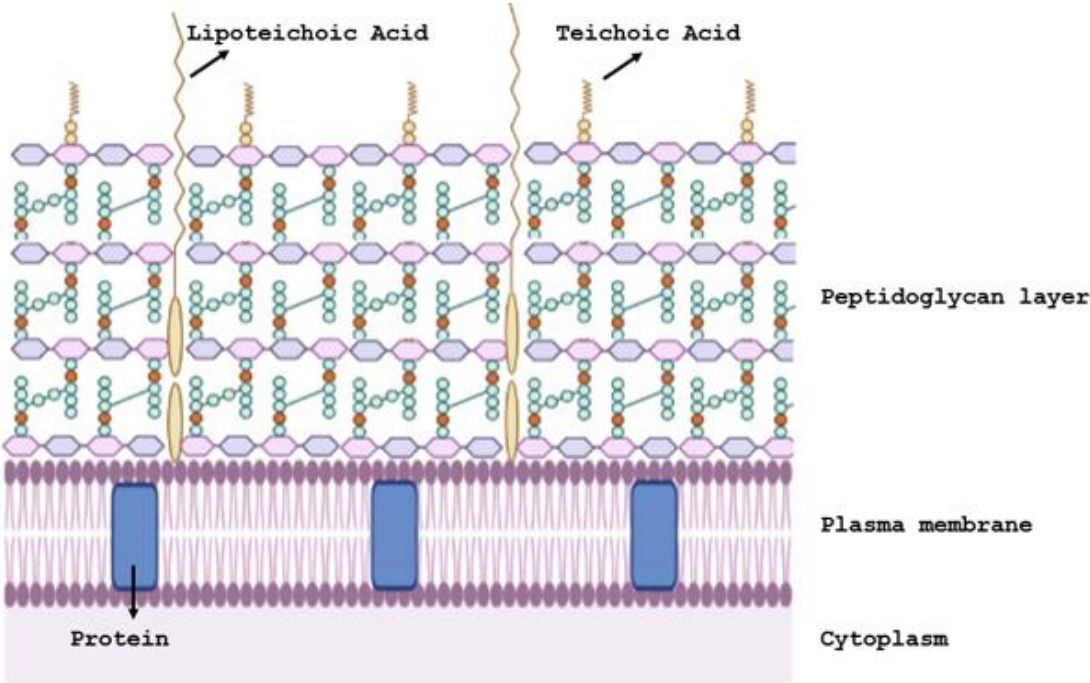
Gram-positive Cell wall
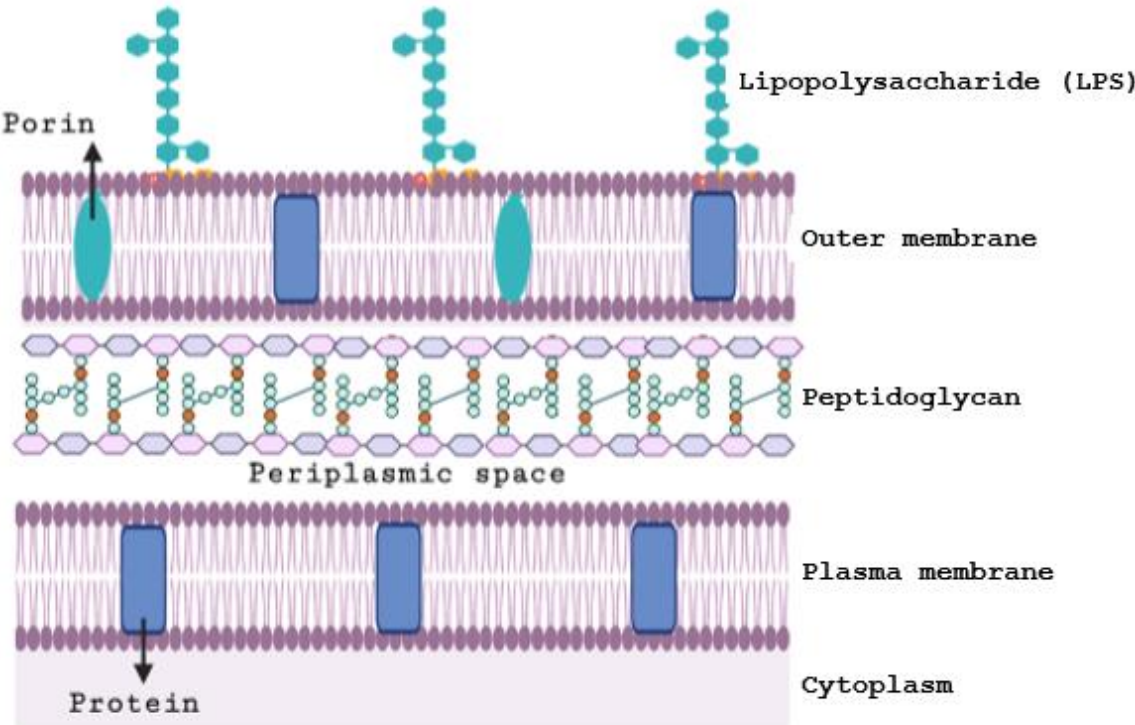
Gram-negative Cell wall

Figure 1-1. Differences in the structure of gram-positive and gram-negative bacteria. The thick layer of murein and peptidoglycan and absence of the outer lipid membrane in gram-positive bacteria retains the crystal violet-iodide complex even after the treatment with alcohol. The cell wall appears purple after the gram staining procedure. In contrast, gram-negative bacteria have a comparatively thin layer of peptidoglycan, which does not retain the color of the crystal violet iodide complex and appears pink. This can be visualized under a light microscope to differentiate the type of bacteria.

Image is created with BioRender.com.

Figure 1-2

Cell Membrane Disruptors

Polymixins

Cell Wall Synthesis Inhibitors

β-lactams
Cephalosporins
Carbapenems
Glycopeptides

DNA Synthesis Inhibitors

Quinolones

Transcription Inhibitors

Rifamycins

Translation Inhibitors

Aminoglycosides
Tetracyclines
Chloramphenicol
Oxazolidinones
Macrolides

Cell Wall Synthesis

DNA

RNA

Protein

Folate Synthesis

Folate Synthesis Inhibitors

Sulfonamides
Trimethoprim

Figure 1-2. Different classes of antibiotics and the mechanism of their actions.

Image is created with BioRender.com.

.

Figure 1-3
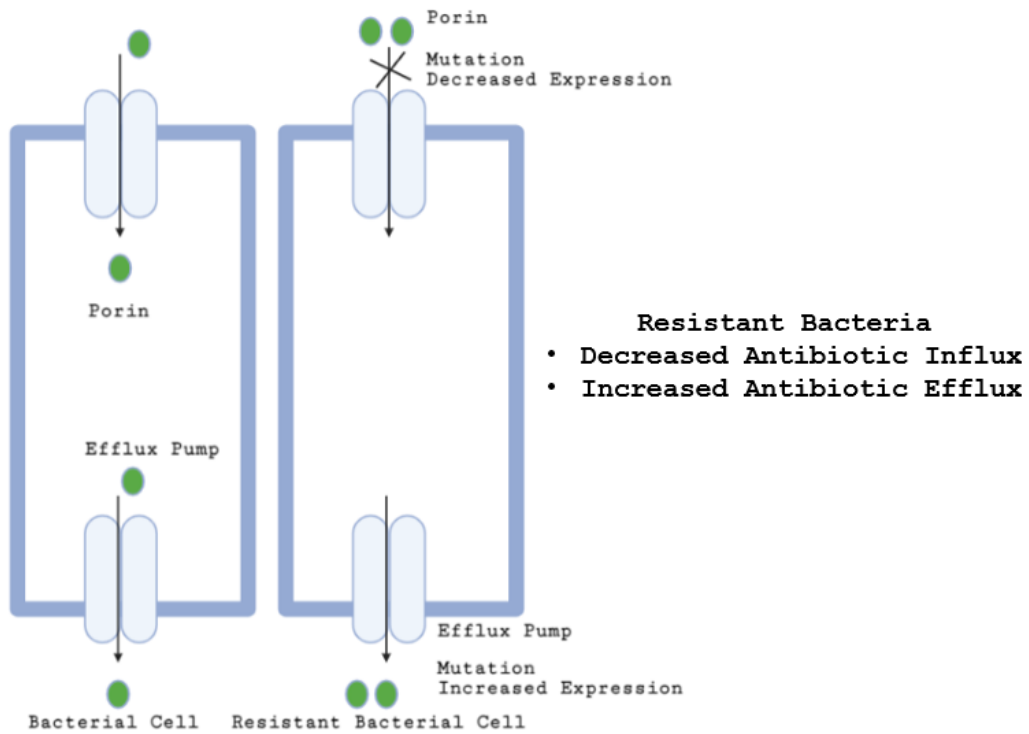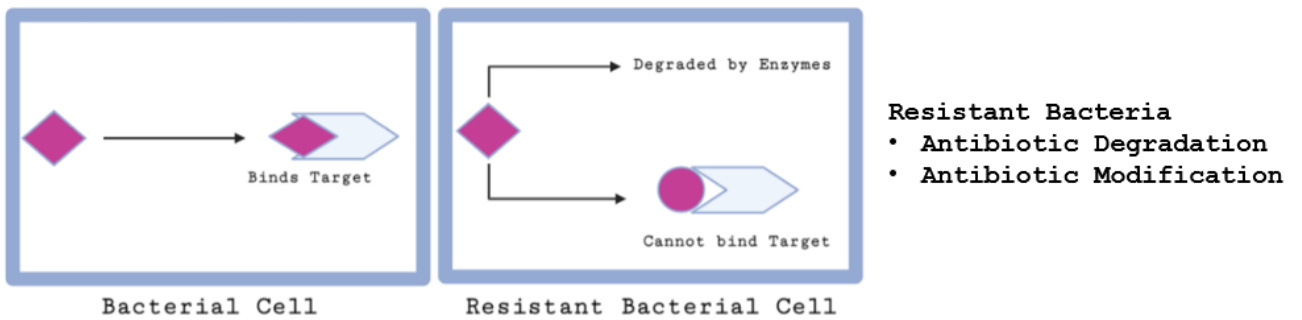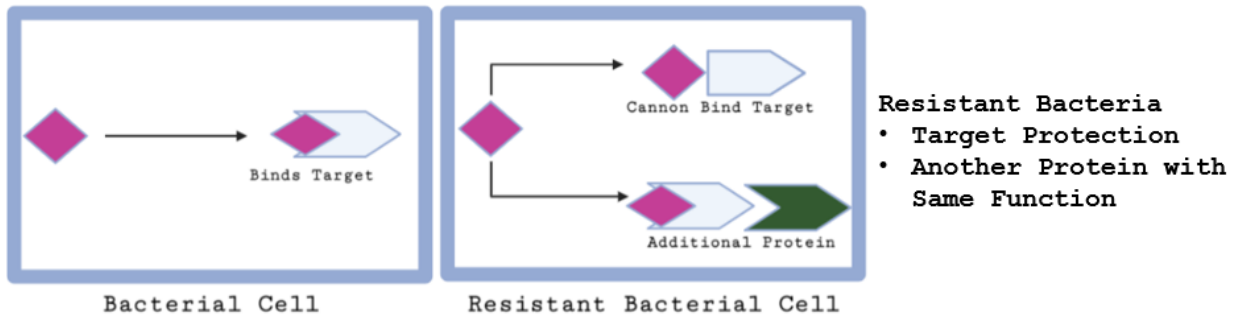
Figure 1-3. Mechanism of antibiotic resistance. Bacteria can develop antibiotic resistance in three separate ways. **A)** The bacteria can decrease the influx and increase the efflux of antibiotics by mutations or increased or decreased expression of porins and pumps. **B)** The bacteria can also modify the antibiotics in different ways such as degradation or addition of various chemical groups. **C)** The bacteria can also change the antibiotic target.

Image is created with BioRender.com.

Figure 1-4

Selection of
Pre-existing Resistant
Cells

Antibiotic
Inhibition

Resistance

All Resistant Cells

Emergence of
Persister Cells

Antibiotic
Inhibition

Revival of
Pathogens

Sensitive Cells with
Persisters
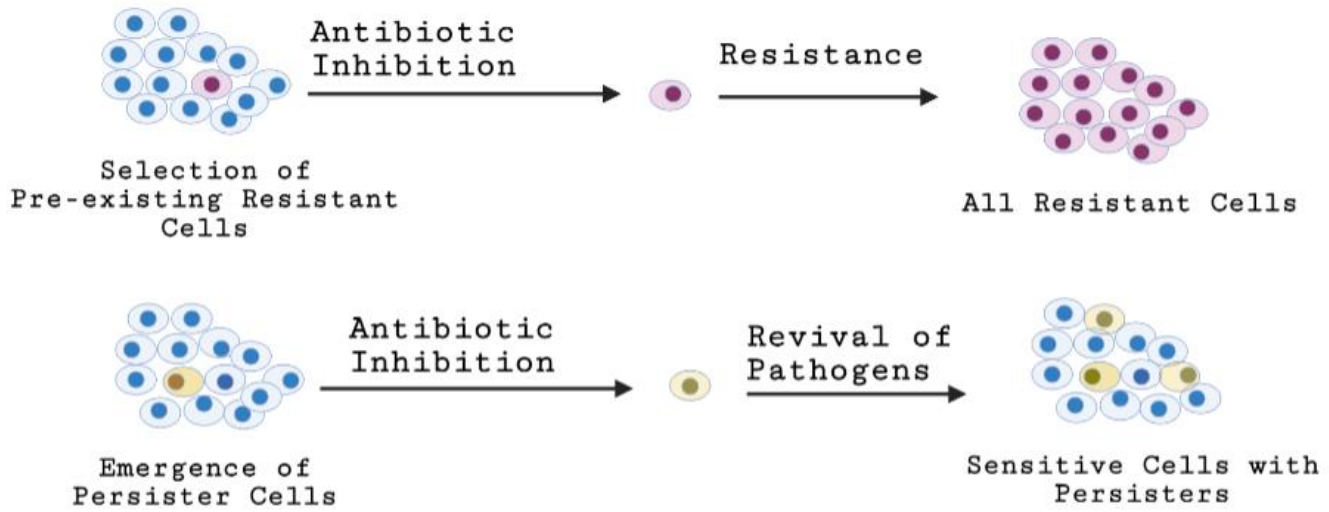
Figure 1-4. Formation of Persister cells. When antibiotic is used to treat bacterial infections, a small subset of cells remains dormant but alive and are not affected by the antibiotics. These are called persister cells. After antibiotic treatment is removed, these persister cells can resuscitate, proliferate, and cause recurrent disease.

Image is created with BioRender.com.

Figure 1-5

A)

De novo
First Generation Library

↓ ↘

Lipid Vesicle-Based Screen

Microbe Sterilization-Based Screen

↓ ↓

ARVA
RRGWALRLVLAY

NATT
RRGWNLALTLTYGRR

↓ ↓

Second Generation Library

B)

ARVA based Second-Generation Library

↓

Double Broth Sterilization

↓

DBS1,DBS2,DBS3
DBS4,DBS5

↓

D-CONGA

↓

D-CONGA Variants

C)

ARVA based Second-Generation Library

↓

DBS1,DBS2,DBS3
DBS4,DBS5

↓

D-CONGA

↓

D-CONGA Variants

↓

D-CONGA-Q7

↓

D-CONGA and D-CONGA-Q7 based Third-Generation Library

↓

46 Peptides

Figure 1-5. Schematic representation of Synthetic Molecular Evolution (SME) that led to the discovery of D-CONGA and D-CONGA-Q7. (A) A 1st generation library was designed de novo and was screened against lipid vesicles to produce ARVA. The same library was screened against bacteria and a fungus to produce NATT. Both peptides are potent, broad-spectrum antimicrobial peptides but lose their activity in the presence of eukaryotic cells. **B)** A 2nd generation library was designed using ARVA and NATT as templates and was screened by double radial diffusion to give the DRD peptides, by hybrid radial diffusion and broth dilution sterilization method to give the RDBS peptides, and by double broth dilution sterilization to give the DBS peptides. The DBS peptides were the best peptides out of the nine selected from the screen. DBS peptides gave rise to the consensus sequence (CON), and its D-amino acid variant D-CON. Among a number of rational variants tested, the peptide D-CONGA was identified, which was a more potent antibiotic than DBS peptides. C) D-CONGA-Q7 is formed by the insertion of glutamine at the seventh position of D-CONGA, which is by far the best antimicrobial peptide from this screen. **C)** A 3rd generation library was designed based on D-CONGA-Q7.

Image is created with BioRender.com.

CHAPTER 2: Synthetic molecular evolution of host cell-compatible, antimicrobial peptides effective against drug-resistant, biofilm-forming bacteria

Introduction

In vitro assays for antimicrobial activity against diverse strains of bacteria, including those resistant to conventional antibiotics, show that AMPs are a potent broad-spectrum antibiotic that sometimes does not induce resistance[124]. Yet, AMPs have not been able to establish a significant clinical impact to date. *In vitro* assays cannot replicate the complex environment that antibiotics are presented *in vivo*. Proteolytic degradation, binding to serum proteins, host cell toxicity, and clearance by glomerular filtration are some of the factors that hinder the performance of AMPs[125]. There is also strong evidence that host-cell and tissue binding is a significant determinant of the loss of activity in antimicrobial peptides. AMP interactions with bacterial membranes have been extensively investigated[126–131]. These studies indicate that AMPs sterilize bacteria by binding selectively to bacterial membranes and disrupting them, ultimately leading to cell lysis and death[128,132–135].

However, most mechanistic information has been derived from experiments done with synthetic phospholipid bilayers. Biological membranes are much more complicated than synthetic bilayers. The simple, synthetic systems are not entirely predictive of interactions with biological membranes. The proteins incorporated in the biological membrane, the carbohydrate-based extracellular macromolecules, and anionic intracellular macromolecules such as nucleic acid can bind and modulate AMP behavior[136–138]. Starr et al., from our laboratory, expanded the binding studies from synthetic bilayers to eukaryotic cells. Using human red blood cells (RBCs), a consistent and experimentally reliable generic

surrogate for all host cells and tissue, he demonstrated that the presence of eukaryotic cells strongly inhibits the activity of many natural and synthetic AMPs. While AMPs, naturally, have a higher affinity to bacterial cells due to electrostatic interactions, this selectivity is not enough to prevent weak binding to eukaryotic cells. This host cell binding decreases the bioavailability of antibiotics, lowering their potency *in vivo*. At physiologically relevant concentrations of cells, pre-incubation of AMPs with RBCs leads to the loss of AMP activity, especially when combined with other impediments[118]. A kinetic network model for this scenario is represented in figure 2-1.

In another study, Starr et al. demonstrated that in addition to host cell binding, proteolysis is also a significant factor in AMP activity loss. AMPs, when incubated with RBCs, were readily cleaved into fragments of various sizes with very low sequence specificity. Many AMP sequences, including synthetic and natural AMPs, are susceptible to degradation by this proteolytic activity. However, the degradation rates vary substantially. In this study, the proteolytic degradation of AMPs was directly attributed to the unique enzymes associated with the cytosols of RBCs[117]. However, this activity effectively mimics the proteolytic activity of human serum as well.

Biological stability and availability are primary concerns when assessing the therapeutic potential of peptide drugs. The implications of the work described above, regarding the loss of drug activity due to host cell binding and protease degradation, are also very significant for the design of experiments that use human RBCs to develop therapeutics against diseases such as malaria, anemia, and sickle cell disease[139,140]. It is especially critical for AMP research as RBCs have been widely used as a model system for toxicity assessment of peptides. More broadly, the impediments caused by RBCs, through

binding and proteolysis, effectively mimic the environmental conditions experienced by peptide drugs *in vivo*. Our current study aims to find peptides with increased hemocompatibility (i.e., antibacterial activity in the presence of RBCs) through a screening-based approach and targeted sequence engineering with these considerations in mind.

The impediments caused by protease degradation and host cell interaction can be selected if the initial design and discovery to preclinical characterization is done in the presence of concentrated host cells. The peptides can be preincubated with RBCs before the addition of bacterial cells. Involving host cells during the screening process will also create a very stringent condition for the selection of hemocompatible peptides. Thus, peptides that are active after the incubation with host cells will have high selectivity and low toxicity. Also, the selected peptides that maintain their bactericidal activity will not be susceptible to proteolytic degradation or host cell binding. This strategy was employed in high-throughput screening by our laboratory, which successfully led to the selection of hemocompatible peptides with superior antimicrobial and antibiofilm activities. This screening employed an approach called synthetic molecular evolution (SME) developed by our laboratory. SME refers to the synthesis of small iterative peptide libraries based on characterized parent AMPs, and screening of the library to select superior AMPs, followed by rational design to improve these selected AMPs. Ultimately, this approach is used to discover evolved peptides that have increasingly potent and selective activity against drug-resistant bacteria.

A peptide library with 28,800 members was synthesized based on the parent AMP, ARVA (figure 2-2). ARVA is a synthetic AMP that has potent broad-spectrum

antimicrobial activity *in vitro*. However, like many other AMPs, ARVA loses its bactericidal effects in the presence of eukaryotic cells because of binding and proteolysis. The resultant AMPs were expected to retain the high bactericidal activity of ARVA and gain functional activity in RBCs. Three different approaches were used to screen the library. Two peptides, DRD1 and DRD2, were selected from the first screening approach, the double radial diffusion (DRD) assay (figure 2-3). DRD assay measures the antibiotic's potential to inhibit bacterial growth by measuring the zone of inhibition (ZOI) on agar plates. ZOI was measured in the absence and presence of $1x10^8$ RBCs/ml. Two iterations of the screen were performed, one against *P. aeruginosa* and *E. coli* and one against *P. aeruginosa* and methicillin-resistant *S. aureus* (MRSA). DRD1 was selected because of its high ZOI against *P. aeruginosa* and *E. coli*, and DRD2 was chosen for its potency against *P. aeruginosa* and MRSA. The second approach was a mixed assay which employed radial diffusion assay against *E. coli* and broth sterilization assay against *P. aeruginosa* (RDBS). RDBS approach screened peptides against *E. coli* and *P. aeruginosa* in radial diffusion and more stringent broth dilution assay simultaneously. Two peptides, RDBS1 and RDBS2, were selected through this approach (figure 2-3). However, the post-screen characterization of the four peptides discovered through the two approaches showed they did not have great broad-spectrum activity.

To circumvent this problem, a third approach using double broth sterilization (DBS) assay was utilized. Five peptides (DBS1, DBS2, DBS3, DBS4, and DBS5), which could sterilize both *E. coli* and *P. aeruginosa* in minimum inhibition concentration (MIC) of less than 10 μM were selected from this screening (figure 2-4 B). Post-screen characterization showed DBS1 and DBS4 to be the most potent antibiotic among the nine

selected peptides. Rational variation in the sequences of these nine peptides led to the synthesis of nine more variants (figure 2-5). The D-form of the consensus sequence of all the selected peptides, D-CON, was one of the best variants against gram-negative bacteria. However, D-CON had poor activity against the gram-positive *S. aureus*. Another variant, D-CONGA (D-CON Glycine Absent), made by deleting the G from the ends of D-CON, was characterized to be the best peptide from this library.

Thus, this study identified antimicrobial peptides (AMPs) that retain activity in the presence of eukaryotic cells by using a synthetic molecular evolution (SME) based approach. Dr. Charles. G. Starr, my predecessor in this project, discovered D-CONGA and demonstrated that variation in the sequence of antimicrobial peptides selected from primary screening of iterative peptide library can lead to identification of peptides that have superior antimicrobial activity, solubility, and lower cytotoxicity against red blood cells (RBCs). He performed assays to show the superior broad-spectrum antimicrobial activity of D-CONGA and some of the evolved peptides from the screen. I inherited his work and expanded the characterization of D-CONGA and some other selected peptides from the screen. In the following work, we show that D-CONGA, a variant obtained by rational modification of the consensus sequence of peptides selected from the stringent screening of iterative, second-generation antimicrobial peptide library is highly effective *in vitro* against all ESKAPE pathogens in the presence of RBCs and serum. The peptide also has broad-spectrum anti-biofilm activity *in vitro* and does not develop resistance against gram-negative *P. aeruginosa* up to 10 generations[121].

Methods and Materials

Peptides and antibiotics

Peptides were either synthesized in the lab using solid-phase peptide synthesis (SPPS) method or were obtained from Bio-Synthesis Inc. (Lewisville, Texas). The purity of each was >95% by HPLC. Antibiotics were obtained from various vendors. Unless otherwise stated, all solutions were prepared by dissolving lyophilized peptide or antibiotic powders in 0.025% v/v) acetic acid. Peptide sequences are provided in figure 2-3 A, 2-4 A, and 2-5 A.

Bacterial strains and growth conditions

E. coli (ATCC 25922), *S. aureus* (ATCC 25923), *P. aeruginosa* (PA01), *E. faecium* (ATCC 19434), *K. pneumoniae subsp. Pneumoniae* (ATCC 13883), *A. baumannii* (ATCC 19606), and *S. enterica subsp. Enterica* (ATCC 14028) were used in this study. An overnight culture was prepared by adding a colony of bacteria into 5 ml fresh tryptic soy broth (TSB) and incubating it overnight in 37 °C. Subcultures, prepared by inoculating 25 mL of fresh tryptic soy broth (TSB) with 200 µl of an overnight culture, were grown to log phase (OD600 = 0.3−0.6), after which cell counts were determined by measuring the OD600 (1.0 = 5×10^8 CFU/mL for *E. coli,* 1×10^9 CFU/mL for *S. enterica,* , 4×10^8 CFU/mL for *K. pneumoniae,* 4×10^8 CFU/mL for *P. aeruginosa*, 3×10^8 CFU/mL for *E. faecium* 1.5×10^8 CFU/mL for *S. aureus*,). Bacterial cells were diluted to appropriate concentrations in either TSB or PBS, depending on the assay.

Human serum and erythrocytes

Fresh human serum (OTC) and human O+ erythrocytes were obtained from Interstate Blood Bank, Inc. (Memphis, TN). Serum was vacuum filtered through a 0.45 µm filter to remove precipitates. RBCs were subjected to four cycles of centrifugation at 1000xg with

resuspension in fresh PBS. Following the final wash step, the supernatant was clear and colorless. RBC concentration was determined using a standard hemocytometer.

Broth dilution assay

Peptides were prepared at 5-times the final concentration needed in 0.025% acetic acid. The peptides were serially diluted by a factor of 2:3 horizontally across a 96-well plate from Corning in PBS. The final volume of the peptide in each well was 25 μl. One column of wells was reserved for controls (TSB and RBCs/ Bacterial Cells and RBCs). 50 μl of Type O+ human RBCs in PBS at 2.5x10^9 cells/mL was added to each well. The plate was incubated at room temperature for 30mins. 50 μl of TSB, inoculated with 5×10^5 CFU/mL of bacteria, was added to all necessary wells. Plates were incubated overnight at 37 °C. Because the RBCs make the determination of growth/sterilization difficult, 10 μl from each well was transferred to a fresh plate with 100 μl of TSB and incubated overnight, again at 37 °C. This plate was read at 600 nm to determine whether bacterial growth had occurred. Plates with OD600 < 0.1 were considered sterilized. Peptides were assigned 30 μM MIC when there was no sterilization observed. In these cases, the MIC was noted as >30 μM, and peptide was considered to have no activity against that bacteria.

Hemolysis assay

Peptides were prepared at twice the final concentration needed in 0.025% acetic acid. The peptides were serially diluted by a factor of 2:3 horizontally across a 96-well plate from Corning in PBS. The final volume of the peptide in each well was 50 μl. To each well, 50 μl of RBCs in PBS at 2x10^8 cells/mL was added. As a positive lysis control and negative control, 1% triton-X and pure RBC were added to corresponding wells. The plate was incubated at 37 °C for 1 hour, after which it was centrifuged at 1000xg for 5 minutes. After

centrifugation, 10 µl of supernatant was transferred to 90 µl of DI H_2O in a fresh 96-well plate. The absorbance of released hemoglobin at 410 nm was recorded, and the fractional hemolysis was calculated based on the 100% and 0% lysis controls.

Selection for stable resistance

Antibiotics were prepared at 5-times the final concentration needed in 0.025% acetic acid and serially diluted by a factor of 2:3 horizontally across a 96-well plate from Corning in PBS. The final volume of the antibiotic in each well was 25 µl. 100 µl of TSB, inoculated with $5x10^5$ CFU/mL of *P. aeruginosa* (PA01), was added to all necessary wells. Plates were incubated overnight at 37 °C. PA01 from the well that contained the highest concentration of antibiotic that allowed for bacterial growth was collected for overnight passaging without antibiotic. Treatments by the same antibiotics were carried out the next day, and the entire process was repeated until resistance or the tenth passage. Glycerol stocks of all generated resistance strains of PA01 or strains at the tenth stage without any resistance were snap-frozen in liquid nitrogen and stored for later testing. These selected strains from the tenth passage were then cross treated against antibiotics other than the one they were selected against.

Biofilm assay using CFU reduction method.

A 1:10 dilution of the overnight culture of *P. aeruginosa* (PA01) was prepared in Luria Broth (LB). 125 µl of this dilution was added to each well across the 96-well plate from corning. The bacterial cells were allowed to grow at room temperature for 48 hours, which is sufficient for biofilm formation. 2 days later, the media was removed from each well, so only biofilm remained on the walls and bottom of wells. 150 µl of 50 µM, 25 µM, 12.5 µM, and 6.25 µM of the antibiotics were prepared and added to the wells with biofilm.

150 µl of sterile PBS was used for control. The plate was incubated with antibiotics for 2 hours, following which the antibiotics were removed from each well. After two washes with distilled water, 150 µl of PBS was added to each well. The sides and the bottom of the wells were scraped off using sterile pipet tips. The resultant solution was serially diluted five times by a factor of 1:10. 10 µl of each dilution was spot plated on a fresh LB agar plate. The plate was incubated over-night, and colonies on each spot were counted the following morning. The effect of the antibiotics on the PA01 biofilm was assessed based on the reduction in colony forming units (cfu) in antibiotic-treated wells compared to untreated wells.

Biofilm Assay Using Confocal Microscopy

Streptococcus mutans (S. mutans) (UA159) was grown overnight in a brain-heart diffusion (BHI) broth at 37 °C and 5% CO_2. Following 1:10 dilution of the overnight culture in 10 ml of semi-defined biofilm medium with glucose (18 mM) and sucrose (2 mM) (BMGS) added as supplemental carbohydrate sources, 200 µl of *S. mutans* was added to an eight-well chambered cover glass. Aerobic *S. mutans* biofilms were cultured on the eight-well chambered cover glass at 37 °C and 5% CO_2 for 3 days with BMGS medium changed daily. After washing twice with PBS, biofilms were then treated with 50 µM, 25 µM, and 12.5 µM AMP, or PBS for control, respectively, for 4 hours. After the treatments, biofilms were stained with BacLight fluorescent dyes, Syto9 and Propidium Iodide, for 15 minutes. Syto9 is a nucleic acid stain, while propidium iodide is a cell impermeant die. After a wash with PBS, the stained biofilm was then imaged using an inverted 40X oil objective. Confocal microscopy was performed with a Zeiss LSM 700 microscope. Confocal z-

stacks and simulated xyz 3D images were acquired and generated using Zeiss 10.0 software. Images were further analyzed using Comstat2 software.

Results

Based on the binding and proteolysis data, Starr and Wimley hypothesized that they could achieve a gain of function in AMPs by applying selective pressures during initial AMP screening for bactericidal activity with down-selection based on solubility, hemolysis, and host cell inhibition. They developed a 28,800 membered iterative second-generation library based on the peptides selected from the first-generation, *de novo* designed, β-sheet-rich peptide library. They designed assays to screen the second-generation library in the presence of concentrated human red blood cells. Both the libraries were synthesized on a "one-bead one-compound technique". The first-generation library was screened for synthetic lipid vesicle permeabilization. However, as we have established, phospholipids are not a perfect representative of bacterial and eukaryotic cell membranes. The peptides selected from the *de novo* library, such as ARVA and NATT, were potent and broad-spectrum for microbial sterilization in standard laboratory assays. However, like many other AMPs, ARVA and NATT lost all their activity in the presence of host cells. It was demonstrated that ARVA and NATT bind to the host cells and are also susceptible to RBCs induced proteolysis. They also had low solubility and caused high hemolysis. In this study, we used SME based approach to select host cell-compatible AMPs. Host-cell compatible refers to peptides that preferentially binds to bacteria and not the eukaryotic cells or tissues. A library was synthesized based on ARVA, and antimicrobial screens were performed with 1×10^9 human red blood cells (RBCs)/mL, a dense cell suspension with 20% of cell density in blood. The screen was designed to select for peptides that were

resistant to binding and proteolysis and thus, retained broad-spectrum antimicrobial activity of ARVA even in the presence of host cells. The resulting host cell compatible AMPs that have evolved are highly effective *in vivo*[121].

Characterization of the antimicrobial activity of selected peptides and their variants

Nine peptides were selected from the initial screen. In the screen, these peptides were able to sterilize *E. coli* and *P. aeruginosa* in concentrations less than 10 μM and had hemolysis of less than 5% at a peptide concentration of 100 μM (figure 2-6). The antimicrobial activities of the selected peptides against gram-negative ESKAPE pathogens was assessed. ESKAPE bacteria include the common human pathogens*: Enterococcus faecium, Staphylococcus aureus, Klebsiella pneumoniae, Acinetobacter baumannii, Pseudomonas aeruginosa*, and the *Enterobacteriaceae*, which consist of *Enterobacter, Escherichia*, and *Salmonella* species. Post screen assays were performed with and without 1×10^9 human RBCs/mL using both protease susceptible L-amino acid peptides and protease resistant D-amino acid peptides. The first four peptides selected from double radial diffusion (DRD) and radial diffusion-broth sterilization (RDBS) screens had poor antimicrobial activity against the ESKAPE pathogens (figure 2-3 B). We should note that the post-screen characterization assays are more stringent than the screen as well as the typical MIC assays reported in the literature. In the assays used for the characterization, peptides are preincubated in concentrated RBCs for 30 minutes to allow binding and proteolysis. The bacteria is also not incubated in minimal media prior to the addition of growth media, which is a standard practice in other MIC assays. In fact, 1×10^5 bacterial cells/ml, which are in exponential phase in growth media, are directly added to peptides preincubated in RBCs. In this case, bacterial cells are actively dividing and are healthy

enough to overcome any antibiotic that does not rapidly sterilize all the cells. Thus, only a very potent antibiotic can sterilize all the bacteria in this assay. This is probably why the first four peptides performed poorly even against the same organisms they were able to inhibit in the screen.

The five peptides selected from the double broth sterilization (DBS) assay were the best antibiotics from the library (figure 2-4 B). In the absence of RBCs, the bactericidal activity of L- and D-DBS peptides were almost identical. The addition of RBCs reduced the activity of L-DBS peptides significantly but did not have much effect on the D-DBS peptides. As expected, L-DBS peptides were degraded by proteolysis while D-DBS peptides resistant to proteolysis were stable and available for activity. The D-form of two of the DBS peptides, D- DBS1 and D- DBS4, could sterilize all the ESKAPE pathogens, including gram-positive *S. aureus* and *E. faecium*, in concentrations $\leq$ 10 μM in the presence of concentrated RBCs. The hemolysis for all the DBS peptides was less than 8% (figure 2-6). They were also very similar in sequence, suggesting convergence to a small part of the library's sequence space. The terminal cassette on N and C terminus of all selected peptides, except DBS5, was RR. DBS5 had RR on the N terminus and R on the C terminus. The hydrophobic core in the center of all the peptides began with invariant WA followed by three positions that could contain either R or another nonpolar amino acid. The selected positive peptides all had one or two R residues in that region, more often in positions 5 and 6. The sequence WARRL in positions 3 to 7 was observed in five out of the nine positives, including the highly active DBS1 and DBS4. In the five superior DBS-positive peptides, position 7 was always L. The three DBS peptides, which had comparatively higher antibacterial activity, DBS1, DBS3, and DBS4, all had the same

sequence until position 7. The C-terminal region of the library core was hydrophobic. Overall, the selected sequences were more hydrophobic than the average library member, always containing two or three aromatic residues in the three varied positions (figure 2-3 A and 2-4 A).

Based on the sequence analysis and characterization of the selected peptides, rational variants were designed (figure 2-5). One of the variants was the DBS consensus sequence, RRGWARRLAFAFGRR, which was aptly named CON. Removal of the invariant glycines from the D-form of the CON peptide made D-CONGA (D-amino acid CONsensus with Glycine Absent). D-CONGA has superior bactericidal activity against all seven ESKAPE pathogens, including the gram-positive species *S. aureus* and *E. faecium,* than any selected or variant peptide from the library. Even in the presence of 20% human serum and 20% serum + 20% human RBCs, the activity of D-CONGA was not strongly affected. D-CONGA also caused very low hemolysis of 2% (figure 2-6).

Assessment of resistance pattern of the evolved peptides

We tested the higher-performing peptides in a *P. aeruginosa* model of stable antibiotic resistance. *P. aeruginosa* is known to be either inherently resistant or prone to induce rapid resistance to many conventional antibiotics. There are also instances of *P.aeruginosa* developing resistance to AMPs by altering the LPS in its outer membrane. For this reason, we chose *P. aeruginosa* to test whether our best peptides from the screen, DBS1, and D-CONGA, could induce resistance. We also performed the experiments with the parent peptide, ARVA, and four conventional antibiotics to compare the resistance pattern. We grew bacteria in serial dilutions of antibiotic and selected the bacteria that grew at the highest concentration of antibiotic to be re-cultured overnight in the absence of

antibiotic. Each passage was again treated with a concentration series of antibiotics, and the process was repeated for ten passages. Two of the four conventional antibiotics tested, streptomycin and ceftazidime, developed resistance by the eighth passage. The remaining two conventional antibiotics, ciprofloxacin, and gentamycin showed a gradual, steady increase in MICs with each passage and were approaching resistance at the tenth passage. L-ARVA was resistant to *P. aeruginosa* in a single passage, while D-ARVA developed resistance by the fourth passage. However, L- and D- forms of DBS1 and D-CONGA had consistent MICs against *P. aeruginosa* over ten passages and no measurable increase in resistance (figure 2-7). After the tenth passage, *P. aeruginosa* treated with streptomycin and ceftazidime was tested for resistance against DBS1 and D-CONGA. The resistant pathogen was still susceptible to both the antimicrobial peptides. *P. aeruginosa* treated with D-CONGA failed to develop resistance against L- and D- DBS1 but curiously was resistant to D-ARVA.

Evaluation of the antibiofilm activity of D-CONGA

Three of the lead peptides selected from the screen, D-CON, DBS1, and D-CONGA, were also tested for activity against biofilms formed by gram-negative *P. aeruginosa*. D-CONGA alone was tested against biofilms from gram-positive *Streptococcus mutans (S. mutans)*. We designed a stringent assay in which *P. aeruginosa* biofilm was treated with the AMPs or conventional antibiotics. Following the treatment, the remaining bacterial colony-forming units was assessed. The conventional antibiotics had little effect on the biofilm, even in higher concentrations. On the other hand, the lead peptides D-DBS1 and D-CONGA reduced viable CFUs throughout the biofilm. In fact, D-CONGA was able to sterilize 99% of biofilm cells at a concentration as low as ∼12.5 μM

(figure 2-8). Next, we tested the effects of D-CONGA against robust biofilms formed by the gram-positive bacterium *S. mutans*. This experiment was done on a glass slide, and the impact was assessed by confocal imaging of dead/live cells on the biofilm surface after peptide or vehicle treatment. D-CONGA treatment of stable *S. mutans* biofilms on glass slides resulted in a rapid and almost complete killing of biofilm organisms. Again, the antibiofilm effect of D-CONGA was very robust even in 12.5 µM, which was the lowest concentration tested (figure 2-9).

Comparison of D-CONGA to SAAP 148

We also compared the hemolysis and bactericidal activity of the evolved peptides with SAAP-148 or P148, which, at the time, was the lead product of Madam Therapeutics (Woerdense Verlaat, Netherlands), and was anticipated to enter clinical trials in humans in 2018. The peptide was proposed as an antibiotic against atopic dermatitis, burn infections, MRSA infections, and wound infections[141]. SAAP 148 is a synthetic derivative of LL-37, a natural human AMP that plays a vital role in the defense against local and systemic infections. LL-37 has antimicrobial activity against gram-negative and gram-positive bacteria. Prior to SAAP 148, Breij et al. synthesized OP-145 that contained the antimicrobial region of LL-37. OP-145, when incorporated in a biodegradable bone implant coating, successfully prevented bacterial colonization of the implant and implant-associated osteomyelitis in rabbits[142]. However, like our peptides selected from the first-generation library, potent OP-145 lost its antimicrobial activity in the presence of biological fluids. Hence, Breij et al. synthesized a set of LL-37 inspired peptides hoping that some of these synthetic peptides will have improved antimicrobial and antibiofilm activities under physiological conditions. These peptides were named SAAPs. After the

characterization of the peptides, SAAP-148 emerged as a potent antibiotic against multidrug-resistant pathogens. Breij et al. describe that SAAP-148 is able to sterilize ESKAPE pathogens at concentrations of 0.4 to 12.8 μM in PBS only and in PBS with 50% plasma. The activity of SAAP-148 was two to eightfold lower in plasma than in PBS. SAAP-148 also did not induce resistance to *S. aureus* and *A.baumannii* up to the twentieth generations. In comparison, conventional antibiotic rifampicin showed a rapid four-fold increase in MICs after eight passages and > 4096 fold increase after fifteen passages against *S.aureus*. Similarly, the MIC for ciprofloxacin against *A. baumannii* started increasing after five passages and was approaching resistance with 128-fold higher MIC by the nineteenth passage. SAAP was also able to degrade biofilms made by gram-positive *S. aureus* and gram-negative *A. baumannii* at concentrations as low as 12.8 μM[143].

We assessed the hemolysis and antimicrobial activity of SAAP-148. The MICs for SAAP-148 against all the ESKAPE pathogens were measured by the broth dilution assay optimized in our laboratory. The peptides were preincubated with RBCs prior to the addition of bacteria. The mixture was then incubated overnight. The bactericidal activity of the peptide was recorded the next day through an absorbance reading at 600 nm. The lowest concentration that sterilized 100% of bacteria was accepted as the MIC for the peptide. As mentioned earlier, this assay is different from what is common in literature and is more stringent. The study that described the antimicrobial activity of SAAP-148 adopted a different technique to measure the MIC. They used plasma as their model for eukaryotic cells. Peptides were not allowed to preincubate with plasma prior to the addition of bacteria. The final mixture was only incubated for 2 hours, and the bactericidal activity was expressed as $LC_{99.9}$, that is, the lowest peptide concentration that killed ≥99.9% of

bacterial cells. Hence, the antimicrobial activity was not based on complete sterilization. With our broth dilution assay, SAAP-148 has excellent activity against some of the ESKAPE pathogens in the absence of RBCs. It sterilized *E. coli, K.pneumoniae, A. baumannii, S. enterica,* and E. *faecium* in concentrations from 0.6 to 8.03 μM. However, even in the absence of RBCs, SAAP-148 showed no inhibitory activity against *S.aureus* and *P.aeruginosa* in our assay. The bactericidal activity of SAAP-148 was much lower in the presence of 20% RBCs. Preincubated in RBCs, SAAP-148 lost its activity against all the ESKAPE pathogens except *A. baumannii*. Even against *A. baumannii*, SAAP-148 had a higher MIC of 13.3 μM (figure 2-10). One explanation for the loss of activity of SAAP-148 in the presence of RBCs could be the release of proteases from the cytosol of the blood cells. SAAP-148, in our assay, was extremely hemolytic. Compared to the 2% of hemolysis that D-CONGA has, SAAP-148 caused almost 40-fold higher hemolysis of 78% (figure 2-10). As mentioned earlier, hemolysis releases proteases from the cytosol of RBCs. Since SAAP-148 is synthesized with all L-amino acids, it is susceptible to degradation through proteolysis. SAAP-148 may also lose activity due to host cell binding, as its high hemolytic activity indicates strong RBC binding. Compared to SAAP-148, which is similar to other AMPs that have been studied in clinical trials, our evolved peptides, especially D-DBS1, D-DBS4, and D-CONGA, are much less hemolytic and much more active against ESKAPE pathogens in the presence and absence of RBCs.

Discussion

Antibiotics are highly successful drugs that have transformed medicine and saved millions of lives. However, antimicrobial resistance continues to increase. In contrast, the rate of discovery of novel antimicrobial drug candidates is dwindling. Species of particular

concern are the ESKAPE pathogens, which are especially relevant to nosocomial infection. In this regard, membrane permeabilizing AMPs are a promising class of bioactive compounds that have attracted much research interest in recent years. Thousands of AMPs are described in the literature that show great potential *in vitro*. However, due to various difficulties in designing and screening for peptides without impediments to function *in vivo*, very few AMPs have reached late-stage clinical trials. Among these, there are only three AMPs that have been approved by the FDA. Polymyxin B and E are two complex, cyclic lipopeptides used as last resort drugs against gram-negative bacteria. Daptomycin is also a lipopeptide that has potency against gram-positive bacterial strains. These AMPs interact with the lipid bilayer of bacteria. While this mode of action is very effective, it provides opportunities for the development of resistance. Fortunately, AMPs are very diverse in sequence as well as structure. The AMPs we have identified and characterized in this chapter are cationic. Most cationic AMPs interact with anionic bacterial cytoplasmic membrane to exert their effects. It is very costly for bacteria to modify the entire plasma membrane. Therefore, cationic peptides are less likely to induce resistance.

While there are only three AMPs that have been able to transition from laboratory to clinical use successfully, there have been a lot more AMPs that have reached the late-stage clinical trials and hundred that show great potential in the laboratory. Rejection at a late stage is a common outcome for all classes of drugs. Hence, the failure of AMP clinical trials itself is not of great concern for the field. The greater obstacle is the fact that many AMPs do not advance beyond the laboratory. For more AMPs to be approved for therapeutic use, an even greater number of them need to transition from laboratory research to clinical trials. To fill up the discovery pipeline with novel AMPs, it is paramount to

recognize the impediments leading to their failure. This chapter describes an approach that allows for the design and screen of peptide library in conditions that down selects for the AMPs without the impediments. Synthetic molecular evolution (SME) can be used to identify host-compatible peptides. We successfully identified short linear peptides that work *in vitro* in the presence of red blood cells and serum. Our evolved peptides from the screening of the second-generation library are highly effective against multi-drug resistant ESKAPE pathogens under all conditions studied. These peptides, their next-generation derivative, or other peptides discovered through SME are bound to have greater success clinically. We have also demonstrated that D-CONGA and other identified peptides from this work are superior to SAAP-148, an AMP in a preclinical stage of development.

Moreover, the evolved peptides we describe here do not induce resistance in *P. aeruginosa* under conditions that cause resistance in conventional antibiotics and other AMPs such as our second-generation template peptide, D-ARVA. The primary mechanism by which *P.aeruginosa* develops resistance to the AMPs is through the addition of cationic groups on its LPS, via aminorabinosylation of lipid A. This increase in positive charge on the outer membrane decreases its interaction with AMPs, therefore, inhibiting the membrane permeabilization. Like many AMPs, D-ARVA functions by massive accumulation on LPS as part of its mechanism. The lack of development of resistance in D-DBS and D-CONGA peptides suggests a serendipitous gain of function in the evolved peptides that was not part of the screening and selection process. This indicates that the D-DBS and D-CONGA peptides do not have to accumulate via electrostatic interaction on LPS to permeabilize the gram-negative outer membrane. Perhaps, these peptides can translocate or pass through porins to access the inner membrane directly.

One of the surprising observations from the characterization of the selected peptides is the stark differences in activities of the closely related peptides. The nine selected peptides and the variants all share many similarities in their sequences, as described in the results. For example, the DRD and DBS peptides are very alike, yet their activities *in vitro* are very different. Similarly, the DBS1 and CON sequence are very alike, with only two conservative substitutions in the hydrophobic central core. Comparing the activity of D-forms of the two peptides shows that this small difference leads to complete loss of function against gram-positive bacteria in D-CON peptide. On the other hand, the removal of terminal glycines in D-DBS1 decreased the activity of the resultant peptide. Still, removing the invariant glycines from D-CON created D-CONGA, the most effective peptide overall with the best activity against every organism. This type of results is only possible through our approach of SME. The trial and errors and other QSAR rules would not have predicted this difference.

Previously, molecular optimization of new AMPs was performed by trial and error, which was sometimes guided by machine learning algorithms. Solubility, toxicity, host-cell inhibition, and proteolytic degradation was tested under standard laboratory conditions after the peptides were synthesized. However, at this point of testing, the feedback is less effective. Our approach of screening for the peptides under stringent conditions allows for early down selection for the characteristics we desire in the peptides. Here, we have shown the selected peptides screened against gram-negative bacteria in the presence of RBCs have host-cell compatibility and negligible hemolysis. We then further optimized the selected peptides through rational variation. Characterization of the variants finally led to the discovery of the best peptide from this screen, D-CONGA.

Figure 2-1
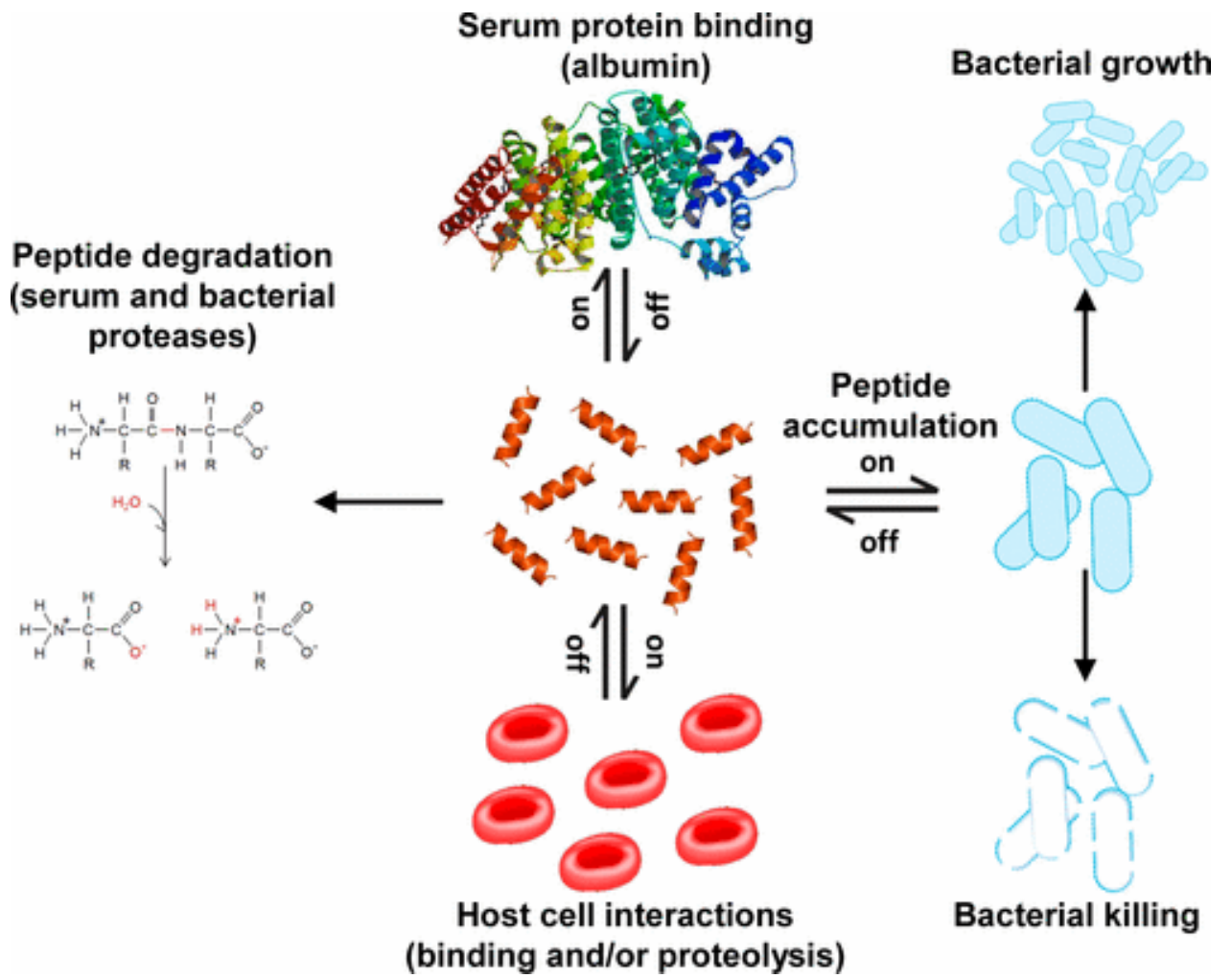
Figure 2-1. Kinetic network model representing the impediments that inhibit the activity of antimicrobial peptides (AMP) *in vivo*. The peptides function by accumulation on the surface of the bacterial cells. This required action for the peptide function may be considered as a portion of a network of kinetic steps that include on and off rates for several binding phenomena and irreversible steps such as proteolytic degradation and bacterial growth.

This image was originally published by Starr et al[144].

Figure 2-2

"ARVA" template sequence

R	R	G	W	A	L	R	L	V	L	A	Y

ARVA-based iterative combinatorial library

1	2	3	4	5	6	7	8	9	10	11	12	13
RR R DD D X	G	W	A	L F A R	R A	L P G R	V F A	L F A S	A	Y S F	G	RR R DD D X

Nonpolar = Black
Aromatic = Green
Polar = Orange
Cationic = Blue
Anionic = Red

Unvaried Residue

Residue Variations

Terminal Cassette

8 Combinatorial Sites and 28,800 Unique Members

60
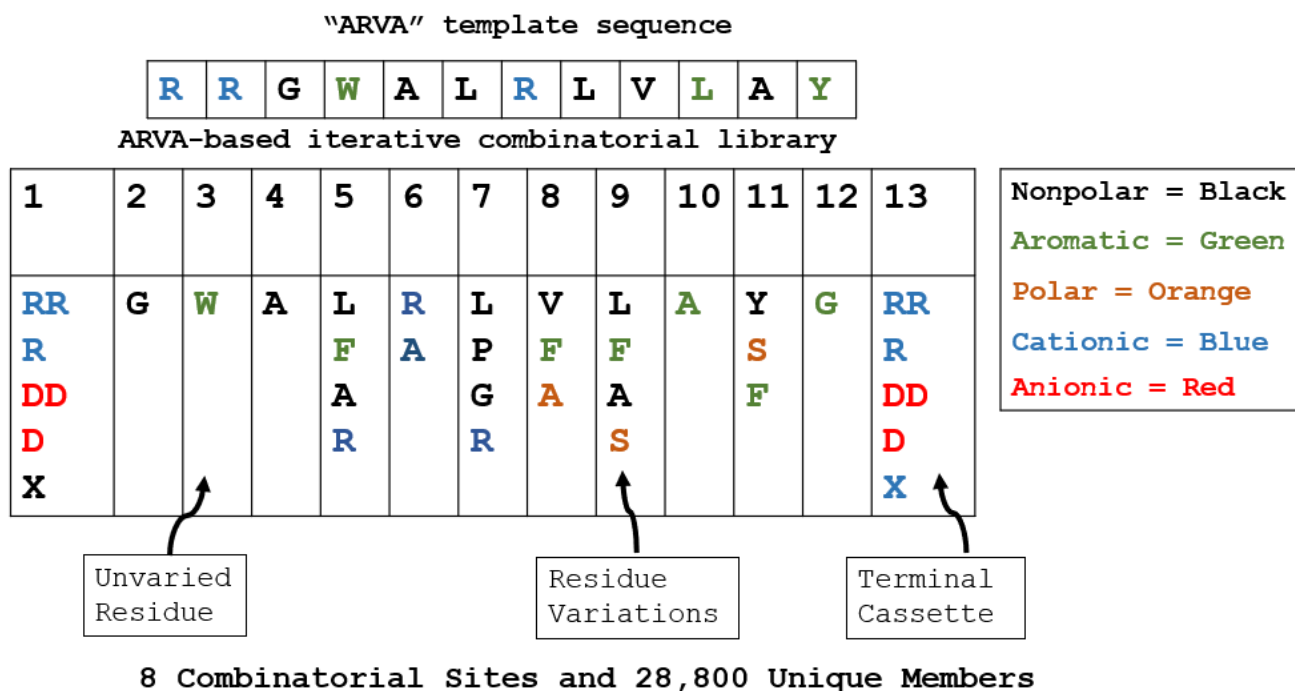
Figure 2-2. Second-generation library design. The 2 to 5 residues listed vertically under each position, and the native residue, are all equally probable. Acidic or basic terminal groups are cassettes of 0, 1, or 2 residues. The difference in the type of residues is denoted by colors as described in the right of the figure.

Figure 2-3

A)

DRD1: RRGWALRPVLAFGRR DRD2: RRGWARRLAAAYGRR	Screen 1: Double Radial Diffusion
RDBS1: RRGWAFRRALAYGRR RDBS2: RRGWARAPAFAFGRR	Screen 2 :Mixed Radial Diffusion + Broth + hemolysis

B)

MC in Broth Dilution (μM)															
Peptide	**EC**		**PA**		**KP**		**AB**		**SE**		**EF**		**SA**		**#<10 μM**
RBC	-	+	-	+	-	+	-	+	-	+	-	+	-	+	**(*+RBC)**
L-ARVA	1.7	22.9	26.0	>30	2.0	29.1	5.4	>30	9.9	>30	3.1	14.3	3.6	>30	6/7
D-ARVA	3.0	19.6	>30	>30	1.4	8.6	7.5	>30	6.6	>30	2.2	14.3	1.3	20.0	1/7*
Sequences Discovered by Double Radial Diffusion (DRD)															
DRD1	>30	>30	14.8	>30	>30	>30	>30	>30	>30	>30	nd	nd	>30	>30	0/6
D-DRD1	7.8	5.5	22.9	16.3	24.5	22.9	>30	>30	12.5	13.3	nd	nd	>30	>30	1/6*
DRD2	18.1	>30	5.1	27.1	>30	>30	25.4	>30	>30	>30	nd	nd	>30	>30	1/6
D-DRD2	8.3	6.3	12.5	12.5	11.6	18.7	>30	>30	13.3	22.9	nd	nd	>30	>30	1/6*
Sequences Discovered by Radial Diffusion + Broth Sterilization (RDBS)=															
RDBS1	22.2	>30	>30	>30	>30	>30	>30	>30	14.8	>30	nd	nd	>30	>30	0/6
D-RDBS1	2.7	2.6	>30	>30	14.8	14.8	>30	>30	5.2	5.2	nd	nd	>30	>30	2/6*
D-RDBS2	8.9	11.6	>30	>30	>30	>30	>30	>30	>30	>30	nd	nd	>30	>30	1/6*

Figure 2-3. High-throughput screening for selection of potent AMPs using DRD and RDBS approaches. A) Sequences of the four peptides selected from two different screen approach. DRD1 and DRD2 were selected from double radial diffusion assay, and RDBS1 and RDBS2 were selected from the mixed radial diffusion and broth dilution assay. **B)** Assessment of antibacterial activity of peptides selected with the first two approaches. MIC values are reported in micromolar peptide concentrations against a panel of ESKAPE bacterial pathogens. The two columns under each organism are for assays performed in the absence (−) and presence (+) of 1 X 10^9 human RBC/mL yellow: MIC ≤ 10 μM; gray: MIC ≥ 25 μM. ">30" means that sterilization was not observed at 30 μM, the highest concentration tested. Values in blue text are for D-amino acid peptides. The column marked "#≤10 μM" is a count of the number of organisms, out of seven, with MIC ≤ 10 μM. Counts are in the absence of RBC for L-amino acid peptides and in the presence of RBCs for D-amino acid peptides.

Figure 2-4

A)

DBS1:	RRGWARRLFFAYGRR
DBS2:	RRGWAARLFAAFGRR
DBS3:	RRGWARRLFAAFGRR
DBS4:	RRGWARRLVFAFGRR
DBS5:	RRGWARALAFAFGR

SCREEN 3: Double Broth Sterilization + Hemolysis

B)

	MC in Broth Dilution (µM)														
Peptide	**EC**		**PA**		**KP**		**AB**		**SE**		**EF**		**SA**		**#<10 µM**
RBC	–	+	–	+	–	+	–	+	–	+	–	+	–	+	**(*+RBC)**
Sequences Discovered by Double Broth Sterilization (DBS)															
DBS1	7.3	>30	4.0	19.2	5.4	8.6	1.7	1.5	1.5	2.2	nd	nd	>30	>30	5/6
D-DBS1	1.6	1.1	1.8	4.6	5.4	6.6	1.4	1.5	1.3	1.8	1.3	5.2	9.6	9.3	7/7*
DBS2	5.7	26.6	3.4	27.1	>30	>30	5.0	>30	7.0	>30	nd	nd	>30	>30	4/6
D-DBS2	4.5	5.2	6.8	11.6	>30	>30	5.9	7.8	3.0	8.3	2.6	9.8	28.0	28.0	3/7*
DBS3	11.5	>30	2.3	20.0	>30	>30	5.4	>30	10.6	>30	nd	nd	>30	>30	2/6
D-DBS3	3.8	4.5	4.9	7.8	>30	>30	7.0	8.9	3.5	7.3	16	19	>30	>30	4/7*
DBS4	15.1	26.6	3.6	19.0	>30	>30	5.4	>30	4.1	>30	nd	nd	>30	>30	2/6
D-DBS4	1.3	1.4	2.2	5.2	5.5	10.2	2.3	4.8	1.5	2.8	1.3	3.6	4.0	4.5	7/7*
DBS5	6.6	15.5	3.8	22.1	14.8	>30	2.6	>30	7.0	>30	nd	nd	>30	>30	4/6
D-DBS5	3.4	13.3	4.6	8.9	8.5	12.5	3.5	7.3	10.9	14.3	>30	>30	>30	>30	2/7*

64

Figure 2-4. High-throughput screening for selection of potent AMPs using DBS approach. A) Sequences of the five peptides, DBS1, DBS2, DBS3, DBS4, and DBS5 selected from the double broth sterilization approach of the library screen. **B)** Assessment of antibacterial activity of peptides selected from double broth sterilization approach. MIC values are reported in micromolar peptide concentration against a panel of ESKAPE bacterial pathogens. Definitions and the color codes are identical to those in **2-3 B**.

Figure 2-5

A)

DBS1-G	RRWARRLFFAYRR	DBS1 minus glycines
Con	RRGWARRLAFAFGRR	Consensus sequence
D-Con	rrGwarrlafafGrr	D-aa Consensus
Con+LR	RRGWARRLLRAFAFGRR	Consensus with added LR
Con+AF	RRGWARRLAFAFAFGRR	Consensus increased hydrophobicity
Con-AF	RRGWARRLAFGRR	Consensus decreased hydrophobicity
Con RtoK	KKGWAKKLAFAFGKK	Consensus with K instead of R
D-CONGA	rrwarrlafafrr	D-Consensus minus Glycines

B)

Analysis of Rational Variants															
Peptide	EC		PA		KP		AB		SE		EF		SA		#<10 μM
RBC	-	+	-	+	-	+	-	+	-	+	-	+	-	+	*+RBC
D-DBS1	1.6	1.1	1.8	4.6	5.4	6.6	1.4	1.5	1.3	1.8	1.3	5.2	9.7	9.3	7/7*
DBS1-G 1	5.2	>30	4.2	26	>30	>30	6.6	nd	3.1	nd	nd	nd	18.7	>30	4/6
Consensus	12.5	>30	2.8	13.3	>30	>30	13.8	22	6.6	>30	nd	nd	>30	>30	2/6
D-Con	1.6	1.3	4.5	6.8	14.8	9.9	7.5	8.6	1.6	2.0	nd	nd	26.3	28.3	5/6*
Con+LR	7.8	>30	2.0	7.8	>30	nd	2.7	nd	2.9	nd	nd	nd	>30	>30	4/6
Con+AF	5.5	28.0	2.5	5.2	2.6	nd	6.2	nd	1.5	nd	nd	nd	26.3	>30	5/6
Con-AF	>30	>30	>30	>30	>30	nd	>30	nd	>30	nd	nd	nd	>30	>30	0/6
D-Con RtoK	7.3	8.9	20.7	23.7	>30	>30	>30	>30	22.2	nd	nd	nd	>30	>30	1/6
D-CONGA	1.0	0.7	1.9	2.8	4.4	3.8	4.4	4.4	1.3	2.0	2.3	4.1	5.7	7.0	7/7*
D-CONGA + 20% serum	2.8	6.4											14.8	10.9	

Figure 2-5. Rational Variants of the selected peptides. A) Sequences of the rational variants of DBS peptides that were tested and the rational for each variant. **B)** Assessment of antibacterial activity of rational variants of peptides selected from the screen of the second-generation AMP library. MIC values are reported in micromolar peptide concentrations against a panel of ESKAPE bacterial pathogens. Definitions and the color codes are identical to those in **2-3 B** and **2-4 B**.

Figure 2-6

MC in Broth Dilution (µM)	
Peptide **RBC**	**Hemolysis (100 µM)**
L-ARVA	0.19
D-ARVA	0.25
Sequences Discovered by Double Radial Diffusion (DRD)	
DRD1	0.01
D-DRD1	0.01
DRD2	0.02
D-DRD2	0.02
Sequences Discovered by Radial Diffusion + Broth Sterilization (RDBS)	
RDBS1	0.01
D-RDBS1	0.01
D-RDBS2	0.01

MC in Broth Dilution (µM)	
Peptide **RBC**	**Hemolysis (100 µM)**
Sequences Discovered by Double Broth Sterilization (DBS)	
DBS1	0.04
D-DBS1	0.05
DBS2	0.08
D-DBS2	0.08
DBS3	0.03
D-DBS3	0.04
DBS4	0.03
D-DBS4	0.02
DBS5	0.08
D-DBS5	0.06

Analysis of Rational Variants	
Peptide **RBC**	**Hemolysis (100 µM)**
DBS1-G	0.10
Consensus	0.09
D-Con	0.09
Con+LR	0.15
Con+AF	0.37
Con-AF	0.03
D-Con RtoK	0.02
D-CONGA	0.02

Figure 2-6. Hemolysis data for all the selected peptides and rational variants. The cytotoxic effects of the selected peptides and the rational variants on red blood cells are represented by fractional hemolysis of 1 X 10^8 human RBCs/ml at 100 µM peptide. Yellow indicates ≤5% hemolysis.

Figure 2-7
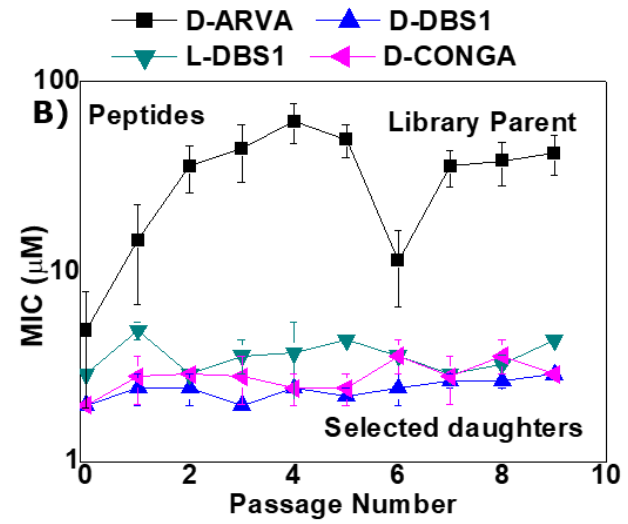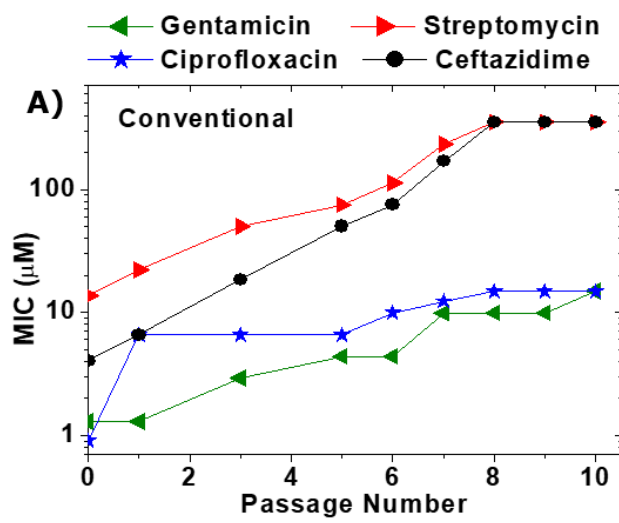
Figure 2-7. Selection for resistance. A culture of *P. aeruginosa* in log phase growth in TSB media was treated with serial dilutions of **A)** four conventional antibiotics and **B)** four antimicrobial peptides**.** The bacteria that grew in the highest concentration of antibiotic were cultured overnight in the absence of antibiotic and then treated similarly next day. This was continued for 10 passages to select for stable resistance mutants. MICs for each passage are shown in A and B. The highest concentrations tested were 350 μM for conventional antibiotics and 67.5 μM for AMPs.

Figure 2-8
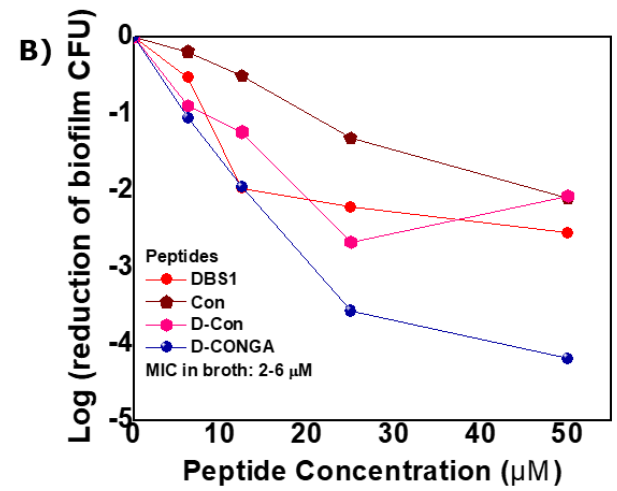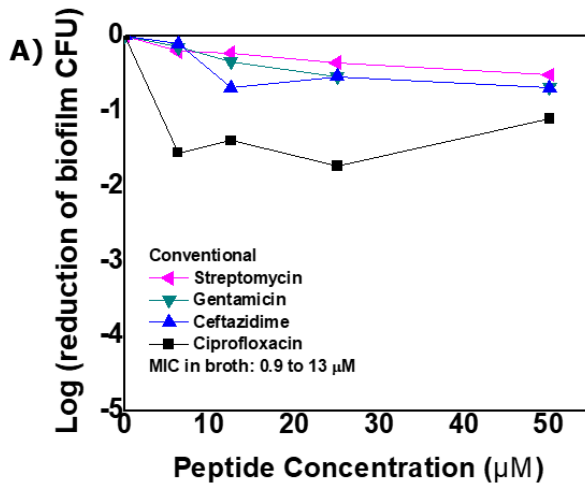
Figure 2-8. Activity against bacterial biofilms made by *P.aeruginosa*.

P. aeruginosa were grown for two days to form biofilms, washed extensively to remove loosely adhered bacteria, and treated with **A)** four conventional antibiotics or **B)** four higher performing antimicrobial peptides. After treatment, the biofilms were scraped and homogenized. Counting of viable colony forming units was done by serial dilution and plating on nutrient agar.

Figure 2-9

Streptococcus mutans

A)

0   12.5   25   50

D-CONGA concentration (μM)

B)
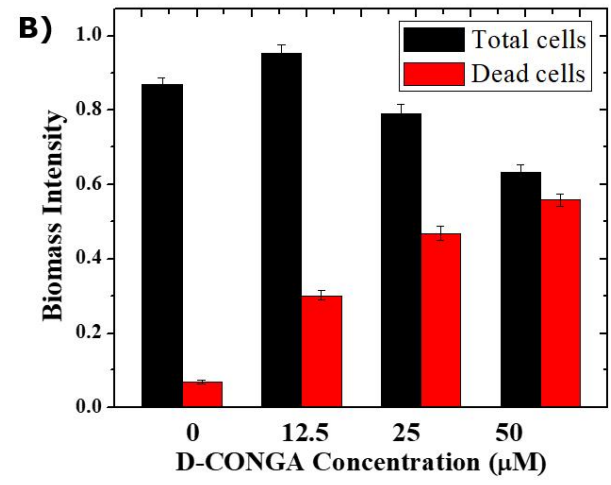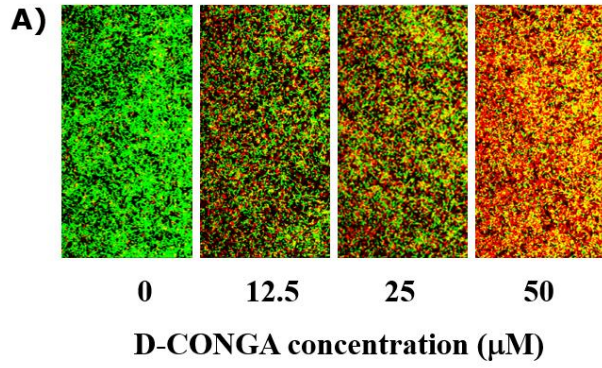
Figure 2-9. Activity against bacterial biofilms made by *S. mutans*. A) Robust biofilms formed by *S. mutans* were treated with increasing concentrations of D-CONGA and imaged by confocal microscopy in the presence of Syto9 (green), which stains all cells, and propidium iodide (red), which stains only dead cells. **B)** Quantitation of total biomass (total cell count) and dead cell counts was done as described elsewhere.

Figure 2-10

MIC in Broth Dilution (μM)															
Peptide	EC		PA		KP		AB		SE		EF		SA		#<10 μM	Hemolysis
RBC	-	+	-	+	-	+	-	+	-	+	-	+	-	+	(*+RBC)	at 100 μM
D-DBS1	1.6	1.1	1.8	4.6	5.4	6.6	1.4	1.5	1.3	1.8	1.3	5.2	9.6	9.3	7/7*	0.05
D-DBS4	1.3	1.4	2.2	5.2	5.5	10.2	2.3	4.8	1.5	2.8	1.3	3.6	4.0	4.5	7/7*	0.02
D-CONGA	1.0	0.7	1.9	2.8	4.4	3.8	4.4	4.4	1.3	2.0	2.3	4.1	5.7	7.0	7/7*	0.02
SAAP-148	0.6	>30	>30	>30	1.6	>30	6.55	13.33	8.03	>30	1.9	>30	>30	>30	5/7	0.78

Figure 2-10. Comparison of bactericidal characteristics of evolved peptides to SAAP-148, against ESKAPE pathogens. The MIC values for each antimicrobial peptide are reported in micromolar concentrations. Definitions and the color codes are identical to those in **2-3 B)** and **2-4 B**), and **2-5 B)**. The column marked "hemolysis" is the fractional hemolysis of 1×10^8 human RBC/mL at 100 μM peptide. Yellow indicates ≤5% hemolysis.

CHAPTER 3: Evaluation of cytotoxicity of selected antimicrobial peptides (AMPs) in mammalian cells and assessment of their suitability for therapeutic use against multi-drug resistant bacterial infections using a murine wound infection model.

Introduction

In chapter 2, we demonstrated that synthetic molecular evolution (SME) can be implemented successfully in the synthesis and screening process of a peptide library to identify host cell-compatible antimicrobial peptides (AMPs). Host cell-compatible peptides refer to those AMPs that selectively inhibit and kill bacteria while maintaining very low mammalian cytotoxicity. This selectivity of AMPs for bacteria is attributed to the differences in prokaryotic and eukaryotic cell membranes. Bacterial membranes are negatively charged, while mammalian cell membranes are mostly neutral. Cationic AMPs, therefore, are expected to preferentially bind to anionic bacteria over mammalian cells. The cholesterol present only in the mammalian cells is also suggested to contribute to the selectivity of AMPs for bacteria[1–4].

We use red blood cells (RBCs) as the model eukaryotic cells. The human red blood cells (RBCs) that we use do not contain nuclei or internal membranes. While we selected the peptides for their low toxicity against RBCs, we do not know how they interact with nucleated mammalian cells. RBCs represent a source from which pure plasma membrane can be isolated for further biochemical analysis. They are used extensively for the study of membrane structure. In 1925, two Dutch scientists, E. Goerter and R. Grendel, extracted membrane lipids from RBCs and provided the first evidence that biological membrane consists of lipid bilayers[5,6]. Nucleated mammalian cells differ from red blood cells on the membrane lipid composition. In fact, in contrast to

red blood cells, nucleated cells of the same type can have differing lipids and proteins on their membrane as they organize into tissues. For example, epithelial cells are polarized when organized into tissues, with different cells responsible for performing distinct functions. The epithelial cells in the intestine, for instance, are divided into the apical surface, which faces the intestinal lumen that absorbs nutrients, and the basolateral surface, which faces underlying connective tissue involved in blood supply. The membrane composition of these cells varies based on their position and function. Therefore, it is critical to assess the interaction of these AMPs with nucleated cells to more comprehensively evaluate their selective toxicity before we consider their appropriateness for application to infection sites[6,7].

In this chapter, we will compare the cytotoxicity of parent peptide, ARVA, with the selected peptides and their rational variants from the screening of the second-generation library. We used two different methods to measure the cytotoxicity of these peptides against HeLa cells. SYTOX Green nucleic acid stain is an excellent green-fluorescent nuclear and chromosome counterstain impermeant to live cells. Membrane integrity has long been used as a criterion for the definition of cell viability. Therefore, the entrance of SYTOX Green into the cells signifies dead cells. The cytotoxicity of the AMPs against HeLa cells was measured based on the fractional entry of SYTOX Green into the cells treated with peptides. The fluorescent signal from cells treated with MelP5, an extremely lytic peptide, represented 100% SYTOX entry or cell death. SYTOX Green entry into the cells treated with AMPs compared to the cells treated with MelP5 allowed for the calculation of cytotoxicity for each peptide. We also used Alamar Blue cell viability assay to measure the percentage of live cells after the incubation with AMPs.

Alamar Blue functions as a cell health indicator by using the reducing power of living cell mitochondria to measure viability quantitatively. Resazurin, the active ingredient of the Alamar Blue reagent, is a non-toxic, cell-permeable compound that is blue and non-fluorescent. However, upon entering living cells, resazurin is reduced to resorufin, a compound that is red in color and highly fluorescent. Again, MelP5 was used to obtain 100% cell death. The percentage of viable cells after treatment with each AMP was calculated by normalizing the fluorescent signal of cells treated with AMPs to those treated with MelP5.

The assays were performed in two different conditions. Cytotoxicity of peptides against HeLa cells was measured in serum-free Dulbecco's modified eagle's medium (DMEM) and a more relevant, complete medium. Complete medium is DMEM substituted with 10% fetal bovine serum (FBS) as a nutrient source, required for the healthy growth of mammalian cells. EC_{50} was calculated for each AMP. An EC_{50} is a statistical estimate of the concentration of a toxicant, in this case, AMP, in the ambient medium necessary to produce a particular effect in 50% of a large population[8]. For our experiments, EC_{50} is the concentration of AMP that causes 50% of SYTOX Green entry into the cells or causes 50% of cell death as represented by a lower reduction of resazurin in Alamar Blue assay. We considered that our AMPs are membrane permeabilizing antibiotics, and SYTOX Green is impermeant to cells unless the cellular membrane is compromised. The fractional entry of SYTOX Green allows us to quantify the real-time membrane permeabilization activity of AMPs. In contrast, the metabolic reduction of resazurin to resorufin in Alamar Blue assay enables us to measure live/dead cells without considering the membrane disruption caused by the AMPs. Furthermore, Alamar Blue

has also displayed interaction with cell culture media and serum. This can affect the signal produced during the assay and the interpretation of cytotoxicity data [9,10]. We also concluded that the presence of serum in media better mimics the *in vivo* conditions of the mammalian cells where they are healthy and growing. Hence, after analyzing the differences in EC_{50} in different assays and media, we concluded that SYTOX Green assay in the media with 10% FBS is the best technique to measure the cytotoxicity of our AMPs. We have used this method for all further experiments to calculate peptide cytotoxicity.

Cancer cell surfaces are different than non-cancer cells. One of the major differences is the exposure of negatively charged lipid phosphatidylserine (PS) on the outer leaflet of the cancer cell membrane, which in non-cancer cells exhibits an overall neutral charge[11,12]. Another factor that contributes to the increase in anionic groups on the membrane of cancer cells is the over-expression of sialic acid residues, which are linked to glycoproteins (e.g., mucins) and glycolipids. Increased sialylation has been reported on cancer cells from epithelia, breast, ovaries, lung, colon, and pancreas[11,13–15]. The selected AMPs were screened in the presence of RBCs to be host cell-compatible with selectivity for bacterial cells. The higher cytotoxicity of AMPs against HeLa, an immortal cancer cell line, can be attributed to the anionic cell membrane, which is similar to bacteria than normal human cells. Therefore, we performed the SYTOX Green assay using the D-DBS peptides and D-CONGA in WI-38, a normal diploid human cell line composed of fibroblasts derived from lung tissue. True to our hypothesis, the tested AMPs had much higher EC_{50} against WI-38 than HeLa cells.

Next, we assessed the efficacy of our lead candidate, D-CONGA, in a mouse

model of skin and soft tissue infections (SSTIs). SSTIs are one of the leading causes of

hospital-acquired infections. They occur especially on wounds, burns, surgical sites,

chronic skin ulcers, and medical devices such as catheters[16,17]. Globally, methicillin-

resistant *Staphylococcus aureus* (MRSA) and multidrug-resistant *Pseudomonas*

aeruginosa are two major opportunistic pathogens that cause community-acquired and

nosocomial infections. They are the most prevalent pathogens isolated from the

structurally abnormal airways, such as those in cystic fibrosis and other chronic lung

diseases[18,19]. They are also rampant in chronic wound infections and in SSTIs frequently

associated with immune-compromised individuals like on the foot ulcers of a diabetic

person or in the ears of patients with chronic suppurative otitis media[20–22]. They also

cause biofilm-infected infections, which are even harder to treat in the current antibiotic

resistance crisis[20,23–25]. MRSA was responsible for estimated 323,000 infections in

hospital patients and 10,600 deaths in 2017 in the United States[26]. In the same year,

multidrug-resistant *Pseudomonas aeruginosa* caused an estimated 32,600 infections

among hospitalized patients and 2,700 estimated deaths[26].

Currently, the most practiced procedure for SSTIs treatment is systemic antibiotic

therapy[27]. Long-term systemic antibiotic therapy is associated with increased

development of drug resistance and side effects[28,29]. Moreover, systemic therapy for

SSTIs is not always effective. Antibiotics, when used systemically, need blood vessels

for transfer to infection sites. Most SSTIs, such as burn wounds, do not have functional

blood vessels[27]. A potential alternative to systemic therapy could be topical antibiotics,

which can be directly applied to the wound bed in high concentrations, bypassing the

need for an intact local circulatory system. The use of antibiotics topically reduces the

potential for systemic toxicity, limits the exposure of the drug to normal flora, and

permits the use of drugs that cannot be used systemically[30–32]. Therefore, we decided to

use the topical application technique on an established splinted full thickness excisional

wound infection model to assess the efficacy of our lead candidate, D-CONGA, against

MRSA and *P.aeruginosa*[33–35]. There is a wide array of wound infection models in mice,

such as tape strip model, incisional wound model, burn wound model, and wound models

that use biopsy punch. All of these models have advantages of their own. However, while

most of these models are useful in quantifying the infection via measurement of bacterial

burden, very few allow evaluation of the efficacy of a topical treatment and the

estimation of wound healing[36–39]. Higher phylogeny mammals, including humans, heal

predominately via re-epithelization and granulation tissue formation while the murine

wound heals primarily through contraction[40]. The wound model we are using integrates a

wound splint by use of sutured silicone ring. The silicone ring prevents contraction and

mimics human wound healing by forcing re-epithelialization and formation of

granulation tissue[33,41]. This splinted wound model has been used previously for studies

involving wound regeneration and repair[42]. In recent years, it has also been used to study

the effects of antimicrobial treatments on the pathophysiology of infection and the wound

repair process[34,43,44]. In this study, we use splinted full thickness excision wound model to

demonstrate that treatment with D-CONGA inhibits the growth of MRSA and *P.*

aeruginosa in the wound bed and inhibits biofilm formation without impairing the wound

healing process. Lastly, we also characterized the systemic effects of D-DBS4, D-DBS2,

CON, and D-CONGA in mice using intraperitoneal (i.p.) injection of peptide in

phosphate buffered saline (PBS). For D-CONGA, 1-palmitoyl-2-oleoyl-*sn*-glycerol-3-phosphoglycerol (POPG) was also used as a peptide solvent. We monitored the behavior, weight, and wound conditions of all animals through the experiment. We also used the liver from each mouse to measure the liver alanine aminotransferase (ALT) enzyme for evidence of liver toxicity. ALT activity is critical in diagnosing and assessing liver diseases and is widely used as the primary reference estimate for identifying drug-induced liver toxicity [45].

Methods and Materials

Peptides and antibiotics

Peptides were either synthesized in the lab using solid-phase peptide synthesis (SPPS) method or were obtained from Bio-Synthesis Inc. (Lewisville, Texas). The purity of each was >95% by HPLC. Unless otherwise stated, all solutions were prepared by dissolving lyophilized peptide or antibiotic powders in 0.025% v/v) acetic acid and concentrations were determined by absorbance at 280 nm.

Alamar Blue cytotoxicity assay

Hela cells were grown to confluency in T-75 flasks in complete DMEM (10% FBS). The day before cytotoxicity experiments, cells were trypsinized, removed from the flask, and pelleted at 1300 rpm. The trypsin and spent media were discarded, and the cells were resuspended in complete DMEM. The cells were then seeded at a density of 10,000 cells/well in a 96-well tissue-culture plate. The next day, after a wash with sterile PBS, cells were treated with peptides serially diluted in complete DMEM or serum-free media at a concentration of 100 μM (1st), 50 μM (2nd), which was followed by serial dilutions by a factor of 2:3 horizontally across the plate. The final volume in each well was 50 μl. The

cells were incubated with AMPs in 37 °C for an hour. 5 μl resazurin solution was added to the media in each well and mixed thoroughly. In live cells, resazurin, which is purple and non-fluorescent, is reduced to form the red fluorescent dye resorufin. The reduction of resazurin can be monitored by measuring fluorescence, and live/dead cell percentage can be assessed. After 3 hours of incubation in 37 °C, one-time resorufin fluorescence reading in an excitation wavelength of 530 nm and the emission wavelength of 590 nm was performed. Untreated cells and cells treated with highly lytic peptide, MelP5, were used as negative and positive controls to calculate the percentage of viable cells.

SYTOX Green cytotoxicity assay

HeLa cells and WI-38 cells were grown to confluency in T-75 flasks in complete DMEM (10% FBS). The day before cytotoxicity experiments, the cells were plated in a 96-well tissue-culture plate as described in the Alamar Blue cytotoxicity assay above. The next day, in a separate 96-well plate, peptides were serially diluted in complete DMEM or serum-free DMEM with 0.1% SYTOX Green starting at a concentration of 100 μM (1st), 50 μM (2nd), which was followed by serial dilutions by a factor of 2:3 horizontally across the plate. The final volume of the peptide in each well was 54 μl. To perform the cytotoxicity assay, media was removed from the wells and replaced with the peptide solutions. No peptide and 20 μM Melp5, a highly lytic peptide, were used as negative and positive controls, respectively. The plate was read for fluorescence every 5 minutes for an hour with an excitation wavelength of 504 nm and an emission wavelength of 523 nm. Cytotoxicity was calculated based on the 100% and 0% lysis controls.

Murine wound infection model

All animal studies strictly adhered to protocol 131 approved by Tulane School of Medicine's Murine Institutional Animal Care and Use Committee (IACUC). Female CD1 mice at 8-12 weeks of age were anesthetized via intraperitoneal (i.p.) injection of ketamine and xylazine at doses of 90 mg/kg and 10 mg/kg, respectively. Their dorsal surface was depilated using an electric razor and scrubbed with a chlorhexidine solution. A full thickness biopsy wound was generated using a 5 mm biopsy punch (Integra). To function as a splint for the wound, a silicone (Invitrogen) ring 0.5 mm thick with an outer diameter of 10 mm and a hole with a 5 mm diameter was placed over the wound and held to the skin with a surgical adhesive. The entire silicone ring was then covered with Tegaderm (3M), and further adhered using 4-0 braided silk interrupted sutures (Ethicon). Mice were given 0.05 mg/kg buprenorphine immediately following surgery and daily for the next two days to alleviate pain from the procedure. Wound beds were infected by penetrating the Tegaderm with an insulin syringe and injecting $1x10^4$ colony forming units (CFUs) of *P. aeruginosa* (PA01) and MRSA suspended in 10 µL sterile PBS directly onto the wound bed. All bacteria used were pelleted during the early exponential growth phase prior to infection. Four hours after infection, mice were topically treated with 2 mM D-CONGA or 0.025% acetic acid (vehicle control) in a 20µL volume by penetrating the Tegaderm with an insulin syringe and injecting the treatment directly on the wound bed. Treatment was administered every 8 hours for the first 5 days of infection. Mice were imaged daily for two weeks using the *in vivo* imaging system (IVIS)-XMRS (PerkinElmer), and bioluminescence generated from the bacteria was quantified in values of radiance (photons/sec). Weight, activity, posture, coat condition, and wound condition were monitored each day throughout the experiment to ensure the wellbeing of each mouse.

Scanning electron microscopy

Tegaderm dressings were removed from the wounds of each mice on Day 3 after surgery. Tegaderm were washed with PBS and attached to hydroxyapatite discs placed horizontally in 24-well microtiter plates. Following this, the Tegaderm was fixed by placing the discs in 200 µl of 2.5% glutaraldehyde. The fixed samples were dehydrated using increasing concentrations of ethanol and then desiccated with CO_2 critical point drying. The samples were carbon coated and subjected to scanning electron microscopy with a Hitachi S-4800 high-resolution microscope.

Assessment of systemic toxicity

Healthy adult CD1 mice, 25 to 32 g were treated twice per day with i.p. administration of 500 µl of different concentrations of D-CONGA solution or vehicle to evaluate the systemic toxicity of D-CONGA. The vehicle was PBS in most experiments. For a few samples, we used PBS containing 5 mM of 0.1 µM unilamellar lipid vesicles composed of 1-palmitoyl-2-oleoyl-*sn*-glycerol-3-phosphoglycerol (POPG) to slow the dispersal of peptide. For the same reason, we also used chondroitin sulfate and bovine albumin serum (BSA) as solvents for some D-CONGA administrations. PBS was the solvent for all other peptide injections. Mice were monitored for 1 hour after treatment, with subsequent checks performed three times daily. Weight was measured each day prior to treatment. At the study endpoint, after 5 days of treatment, mice were killed by CO_2 asphyxiation and livers were collected. Liver ALT enzyme was measured using a fluorometric kit from Abcam. Liver samples were homogenized in buffer, and the supernatant was used to measure liver ALT enzyme by fluorescence using a coupled enzyme reaction.

Fluorescence from pyruvate standards of known concentrations was used to convert fluorescence to milliunits (mU) of ALT activity.

Results

Evaluation of cytotoxicity of selected AMPs in HeLA and WI-38 cells

Our evolved AMPs exhibit bactericidal activity in the presence of concentrated human red blood cells (RBCs) at concentrations that are not hemolytic. This host-cell compatibility was obtained by screening the library in the presence of concentrated RBCs. However, to decide on the suitability of AMPs for use in mammalian systems, we need to determine the concentrations at which our AMPs are active against a broad-spectrum of pathogens without inducing cytotoxic damage to mammalian cells. In the work described here, we analyzed the toxic effects of selected and rational AMPs from the second-generation library towards two types of mammalian cells, cervical cancer epithelial cells, HeLa, and normal lung fibroblasts, WI-38.

In this chapter, we compare two cytotoxicity assays, Alamar Blue and SYTOX Green, under two conditions; in cell culture media with 10% fetal bovine serum, and in serum free media. This allowed us to compare the effects of AMPs on starved versus healthy cells and also to evaluate the impact of AMPs on HeLa cells in the presence and absence of serum. Based on these results, we used the SYTOX Green assay in complete media to test the toxicity of all AMPs studied against WI-38 cells.

For all cytotoxicity experiments, we express cytotoxicity using EC_{50}, the concentration of peptide that causes 50% of the maximum effect. The Alamar Blue assay measures cellular metabolic activity. The assay is based on the conversion of the blue non-fluorescent dye resazurin, which is converted by mitochondrial and other reductase

enzymes, to the pink, fluorescent resorufin. Resorufin can be measured fluorometrically. There is a direct correlation between resazurin reduction in the growth media and the quantity of living cells in the sample. EC_{50} in this assay refers to the concentration of AMP that causes a 50% loss in cell viability. The SYTOX Green assay measures membrane integrity, which is essential for the normal functioning of the cells. Loss of membrane integrity can be used as a criterion for defining cell viability. Cells with a compromised plasma membrane cannot maintain an electrochemical gradient or retain nutrients and are considered dead[46,47]. SYTOX Green is a membrane impermeant nucleic acid stain. It is excluded from live cells with intact plasma membrane but exhibits green fluorescence upon binding with nucleic acid in dead cells. The green fluorescence can be measured using a plate reader. EC_{50} in this assay represents the concentration of AMP that causes a loss of membrane integrity in 50% of the cell population. MelP5, a lytic peptide, was used to define 100% SYTOX Green entry and 0% resazurin reduction in SYTOX Green assay and Alamar Blue assay, respectively.

The first sets of cytotoxicity assays were performed against HeLa Cells. EC_{50} calculated using Alamar Blue assay was higher than for SYTOX Green for most of the AMPs tested (figure 3-1, 3-2, 3-3, and 3-4). Furthermore, the EC_{50} for each peptide was higher when the experiments were performed in DMEM with FBS than in serum-free media (figures 3-1, 3-2, 3-2, and 3-4). Therefore, AMPs are less cytotoxic to mammalian cells in the presence of serum. This was especially true for parent peptides D- and L-ARVA and the peptides from the first two screening approaches, D-DRD1, D-DRD2, L-RDBS1, D-RDBS1, and D-RDBS2. In fact, Alamar Blue assay in media with serum revealed no toxicity for 5 out of these 7 peptides up to 200 μM, which was the highest

concentration tested. In the same conditions, D-ARVA and D-RDBS1 showed toxicity and had a higher EC_{50} of 156 μM and 207 μM, respectively (figure 3-1). In the absence of serum, the cytotoxicity of all seven AMPs increased (figure 3-2). However, the EC_{50} was still reasonably high (figure 5). The cytotoxicity pattern was similar in SYTOX Green assay, with EC_{50} for AMPs being higher in media with serum than in serum-free media.

From the results in chapter 1, we know that the parent peptides D- and L- ARVA and the peptides from the first two screening approaches (D-DRD1, D-DRD2, L-RDBS1, D-RDBS1, and D-RDBS2), even in D form, do not possess broad-spectrum antimicrobial activity in the presence of RBCs. It was previously demonstrated that L- ARVA undergoes proteolytic degradation in the presence of RBCs and serum at a rate at which an intact peptide is completely absent from solution after eight hours[48]. D-ARVA, on the other hand, is resistant to proteolytic degradation but is still affected by direct RBC binding and by serum protein binding. Hence, these results were not surprising for ARVA[35]. We have not performed any binding or degradation studies with the peptides selected from the first two screening approaches of the second-generation library. However, based on the results from experiments with ARVA, we believe that these AMPs may be similarly affected by binding and degradation in the presence of serum and its proteases, which decrease their bioavailability and, as a result, their cytotoxicity. The evolved peptides DBS1, DBS4, D-CON, and D-CONGA, which were selected and characterized in broth dilution assay and maintained broad-spectrum activity in the presence of RBCs, showed higher cytotoxicity against HeLa Cells in both assays. Among the two assays, the SYTOX Green assay was more sensitive (figures 3-3 and 3-4). Each

AMP had lower EC_{50} against HeLa cells with SYTOX Green assay (figure 5) than Alamar Blue assay.

Many AMPs have inherent cytotoxicity against cancer cells. AMPs possess a cationic structure that allows them to target the membranes of cancer cells better than normal mammalian cells. This is because cancer cells have exposed anionic lipids on the outer surface due to dysregulation of lipid asymmetry. Hence, we performed the final cytotoxicity assays against WI-38 cells, which are normal human fibroblasts. Additionally, based on the first set of cytotoxicity experiments and past research showing inconsistencies with the Alamar Blue assay, we used the SYTOX Green assay for these experiments[9,10]. SYTOX Green directly assesses membrane disruption and is, therefore, more sensitive to membrane permeabilizing AMPs. Lastly, these final cytotoxicity measurements were performed in complete media with 10% FBS to better mimic physiological conditions. As expected, all evolved peptides had lower toxicity in WI-38 cells (figure 3-6 A). The increase in EC_{50} ranged from 3 times for some selected peptides to almost 7 times for D-CONGA (figure 3-6 B). Against WI-38, EC_{50} for all our evolved peptides is much higher than their MICs against all the pathogens tested in chapter 1. Therefore, we concluded that these AMPs are suitable for testing in an *in vivo* infection model.

Assessment of the selected AMPs against gram-positive and gram-negative bacterial infection in a murine wound model

Skin and soft tissue infections, SSTIs, rank among the most common bacterial infections in humans. *MRSA* and multi-drug resistant *P.aeruginosa* are opportunistic pathogens isolated from SSTIs and wound infections. Increasing resistance is reported against

topical antibiotics such as fusidic acid or mupirocin that are often used to treat these infections[49–51]. Thus, new treatment options for bacterial SSTIs are urgently needed. We used our lead peptide, D-CONGA, on a full thickness excisional splinted wound model to evaluate its efficacy for the treatment of SSTIs and chronic wounds. A complex wound environment was established by creating a full thickness surgical punch wound, 5 mm in diameter and 3 mm in depth, on a murine dorsal surface. A biopsy punch was used to penetrate the epidermis, dermis, and panniculus carnosis in healthy adult CD1 mice. A silicone ring was sutured around the wound to prevent healing through skin contraction. Contraction is how a mouse wound heals. A silicone ring forces the wound to heal through re-epithelization and granulation tissue-formation that mirrors human wound healing. Tegaderm, a transparent film dressing, was placed on the wound to maintain a moist environment to promote wound healing. The wounds were infected either with 10^4 CFUs of luminescent *MRSA* or 10^4 CFUs of luminescent *P. aeruginosa*, strain PA01. An insulin syringe was used to penetrate the Tegaderm and dispense the bacteria directly onto the wound bed. To allow for the infection to develop, the first treatment with D-CONGA was performed 3 hours post infection. Weak acetic acid, used as solvent to dissolve the peptide, was used as negative control, and gentamycin treatment was the positive control.

Whole animal luminescence imaging was performed to quantify bacterial burdens. As the infection developed, the wound bed filled with purulence within 12–24 hours. 75 µg of D-CONGA in 20 µl of 0.025% acetic acid was administered every 8 hours for the first 5 days. The Tegaderm was removed on day 3 post-surgery and fixed in 2.5% glutaraldehyde for scanning electron microscopy. This facilitates the drying of the

92

wound, leading to faster healing. For MRSA, the infection was slow was not visible until the next day (figure 3-8 A). When wounds were infected with luminescent MRSA, and treated with vehicle only, they remained infected with high bacterial burdens for 3 subsequent days before spontaneous resolution after the Tegaderm was removed. In contrast, the MRSA infected wounds treated with D-CONGA had a tremendous 4-log decrease in luminescence to close to background levels, at the peak of infection, days 2 and 3 (figure 3-8 B). For *P. aeruginosa infection*, the wound treated with vehicle only displays a dramatic increase in the bacterial burden for 3 days before beginning to resolve on day 4. Again, treatment every 8 hours with 75 μg of D-CONGA in 20 μl of 0.025% acetic acid resulted in 2 to 3 logs of reduction in luminescence at the peak of infection (figure 3-7). In both cases, the silicone rings on mice fell off between days 5 to 8. All the mice were monitored for weight, coat-condition, wound condition, and overall health. These scores indicate that peptide-treated animals remain healthy and have gross wound pathology similar to, or better than, wound healing response in control mice (figure 3-10). Therefore, D-CONGA was efficacious at treating MRSA and *P.aeruginosa* infection in the mouse wound bed.

The peptide treatment of the wound was also able to inhibit significant bacterial colonization. Analysis of the Tegaderm dressings overlay, which were fixed in 2.5% glutaraldehyde, were examined by scanning electron microscopy for bacteria and bacterial biofilms. In vehicle control samples, Tegaderm from infected animals has evidence of individual MRSA-like cocci or *Pseudomonas*-like rods (figure 3-9). These dressings also show complex three-dimensional (3D) matrices containing bacteria, consistent with organized bacterial biofilms. The Tegaderm films from animals treated

with D-CONGA illustrated clear inhibition in bacterial colonization and no evidence of organized biofilms. 4 out of 10 vehicle treated controls displayed large numbers of MRSA-like bacteria in randomly selected areas. However, D-CONGA treated samples had no bacteria in any of the 11 samples ($P = 0.035$ for the proportion of positive samples, $P < 1 \times 10^{-5}$ for cell count). For *P. aeruginosa*-infected animals, *Pseudomonas*-like bacteria were observed in 12 out of 15 vehicle control samples. No bacteria or biofilm-like organization was observed in any of the 15 peptide-treated samples ($P < 1 \times 10^{-5}$).

Characterization of Systemic Toxicity

We also characterized the systemic effects of our evolved AMPs in female CD1 mice. Different concentrations of L-CON, L-DBS2, D-DBS4, and D-CONGA in phosphate buffered saline (PBS) were given to mice for 5 days through intraperitoneal (i.p.) injections (figure 3-11 A). Mice were not able to survive more than one L-CON administration at either 50 or 100 μg concentrations. In contrast, L-DBS2 and D-DBS4 were non-toxic to mice up to 100 and 400 μg of concentrations, respectively, until the end of 5 days of treatments. However, immediately after the administration of these peptides, the majority of mice showed temporary effects on behavior demonstrated by hunched postures and uncoordinated movements. D-CONGA i.p injections were safe to mice up to 25 μg in PBS and 200 μg in 2-oleoyl-1-pamlitoyl-sn-glyecro-3-glycerol Fec (*POPG*) lipid when administered once a day for 5 days. At these concentrations, mice treated with D-CONGA displayed no behavioral effects, weight loss, or liver toxicity. However, at higher concentrations of 50 or 100 μg dose per day, administrations of D-CONGA led to severe decline in mouse health with significant hunching and moribund

94

behavior, sometimes even after a single treatment. Livers were collected from all the mice that survived treatments from various peptides at the end of 5 days of the experiment. Measurement of alanine aminotransferase (ALT) activity showed no liver toxicity in any of these mice (figure 3-11 B).

Discussion

The therapeutic benefits of AMPs against pathogens, including the multi-drug resistant strains, are well investigated and recognized. The literature shows recent developments in the discovery and characterization of broad-spectrum natural and synthetic AMPs[52–54]. However, the investigation of the wound healing properties of AMPs is still emerging. Recently, their value as topical formulations has been recognized. Some AMPs in topical formulations, like polymyxins or gramicidins, are already in the market. Others, such as Pexiganan (Locilex®), Lytixar, OP-145, or Novexatin, are in late-stage clinical trials[55,56]. In this chapter, we evaluate the cytotoxicity of the evolved AMPs from our second-generation peptide library against mammalian cells. We also demonstrate the suitability of our lead peptide, D-CONGA, for therapeutic use by assessing its efficacy on a full thickness excisional splinted wound model. We show that D-CONGA can inhibit infections caused by opportunistic pathogens, MRSA, and multi-drug resistant *P.aeruginosa*, in wound infections. Additionally, D-CONGA can also prevent the formation of biofilms in these wounds. D-CONGA could prove a novel method of preventing antibiotic resistance, simultaneously providing a new broad-spectrum topical treatment option against wound pathogens and accompanying biofilm infections.

The differentiation of microbial and human cells is essential for AMPs to resolve bacterial infection while also limiting antimicrobial-related damage to host cells. Cytotoxic profiling of AMPs is thus necessary for the determination of their suitability for use in humans. Membrane integrity is the most important feature to be considered while evaluating eukaryotic cell toxicity. Those cells with disrupted membrane allow non-permeable molecules into and out of the cells and are non-viable. Different cytotoxicity assays can be used to quantify live or dead cells by measuring the passage of these molecules either in or out of cells. AMPs exert their effects by permeabilization of bacterial membranes[57]. Hence, we assessed the cytotoxicity of selected peptides using two different assays and compared the cytotoxicity that was measured for each AMP. The two assays use distinct approaches to calculate the cytotoxicity profiles for the AMPs. The Alamar Blue assay measures viable cells by metabolic activity and the SYTOX Green assay quantifies dead cells by membrane permeability.

Alamar Blue assay demonstrated lower toxicities for all selected AMPs against both HeLa and WI-38 cells. SYTOX Green, on the other hand, showed higher cytotoxicity for all AMPs especially when the experiments were performed in serum-free media. Alamar Blue relies on a metabolic pathway that converts resazurin to resorufin. Resazurin is a non-toxic, cell-permeable compound internalized by viable cells and metabolically reduced to the highly fluorescent red compound, resorufin. Resorufin is released from cells into media, and the quantity produced is directly dependent on the number of viable cells. Hence, this assay quantitatively measures the proliferation of cells.

Our second assay, SYTOX Green assay, uses a nucleic acid binding dye that is impermeable to viable cells. However, in the event of cell membrane disruption, SYTOX Green is allowed free entry into the cell. As a result, the dye quickly binds to the nucleic acid and stains dead cells. SYTOX Green exhibits a considerable, almost 1000 fold fluorescence enhancement upon DNA binding[58]. In this assay, the quantity of the dead cells is directly dependent on the amount of dye entry. The cytotoxicity is based on the emitted fluorescence when the dye enters the compromised cell membrane and binds to the DNA. In the first set of experiments performed in HeLa cells, Alamar Blue assay showed lower toxicities for the majority of our AMPs, especially in complete media that contains 10% FBS. EC_{50}, the AMP concentration that produces death in 50% of a cell population, was high for most AMPs in this experimental condition. The toxicities increased (EC_{50} decreased) in serum-free media. The SYTOX Green assay was more efficient for our purpose, with the 0 and 100% SYTOX Green control values relatively more consistent and reliable than the values obtained from Alamar Blue assay. SYTOX Green showed comparatively higher toxicity for most of our AMPs than Alamar Blue assay. The EC_{50} for SYTOX Green assay in the serum-free media was the lowest, and thus, this condition showed the highest toxicity for our AMPs.

It has been demonstrated that even in the absence of cells, Alamar Blue can interact with cell culture media causing the increase in fluorescence. DMEM was one of the media tested which produced a time-dependent increase in signal with Alamar Blue even in the absence of cells required for the metabolic activity necessary for the conversion of resazurin to fluorescent resorufin[9]. Alamar Blue also experiences an apparent decrease in the rate of reduction of the reagent in cell cultures in the presence of

FBS[10]. Furthermore, in many Alamar Blue experiments in 96 well plate format, we find

that the cell-only controls do not match the experimental values extrapolated to zero

peptide concentration. This unexplained offset would require a rescaling of the data to

show the expected transition from 100% viability to 0% viability with increasing peptide

concentration. This rescaling has not been applied to the figures here. In the light of these

conflicting influences in the Alamar Blue results, we decided to perform the rest of the

cytotoxicity experiments with SYTOX Green assay. We also elected to use complete

media for the assays to mimic *in vivo* conditions. Most of our evolved peptides consist of

D-amino acids. Hence, proteolytic degradation is not a concern. Next, as mentioned

earlier, there exist fundamental differences between the cell membranes of malignant

cells and normal cells. Cancer cell membranes typically carry a net negative charge due

to a higher-than-normal expression of anionic molecules. Electrostatic interactions

between the cationic AMPs and anionic cell membrane components of cancer cells may

account for the ability of AMPs to selectively kill cancer cells while sparing healthy

cells[59]. Hence, the higher cytotoxicity of our AMPs in HeLa cells can be attributed to its

cancerous properties. Therefore, for the ultimate set of cytotoxicity measurements we

used the SYTOX Green assay in complete media in WI-38 cells, which is a normal lung

fibroblast cell line. As we anticipated, the cytotoxicity for all our AMPs was much lower

in WI-38 cells compared to HeLa cells. The increase in EC_{50} for the AMPs in WI-38,

compared to HeLa cells, ranged from 3 to 7-fold. These EC_{50} were up to 100-fold higher

than MICs of the evolved AMPs against all the ESKAPE pathogens. Hence, we conclude

that the selected AMPs have potent antibacterial activity without producing any toxic

effects against mammalian cells and is suitable for experiments in an *in vivo* infection model against multi-drug resistant pathogens.

Murine models have been crucial to our understanding of wound healing. However, wound repair in mice does not completely recapitulate wound healing in humans. Murine and human skin have the same layers of cells in the dermis and epidermis. However, they differ in thickness and numbers of different layers, with human skin being thicker, firmer, and attached to underlying tissue while murine skin is thinner and loose. The looseness of the skin is because of the presence of *panniculus carnosus* in the subcutaneous tissue of mice, which is absent in humans. *Panniculus carnosus* consists of a thin layer of muscular tissue that gives great contraction potential to the skin, which is essential because 90% of murine excisional wounds heal mainly by contraction. In contrast, the human dermis is firmly attached to the subcutaneous tissues and has irregular and less pronounced contractions than mice. Hence, wounds in humans heal by re-epithelization and formation of granular tissue[60]. These differences in the biomechanics of healing must be considered when analyzing and interpreting preclinical studies performed using murine infection models.

In this chapter, we used splinted full thickness excisional wound model to evaluate the efficacy of our lead peptide, D-CONGA, as a novel topical treatment for MRSA and multi-drug resistant *P. aeruginosa* wound infection. We demonstrated that treatment with D-CONGA inhibits the growth of MRSA and *P.aeruginosa* in the wound bed, reduces gross pathology, inhibits biofilm formation, and does not impair the wound healing process. Our murine model uses splint to replicate human wound healing. The presence of a splint on the wound eliminates skin contraction. Splinted wounds overcome

the differences in wound healing mechanisms in mice and humans by forcing them to heal through re-epithelialization, cellular proliferation, and angiogenesis, which mirrors the biological processes of human wound healing. In this model, one full thickness excision that includes the *panniculus carnosus* is created on the dorsal surface of adult CD1 mice by using a biopsy punch. A silicone splint is placed around the wound with adhesive assistance and covered by Tegaderm, a transparent occlusive dressing, to keep the wound moist. The splint is then secured with eight interrupted sutures. The dressing is collected and fixed in glutaraldehyde 3 days after initial surgery for biofilm visualization[33,35,61].

D-CONGA effectively treated the MRSA and *P. aeruginosa* infections on the wound bed and prevented significant bacterial colonization (Figures 3-7 to 3-9). Furthermore, SEM performed on the Tegaderm dressing proves that D-CONGA can also inhibit bacterial colonization and biofilm formation on infected wounds. Wound scoring and animal health-related scores demonstrated no differences in gross wound pathology and wound healing response in peptide-treated versus vehicle-treated mice. D-CONGA did not induce any changes on the wound bed that indicate an inflammatory or adverse effect of the peptide. There was a slight decrease in the weight of the mice for the first few days after infection but since the phenomenon was uniform between the peptide-treated and vehicle-treated groups, this was likely due to the wound and infection model itself. The bacterial infection started resolving from Day 4 even in vehicle treated mice. This is due to the effects of murine immune system that has recognized the infection and initiated the response. Additionally, the removal of Tegaderm dressing on Day 3 and subsequent drying of the wound bed also aid the decline in the bacterial burden. In some

cases, after the peptide treatment is stopped on Day 5, the bacterial burden, now unchecked, increases rapidly. Therefore, the data discussed here focuses on the first four days when the bacterial infection is at its peak and not affected by these factors.

As the last part of this chapter, we characterized the systemic effects of L-CON, L-DBS2, D-DBS4, and D-CONGA in female CD1 mice using 5 days of intraperitoneal (i.p.) injection of concentrated peptides in PBS, or in a few cases in PBS with liposomes. L-CON was toxic to mice at 50 μg, the lowest concentration tested. Mice exposed to L-DBS2 and D-DBS4 survived the injections for 5 days up to 100 and 400 μg of concentrations, respectively. Our lead peptide, D-CONGA, was safe to mice up to 25 μg in PBS and 200 μg in POPG lipid when administered once a day for 5 days. At these concentrations, mice treated with D-CONGA displayed no behavioral effects, weight loss, or liver toxicity. However, at higher concentrations of 50 or 100 μg dose per day, administrations of D-CONGA led to severe decline in mouse health. The mice appeared to be moribund with intermittent seizure-like behavior even after only one injection. To avoid further pain, these mice in distress were euthanized. This immediate reaction in the mice injected with the AMPs could be pseudoallergy, characterized by immediate systemic reactions that are indistinguishable to anaphylaxis symptoms[62]. The mechanisms involve the release of mediators from basophils and mast cells but is not induced by Immunoglobulin E (IgE). The condition usually leads to mast cells and basophils to degranulate and typically occurs after the first dose of medication. Pseudoallergy does not mimic antigen-specific immune responses but can induce the release of histamine from mast and other cells, which can activate the complement system mimicking signs of anaphylaxis[62–65]. Another observation worth noting here is

101

the dramatic difference in the systemic effects of D-DBS4 compared to D-CONGA. Despite very close sequence similarity, the toxicity of D-DBS4 is much lower. Thus, we hope to be able to engineer variants of D-CONGA that have lower systemic toxicity. Additionally, the acute reaction to the peptide injections can be further reduced by finding an optimal vehicle that facilitates the slow release of the peptide. It is apparent more research is necessary to identify the most optimal vehicle for AMP delivery. Until then, our AMPs are excellent candidates for topical therapeutics against bacterial infections.

In this chapter, we present preclinical data that demonstrates the success of our evolved AMPs in protecting wounds infected by drug-resistant bacteria. We used synthetic molecular evolution to identify these host cell-compatible AMPs with excellent activities and low cytotoxicity *in vitro* and *in vivo*. We are confident that these peptides will have a greater probability of success in the clinic than other AMPs described in the primary literature. This is exemplified by the analysis of antibacterial activity of SAAP-148 in chapter 2. We expanded our characterization of SAAP-148 and measured its cytotoxicity in HeLa and WI-38 cells using SYTOX Green assay. Compared to our selected peptides, SAAP-148 is highly toxic to HeLa and WI-38 cells (figure 3-12). The *in vitro* activity and cytotoxicity data for SAAP-148, validates our belief that our peptides characterized in chapter 2 and chapter 3, are superior antibiotics to most AMPs in the preclinical stage of development. The approach of SME described here, which incorporates screening of iterative rational libraries under physiologically relevant conditions and allows for orthogonal selection and down-selection based on known impediments, could transform how AMPs are designed, discovered, and characterized.

The use of SME to select for potent AMPs from very early stages of design and selection can increase the population of AMPs therapeutics that get to later stages of development and approval. This, ultimately, will raise the probability that one, or some, will succeed, accomplishing the primary goal of this project.

Figure 3-1

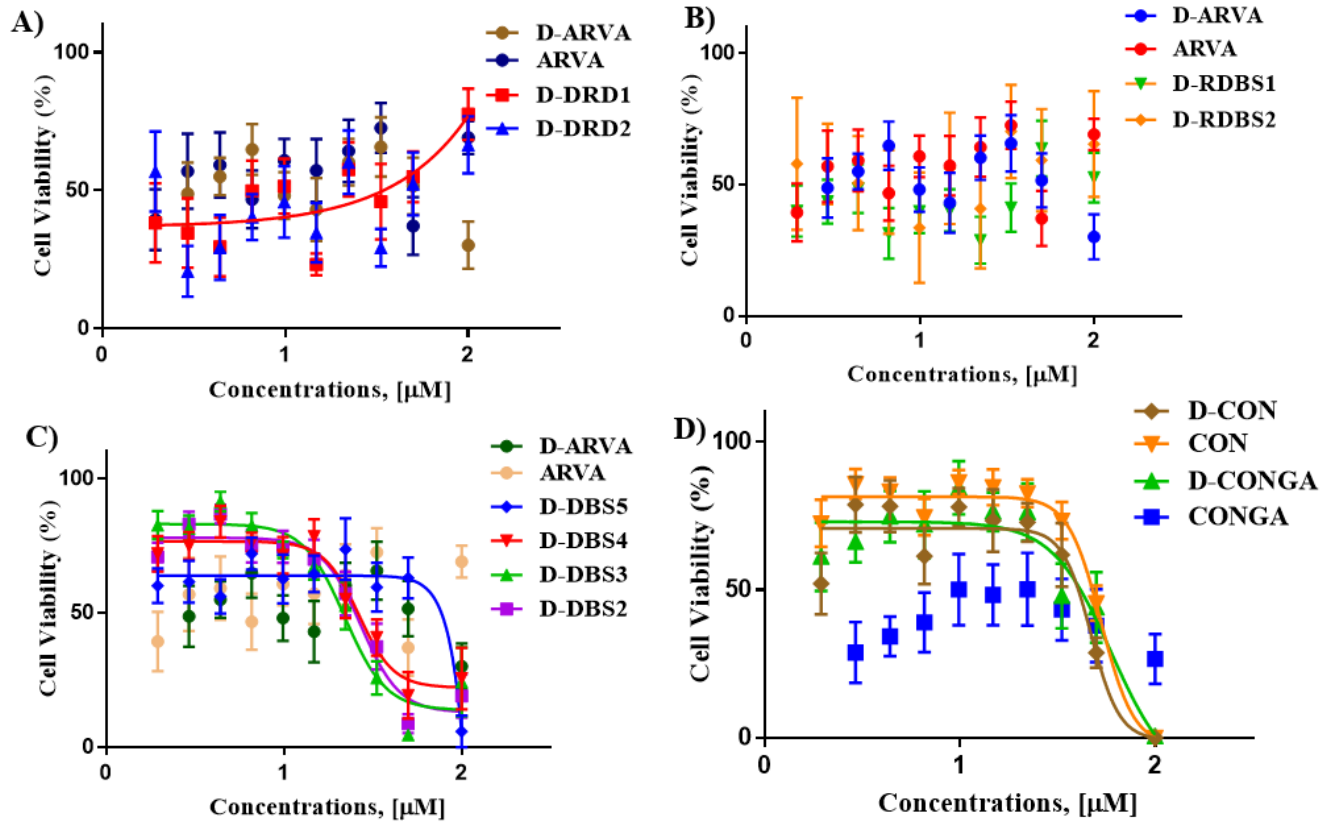

Alamar Blue Assay in Complete Media

Figure 3-1. Alamar Blue assay in complete media. Cytotoxicity of selected antimicrobial peptides (AMPs) and their variants are shown as cell viability % of HeLa cells post treatment with increasing concentrations of AMPs. The assay is performed in serum-free media with 10% fetal bovine serum (FBS). The cytotoxicity of peptides selected from **A)** double radial diffusion approach (DRD), **B)** mixed radial diffusion and broth sterilization approach (RDBS), and **C)** double broth sterilization (DBS) approach is compared to the cytotoxicity of parent peptide, ARVA using Alamar Blue assay that allows the quantification of live cells post peptide treatment. **D)** The cytotoxicity of L- and D-forms of the two best rational variants of the selected peptides, CON and CONGA is also presented.

Figure 3-2

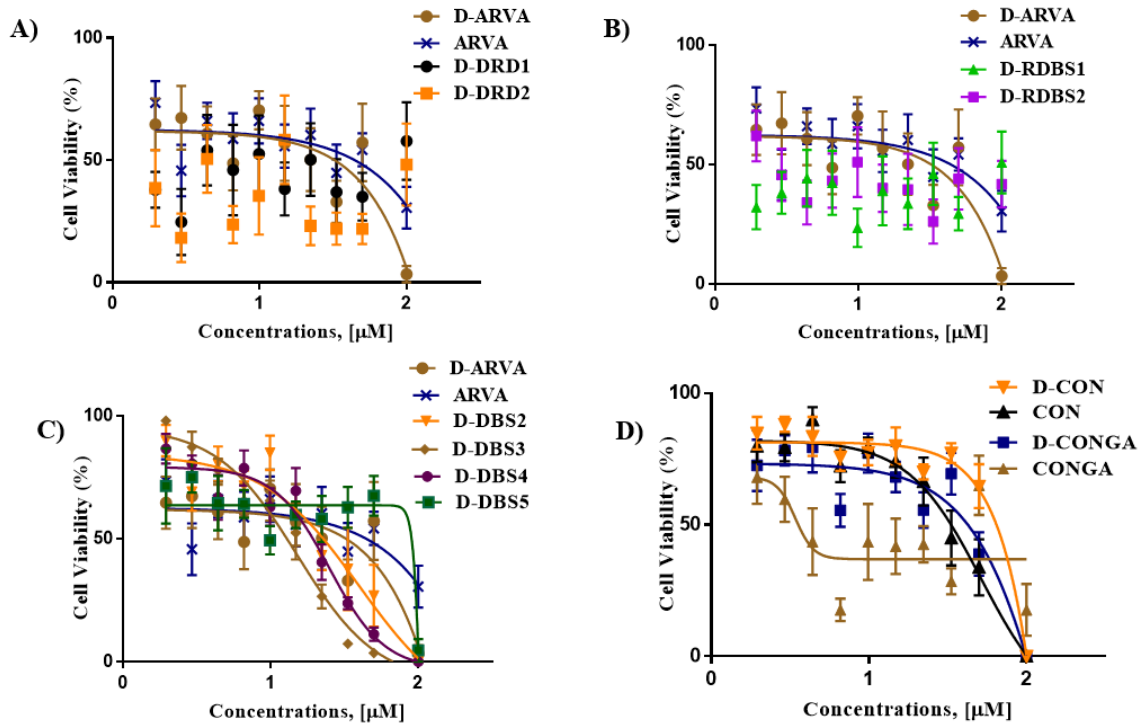## Alamar Blue Assay in Serum-Free Media

Figure 3-2. Alamar Blue assay in serum-free media. Cytotoxicity of selected antimicrobial peptides (AMPs) and their variants are shown as cell viability % of HeLa cells post-treatment with increasing concentrations of AMPs. The assay is performed in serum-free media. The cytotoxicity of peptides selected from **A)** double radial diffusion approach (DRD), **B)** mixed radial diffusion and broth sterilization approach (RDBS), and **C)** double broth sterilization (DBS) approach is compared to the cytotoxicity of parent peptide, ARVA using Alamar Blue assay that allows the quantification of live cells post peptide treatment. **D)** The cytotoxicity of L- and D-forms of the two best rational variants of the selected peptides, CON and CONGA is also presented.
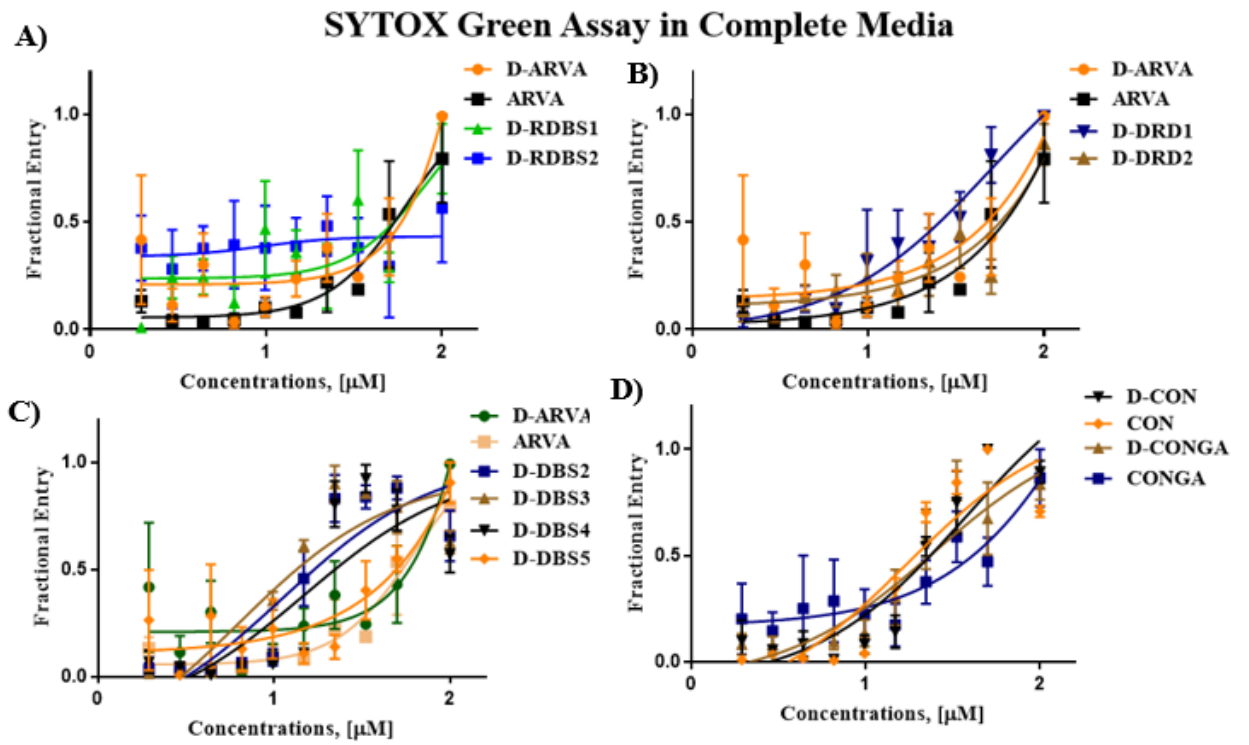
Figure 3-3

Figure 3-3. SYTOX Green assay in complete media. Cytotoxicity of selected antimicrobial peptides (AMPs) and their variants are represented by the fractional entry of SYTOX Green dye in HeLa cells post-treatment with increasing concentrations of AMPs. The assay is performed in complete media with 10% fetal bovine serum (FBS). The cytotoxicity of peptides selected from **A)** double radial diffusion approach (DRD), **B)** mixed radial diffusion and broth sterilization approach (RDBS), and **C)** double broth sterilization approach (DBS) is compared to the cytotoxicity of parent peptide, ARVA using SYTOX Green assay that allows the quantification of dead cells post peptide treatments **D)** The cytotoxicity of L- and D-forms of the two best rational variants of the selected peptides, CON and CONGA is also presented.

Figure 3-4

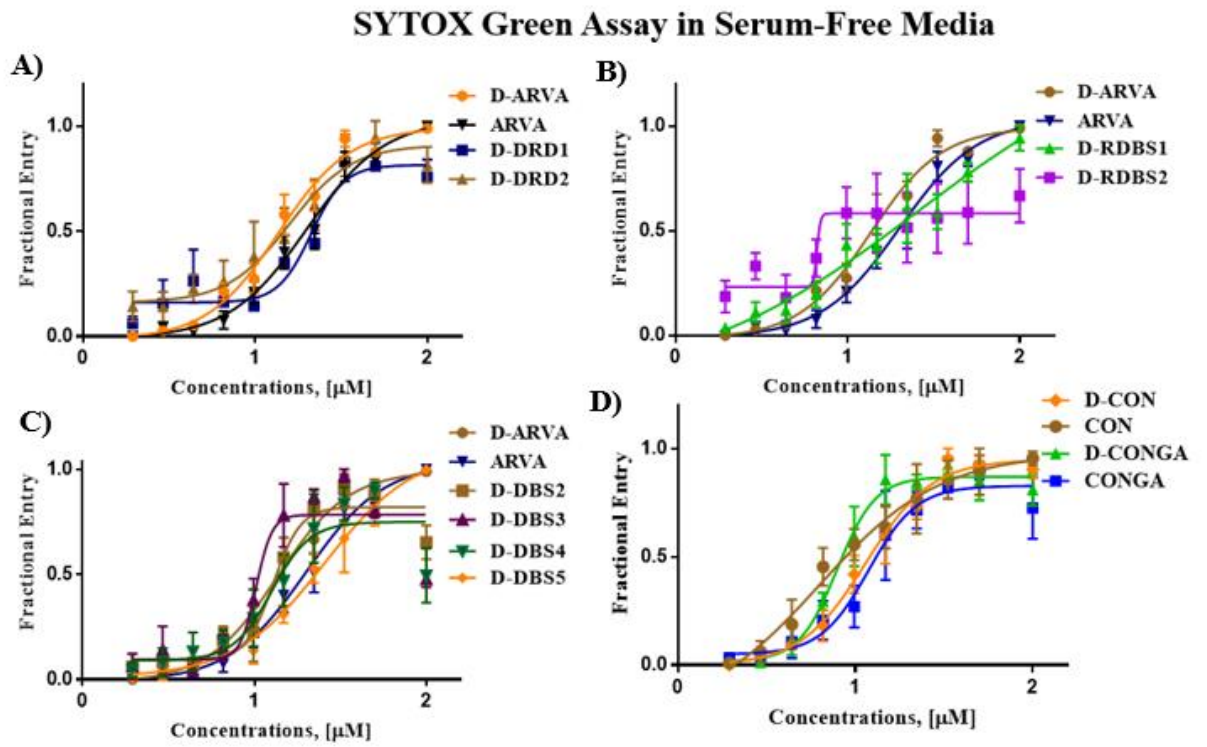**SYTOX Green Assay in Serum-Free Media**

Figure 3-4. SYTOX Green assay in serum-free media. Cytotoxicity of selected antimicrobial peptides (AMPs) and their variants are represented by the fractional entry of SYTOX Green dye in HeLa cells post-treatment with increasing concentrations of AMPs. The assay is performed in serum-free media. The cytotoxicity of peptides selected from **A)** double radial diffusion approach (DRD), **B)** mixed radial diffusion and broth sterilization approach (RDBS), and **C)** double broth sterilization approach (DBS) is compared to the cytotoxicity of parent peptide, ARVA using SYTOX Green assay that allows the quantification of dead cells post peptide treatments. **D)** The cytotoxicity of L- and D-forms of the two best rational variants of the selected peptides, CON and CONGA is also presented.

Figure 3-5

A)

	Cytotoxicity in Hela Cells (μM)			
Peptides	EC$_{50}$-CM (Alamar Blue)	EC$_{50}$-SF (Alamar Blue)	EC$_{50}$-CM (Sytox Green)	EC$_{50}$-SF (Sytox Green)
L-ARVA	500	122.7	68.28	20.42
D-ARVA	156	120.1	170.5	13.86
D-DRD1	500	500	47.84	20.7
D-DRD2	500	500	114.2	17.75
RDBS1	500	195.1	60.77	10.89
D-RDBS1	207.3	500	304.8	43.87
D-RDBS2	500	230.7	500	500
L-DBS1	94.18	38.51	15.98	10.28
L-DBS2	49.91	34.48	14.45	16.22
L-DBS3	33.79	19.17	11.35	10.86
L-DBS4	96.61	44.78	14.35	6.259
L-DBS5	105.1	77.13	28.66	24.89
D-DBS2	25.04	27.67	14.05	13.03
D-DBS3	19.6	14.35	10.49	10.33
D-DBS4	23.72	25.06	15.43	10.06
D-DBS5	102.6	82.17	54.96	29.84
L-CON	60.85	46.69	15.99	6.513
D-CON	59.47	83.72	21.78	11.4
L-CONGA	148.4	123.5	41.63	13.58
D-CONGA	59.35	52.38	16.19	8.404

Cytotoxicity in Hela Cells

B)

Legend:
- Alamar Blue, CM
- Alamar Blue, SF
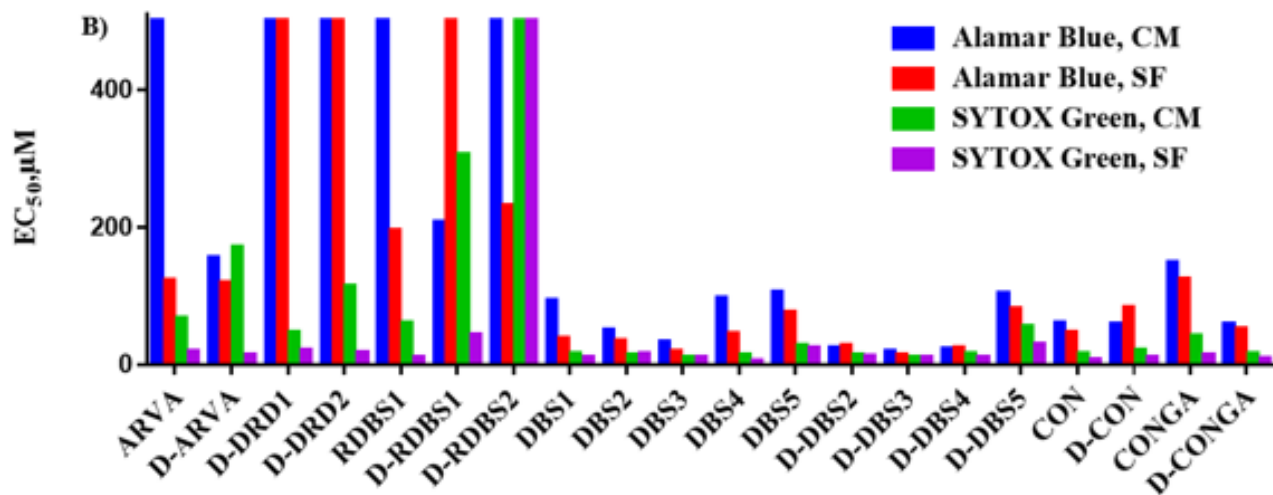- SYTOX Green, CM
- SYTOX Green, SF

Figure 3-5. Comparison of peptide cytotoxicity obtained by Alamar Blue and SYTOX Green assays performed in media with and without serum. A) EC_{50}, a concentration that produces 50% effects in a large population of cells, in this case, cause cytotoxicity, is presented for selected peptides and their rational variants in HeLa cells. The cytotoxicity calculated using two approaches, Alamar Blue assay and SYTOX Green assay, in two media compositions, media with and without serum, is compared to discover the best technique for the determination of peptide cytotoxicity against mammalian cells. The peptides that do not show any toxicity against HeLa cells, in the highest concentration of peptide in that particular condition, are given an EC_{50} of 500. Columns in yellow show our best selected peptides. **B)** Demonstration of the differences in EC_{50} of the same peptides in HeLa cells when cytotoxicity assays and media compositions are varied. Our AMPs show the lowest toxicities with Alamar Blue assay than with SYTOX Green assay. Similarly, cytotoxicity for peptides increases when the assays are performed in serum-free media compared to those completed in media with FBS.

Figure 3-6

A)

SYTOX Green Assay in Complete Media
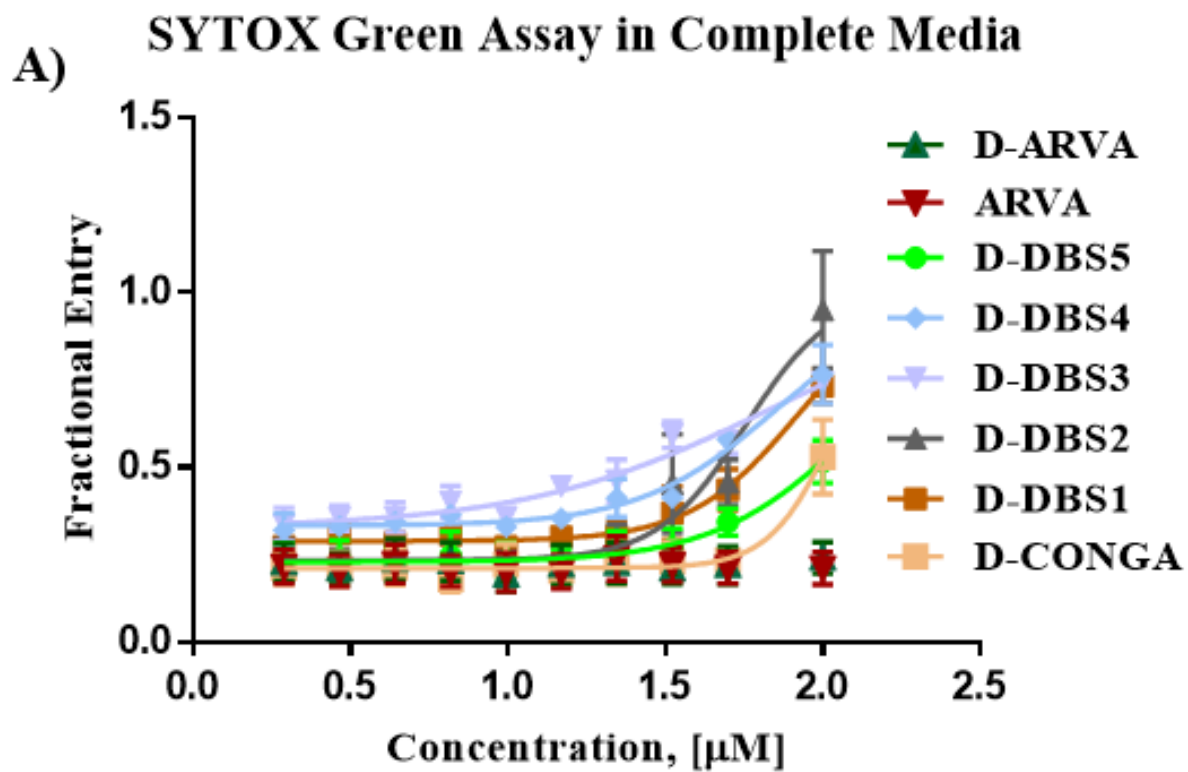
B)

Cytotoxicity in WI-38 cells	
Peptides	Cytotoxicity EC_{50} (μM)
ARVA	500
D–ARVA	500
D-DBS1	82
D-DBS2	57
D-DBS3	71
D-DBS4	72
D-DBS5	130
D-CONGA	110

Figure 3-6. Cytotoxicity of our AMPs in WI-38, normal fibroblast cells. A) SYTOX Green assay was performed in complete media to evaluate the cytotoxicity of our best AMPs in WI-38 cells. The cytotoxicity for each peptide was lower in the fibroblast than cancer cell line, HeLa. **B)** EC_{50} of the best peptides from the second-generation library was higher in WI-38 cells than in HeLa cells.

Figure 3-7
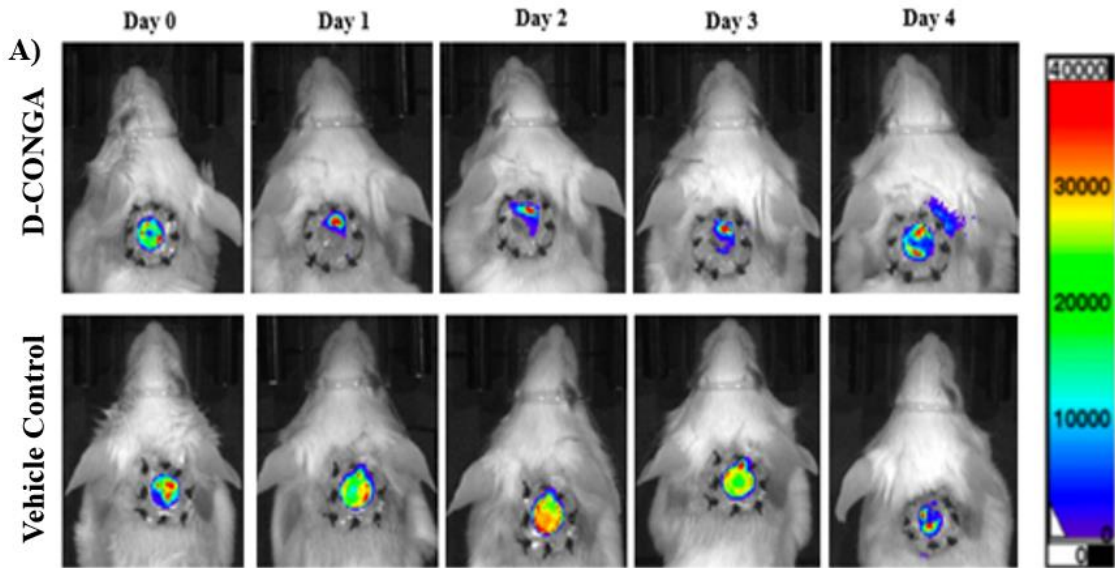
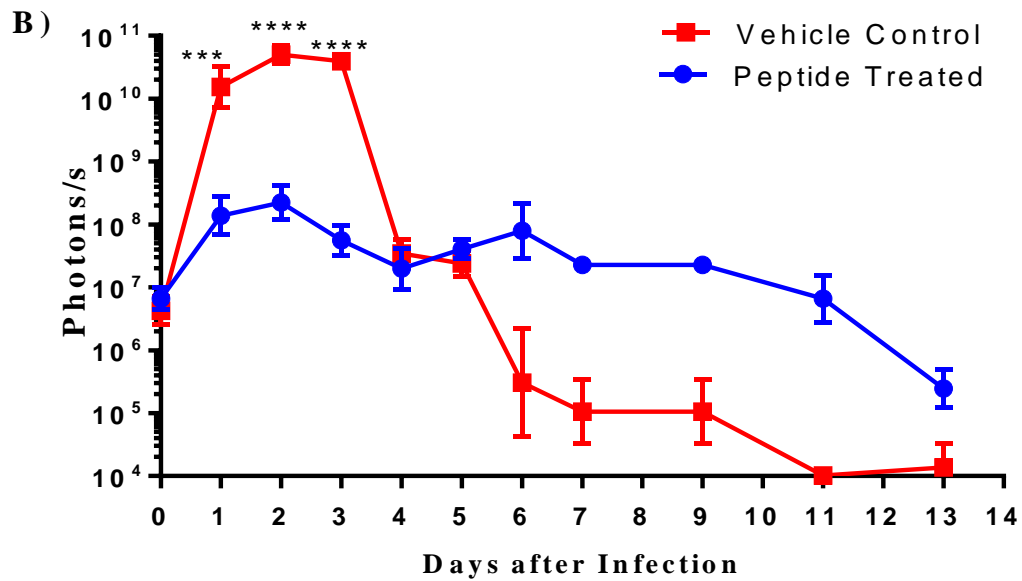**Figure 3-7. The animal model of deep surgery wound infection by *P.aeruginosa.* treated with D-CONGA.** Circular, dorsal puncture wounds were surgically created in healthy, adult CD1 mice, stabilized with a sutured silicone ring, and covered with Tegaderm dressing to better mimic infection and wound healing in humans. Wounds were infected with luminescent *P. aeruginosa* and were treated with D-CONGA peptide or vehicle control every 8 hours until Day 4. An IVIS whole animal imager was used to measure luminescence in all animals once per day for 13 days after infection. **A)** Example of daily images of two mice infected with *P. aeruginosa* are shown. **B)** Total integrated radiance from the wound bed was measured daily in *P. aeruginosa* infected mice. Statistical significance of the pairwise differences are shown, determined with a t-test on log values after applying the Bonferroni correction for multiple comparisons.

Figure 3-8

Figure 3-8. The animal model of deep surgery wound infection by MRSA treated with D-CONGA. The same surgical procedure was followed as described in figure 3-8. **A)** Example of daily images of two mice infected with MRSA are shown. **B)** Total integrated radiance from the wound bed was measured daily in MRSA infected mice. Statistical significance of the pairwise differences are shown, determined with a t-test on log values after applying the Bonferroni correction for multiple comparisons.
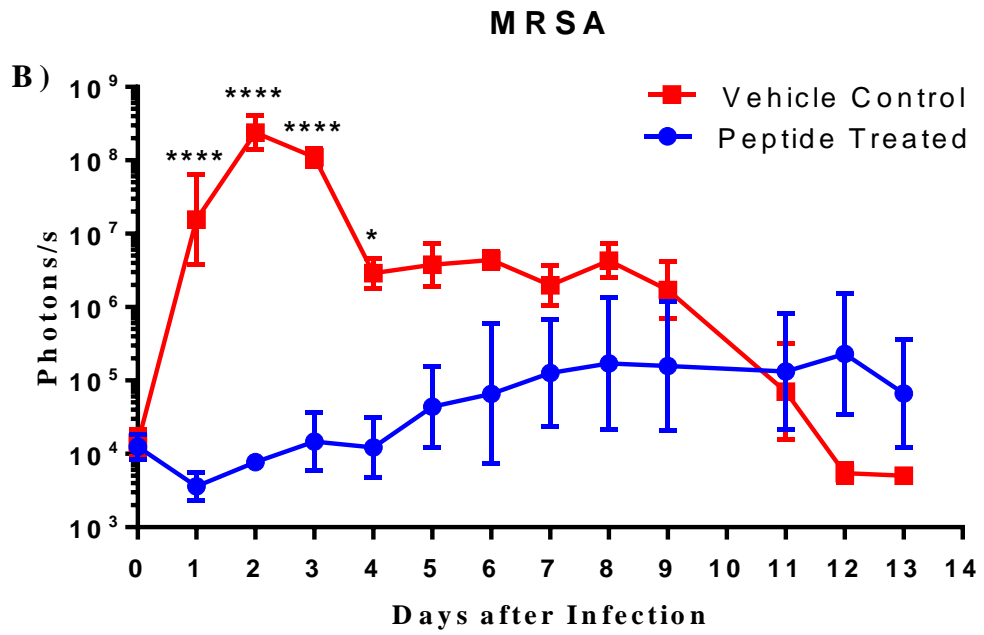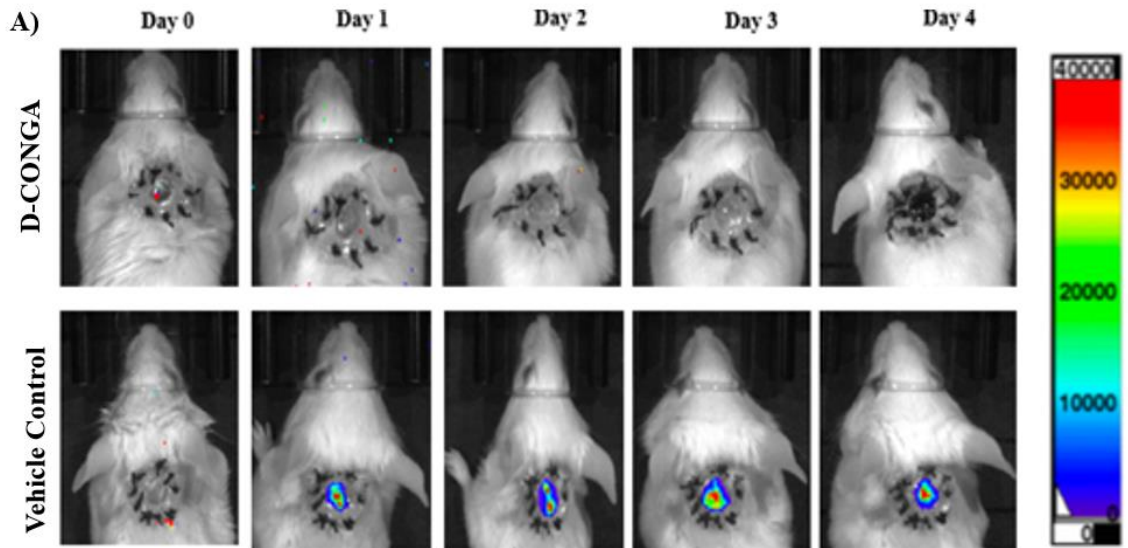
Figure 3-9

A)

MRSA

B)

Pseudomonas aeruginosa
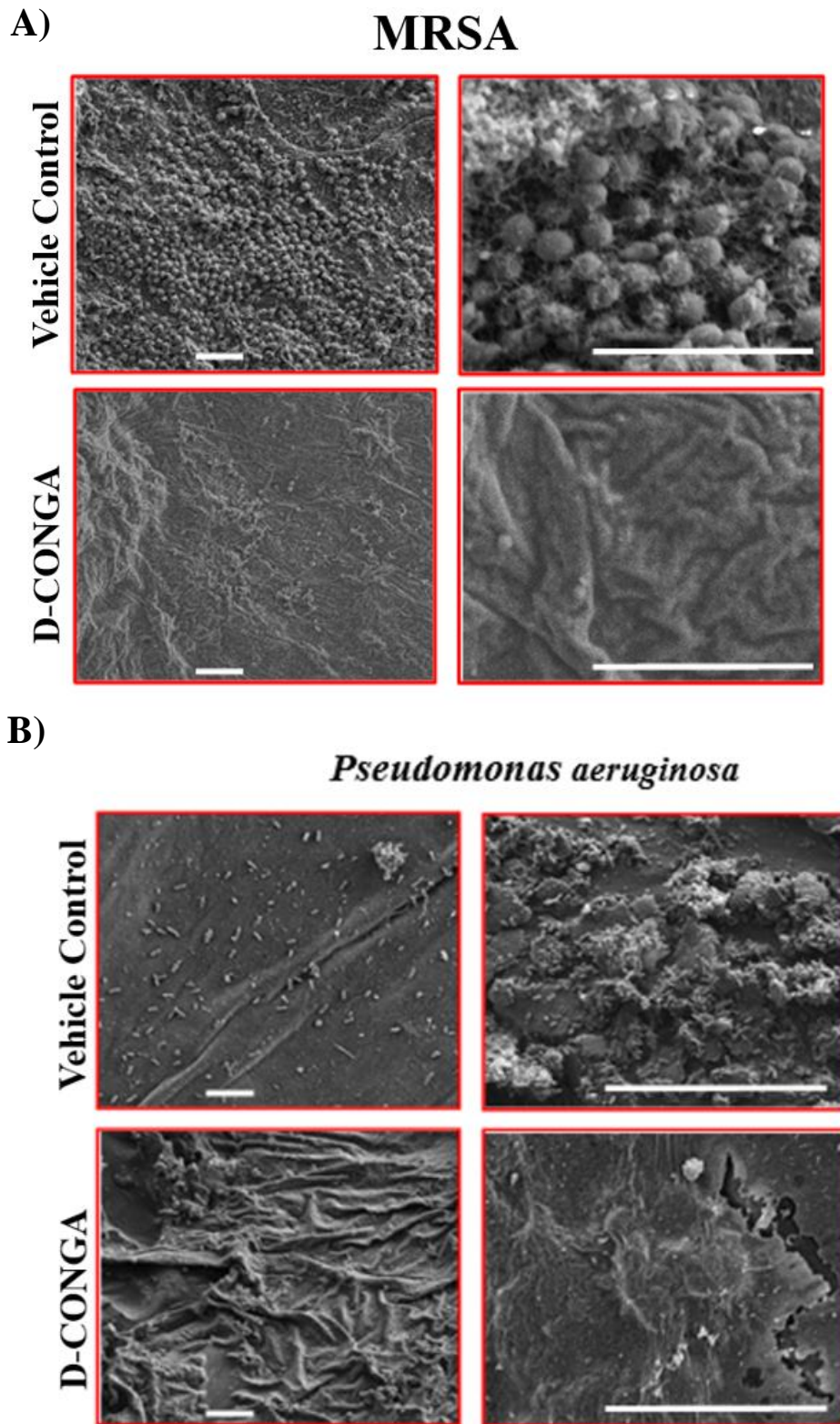
Figure 3-9. Representative scanning electron microscopy images of glutaraldehyde fixed Tegaderm dressing that were removed from experimental animals on Day 3 is presented here. Two different magnifications are shown of different areas. Scale bars are 5 μm in all images. **A)** The top two images show vehicle controls with abundant biofilms and cocci MRSA in all samples. The bottom two images are of the Tegaderm of wound treated 3 times a day with peptides. No biofilm is observed, and only the Tegaderm adhesive is visible. **B)** Similarly, The top two images show vehicle controls with abundant biofilms and rod-like *P.aeruginosa* in all samples. The bottom two images are of the Tegaderm of wound treated 3 times a day with peptides. No biofilm is observed, and only the Tegaderm adhesive is visible.

Figure 3-10
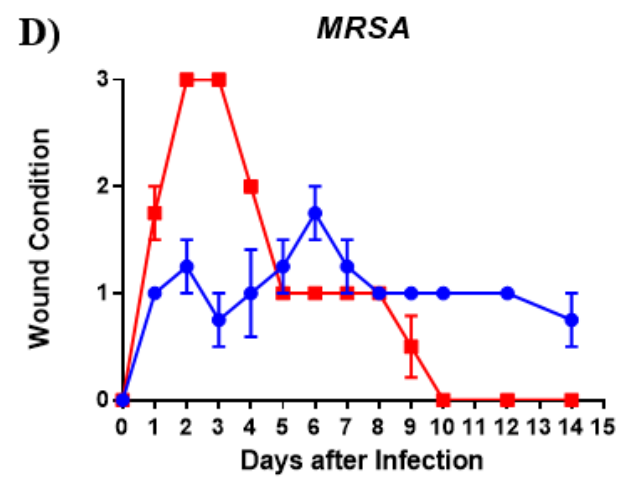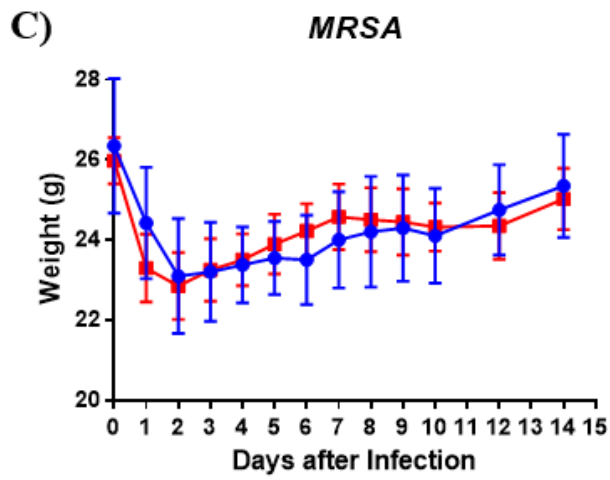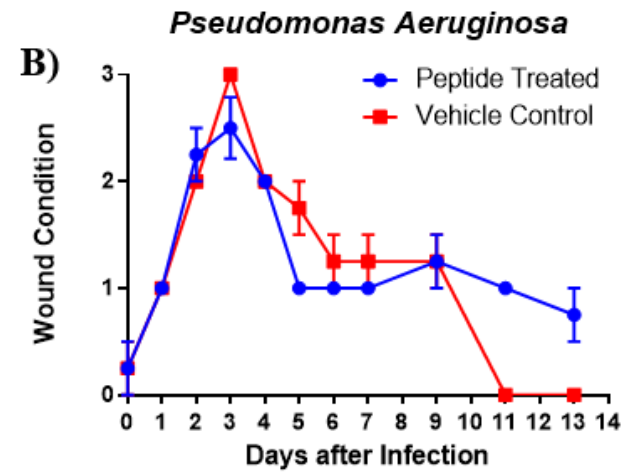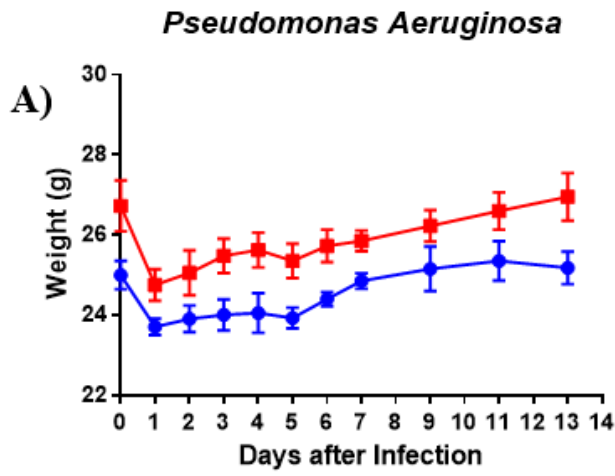
Figure 3-10. Post-surgery mouse monitoring data. A and C) The weights and **B and D**) wound condition of each mice was monitored every day for the 14 days of the experiment. The mice did not demonstrate any weight loss based on different bacterial infections or solvent treatments. There was no difference in the wound condition of mice treated with peptide versus the mice treated with vehicle control in *P.aeruginosa*. In MRSA infected mice, however, the peptide treated group show overall better wound pathology than vehicle control for the first few days of the experiment.

Figure 3-11

A)

Peptides (500 µl)	Weight (g)				
	Day 1	Day 2	Day 3	Day 4	Day 5
Control PBS 1	29.7	30.3	32.1	32.7	32.6
Control PBS 2	27.2	28.2	28.5	29.2	30.2
Control POPG	26.2	25	25.7	26.4	26.2
D-CONGA-12.5 µg	27.3	27.2	27.9	27.3	27.8
D-CONGA-25 µg	28	28	28.9	29.1	29.1
D-CONGA-50 µg	27.8	Deceased	Deceased	Deceased	Deceased
D-CONGA-100 µg POPG	26.9	25.3	25.6	26.4	26.9
D-CONGA-200 µg POPG	30.2	29.5	29.7	31.5	32.2
D-CONGA-400 µg POPG	31.1	28.7	Deceased	Deceased	Deceased
D-DBS4- 100 µg	24.4	25.1	25.5	25.7	27.3
D-DBS4- 200 µg	31.3	30.7	31.1	31.5	31.7
D-DBS4- 400 µg	31.4	30.4	30.6	31.3	30.7
L-CON-50 µg	30.1	Deceased	Deceased	Deceased	Deceased
L-CON-100 µg	29.3	Deceased	Deceased	Deceased	Deceased
L-DBS2-50 µg	30.2	29.7	29.3	28.5	28
L-DBS2-100 µg	28.5	27.7	27.9	27.8	27.9

Alanine Transferase (ALT) activity in Mice Liver
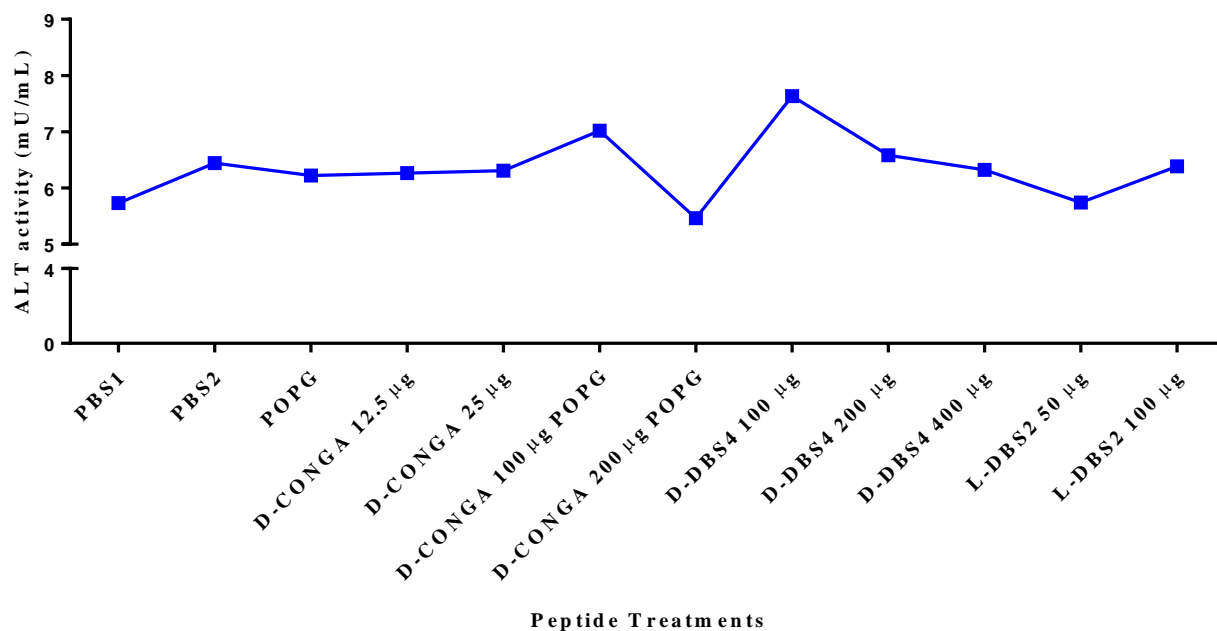
Figure 3-11. Systemic toxicity of AMPs in mice. A) Weights of the mice treated once

per day with i.p. administration of 500 μl of peptide solution or vehicle. The composition

of the injection is given in the first column. Mice were monitored for 1 hour after

treatment with subsequent checks performed three times daily. The ones which showed a

drastic decline in health and behavior were euthanized and are described as "Deceased".

B) At the study endpoint, after 5 days of treatment, mice that survived were euthanized

by CO_2 asphyxiation and livers were collected. Liver ALT enzyme was measured using a

fluorometric kit from Abcam as directed by the manufacturers. Liver samples were

homogenized in buffer, and the supernatant was used to measure liver ALT enzyme by

fluorescence using a coupled enzyme reaction. Fluorescence from pyruvate standards of

known concentrations was used to convert fluorescence to milliunits (mU) of ALT

activity.

Figure 3-12

A) SYTOX Green Assay in HeLa cells

B) SYTOX Green Assay in WI-38 CELLS

SAAP-148
D-CONGA

C)

	SAAP-148	D-CONGA
EC50 (HeLa)	4.206 µM	16.19µM
EC50 (WI38)	12.63 µM	110 µM

Figure 3-12. Comparison of cytotoxicity of our lead peptide, D-CONGA, and SAAP-148. A) Cytotoxicity is represented by the fractional entry of SYTOX Green dyes into HeLa and WI-38 cells in complete media. **B)** EC_{50} for SAAP-148 compared to D-CONGA.

CHAPTER 4: Synthesis and characterization of the rational variants of D-CONGA.

Introduction

In chapters 2 and 3, we have demonstrated that variation in the sequence of antimicrobial peptides selected from the primary screening of an iterative peptide library can lead to the identificatio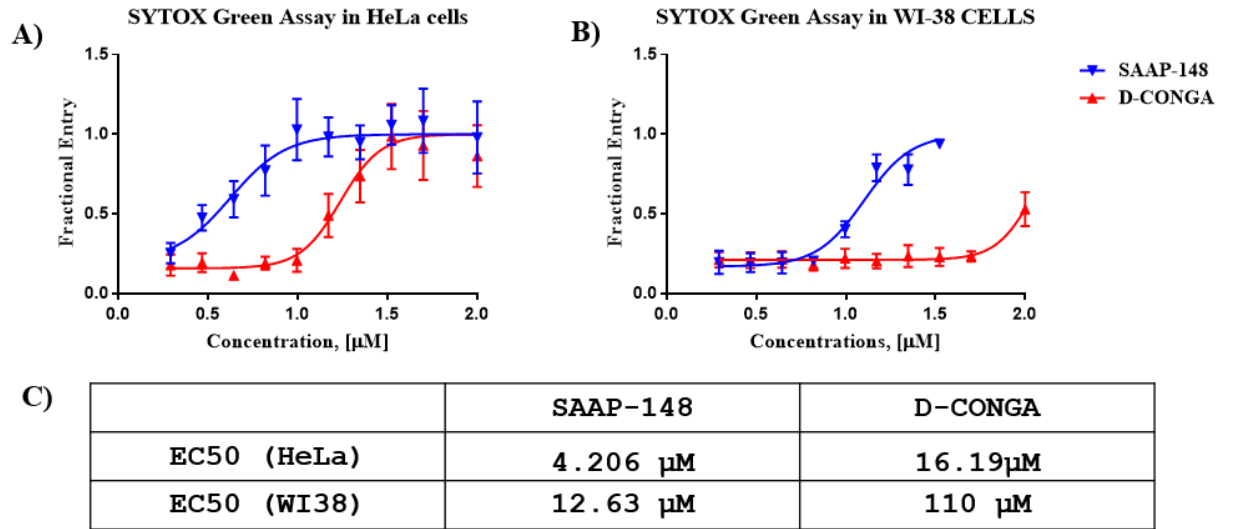n of peptides with improved antimicrobial activity, higher solubility, and lower cytotoxicity against red blood cells (RBCs) and nucleated mammalian cells. This process, referred to as synthetic molecular evolution (SME), led to the discovery of D-CONGA, a rational variant obtained by removing the invariant glycine from the consensus sequence of nine peptides selected from the stringent screening of the second-generation antimicrobial peptide library. D-CONGA is highly effective *in vitro* against all ESKAPE pathogens in the presence of RBCs and serum. The peptide also has anti-biofilms activity in gram-positive and gram-negative bacteria and shows potency against both types of bacteria and their biofilms in relevant infected wound models in mice.

As the next logical step of SME, we decided to make rational variants of D-CONGA. In this chapter, we synthesized 13 variants of D-CONGA. They were broadly divided into four classes; insertions, deletions, swaps, and cyclized. Three variants were formed by the insertion of an amino acid in the seventh position of D-CONGA to split the central hydrophobic core from the polar/cationic N-terminus. Three more were synthesized by deletions of amino acids at different positions in the sequence of D-CONGA. Five more variants were produced through the swapping of amino acids within D-CONGA. Among the swap variants, one had a flipped central hydrophobic core. Two

of the swap variants had residues changed from D to L forms, and the two remaining had central double arginine switched to ones with longer and shorter sidechains. Lastly, two cyclized versions of D-CONGA were synthesized through the hydroxide-terminal group or added glutamate in the N terminal.

Next, to investigate the importance of each residue in D-CONGA in the position and enantiomer forms they appear in, the 13 variants were characterized for their antimicrobial activity against gram-positive *Staphylococcus aureus*, and gram-negative *Escherichia coli* and *Klebsiella pneumonia,* in the presence and absence of RBCs. The cytotoxicity of the D-CONGA variants was tested against the normal fibroblast cell line, WI-38, using the SYTOX Green assay in complete media. Their hemolysis of human RBCs was also measured. Variation of the sequence in D-CONGA produced significant changes in its characteristics. Some variants maintained their antibacterial activity but saw an increase in cytotoxicity. Some others had very low cytotoxicity but displayed a loss of bactericidal function against one or more of the pathogens tested.

Two peptides, created by insertion of amino acids glycine (G) and glutamine (Q) after the sixth position of D-CONGA, were the best antibiotics with the lowest toxicity. Among the two, D-CONGA-Q7 had the higher EC_{50} and similar or lower MICs against all three pathogens tested. D-CONGA-Q7 even surpassed its predecessor D-CONGA in its antibacterial activity. The MICs of D-CONGA-Q7 were less than 5 μM against all three pathogens. Moreover, the cytotoxicity of D-CONGA-Q7 in WI-38 cells was four times lower than that of D-CONGA. D-CONGA-Q7 inhibited the growth of methicillin-resistant *Staphylococcus aureus (*MRSA*)* and *Pseudomonas aeruginosa* on the murine model of deep surgery wound infection. Compared to D-CONGA, treatment of the

infected wound with D-CONGA-Q7 resulted in higher logs of reduction in bacterial burden at the peak of infection. We further characterized the bactericidal activity of D-CONGA and D-CONGA-Q7 against 14 clinical isolates of multi-drug resistant gram-positive and gram-negative bacteria. For comparison, MICs of eight conventional antibiotics against the isolates were also measured. The majority of these isolates were obtained from lung sputum of patients with cystic fibrosis at Tulane Hospital, New Orleans. Other isolates were multi-drug resistant bacterial strains.

Cystic fibrosis (CF) is one of the most frequent types of autosomal-recessive disorder. The morbidity and mortality of most patients with CF is due to pulmonary disease, characterized by chronic lung infections and airway inflammation[1–4]. The most common bacterial species involved in respiratory tract infection in CF is *Pseudomonas aeruginosa*. In fact, 80% of all adult chronic lung infections in CF patients can be attributed to *P. aeruginosa*[5]. *P. aeruginosa* exists in two different forms in the lungs of CF patients, mucoid and non-mucoid forms. Bacterial conversion from non-mucoid to mucoid form in CF patients is defined by overproduction of the exopolysaccharide alginate, a hallmark of chronic infection and predictive of poor prognosis[6]. The second most prevalent pathogen in the lungs of CF is *S. aureus.* Analysis of more than 200 adult patients with CF demonstrated that one-third of CF patients had P.*aeruginosa,* and one-third had a mixture of *P.aeruginosa with S. aureus*[7]. In 2018, over 55% of CF patients cultured for respiratory pathogens were found to be infected with Methicillin-sensitive *S. aureus* (MSSA), and 25% of them with methicillin-resistant *S. aureus* (MRSA)[8]. Additionally, a study from 2010 demonstrated that MRSA detection in the respiratory

tract is associated with worse survival in CF patients than in those who never have a culture positive for MRSA[9].

Although in smaller quantity, many other multi-drug resistant gram-negative bacteria also contribute to the community derived and nosocomial pneumoniae in patients with CF. A study performed over 35 years of time period demonstrated that, while uncommon, approximately 10% of CF airway samples contained drug-resistant *Klebsiella spp.* in any given year[10]. *Klebsiella pneumoniae*, is particularly frequent in the upper respiratory tract of CF patients younger than 12 months[11]. Another gram-negative bacteria, *Acinetobacter baumannii,* is also responsible for pneumonia in CF patients[12]. In a recent study, all but two, of the known strains of *Acinetobacter* spp. were identified from CF patients[13]. Many of these bacterial species are multi-drug resistant, and can form biofilms in the lungs of patients with CF. The biofilm mode facilitated by mucus in the respiratory canal contributes to the chronic severe lung infections responsible for morbidity and mortality of numerous CF patients, and is associated with reduced susceptibility to antibiotics[14–18].

Thus, the lungs of patients with cystic fibrosis (CF) are colonized by a microbial community comprised of many pathogenic species that cause chronic infections and develop quick resistance. It is essentially a giant incubator of pathogens that can be utilized for the identification of antimicrobials that have bactericidal effects against drug-resistant infections. Treatment of CF pulmonary infection includes penicillin such as ampicillin; aminoglycosides, including tobramycin and gentamicin; carbapenems, such as meropenem; fluoroquinolone such as ciprofloxacin; cephalosporins, including ceftazidime and ceftriaxone, and in some cases, antimicrobial peptide colistin, a

polymyxin[19–21]. Aggressive antibiotic treatment can eliminate the bacterial infections

from the lungs of CF patients during the early stages. However, existing antibiotic

regimen, while helpful to reduce the bacterial burden fails when chronic infection is

established. Here, we have compared the antibacterial activity of our lead peptides, D-

CONGA, and its superior rational variant, D-CONGA-Q7, with eight conventional

antibiotics mentioned above, which are extensively used to treat infections caused by

multi-drug resistant pathogens. D-CONGA and D-CONGA-Q7 were able to sterilize all

the resistant isolates. The MICs of D-CONGA-Q7 against all 14 pathogens were less than

15 μM. D-CONGA, while still active, had very high MICs against two strains of

klebsiella, which were among the four pathogens, resistant to all the conventional

antibiotics tested. Not a single conventional antibiotic was able to sterilize all the resistant

bacterial isolates even in the highest concentrations used. Two antibiotics, ampicillin, and

ceftazidime were resistant to all 14 pathogens. Hence, in this chapter, through the

identification of D-CONGA-Q7, we have yet again demonstrated that SME approach that

guided us to design, synthesize and characterize the rational variants of D-CONGA can

be used to discover superior peptides with each generation. The work shown here

recognizes D-CONGA-Q7 as our best AMP to date and a better antibiotic than most

conventional drugs in the market.

Methods and Materials

Synthesis of the variants

All peptides used in this study were synthesized using solid-phase FMOC chemistry and

purified to >95% using high-performance liquid chromatography (HPLC) either in the

laboratory or by Bio-synthesis Inc (Lewisville, TX). The peptide identity was confirmed

through mass spectrometry. Antibiotics were obtained from various vendors. Unless otherwise stated, all solutions were prepared by dissolving lyophilized peptide or antibiotic powders in 0.025% v/v) acetic acid and concentrations were determined by absorbance at 280 nm.

Bacterial Strains and Growth Conditions

E. coli (ATCC 25922), *S. aureus* (ATCC 25923), K. *pneumoniae subsp. Pneumoniae* (ATCC 13883), were used in this study for the bactericidal characterization of D-CONGA variants. Subcultures, prepared by inoculating 25 mL of fresh tryptic soy broth (TSB) with 200 μl of an overnight culture, were grown to log phase (OD600 = 0.3−0.6), after which cell counts were determined by measuring the OD600. Bacterial cells were diluted to appropriate concentrations in either TSB. Sources of clinical bacterial isolates: KP = *Klebsiella pneumoniae*. Strains 6, 46, NDM-1, ST396, ST258C2, St258C3, ST258I2, 398, and CRE were isolated by Dr. J. Kolls, Tulane University from lung sputum of cystic fibrosis patients. PA = *Pseudomonas aeruginosa*. Mucoid and non-mucoid strains were isolated by Dr. J. Kolls, Tulane University form lung sputum of cystic fibrosis patients. KP (Morici) is ATCC# 33495, provided by. Dr. L. Morici, Tulane University. The multidrug resistant *Staphylococcus aureus* strain, MRSA, is SAP400, a USA400 strain of community acquired MRSA. AB = *Acinetobacter baumannii* is a pan drug resistant (PDR) strain isolated in the Tulane Hospital in 2015. Clinical isolates were grown in the same way as the laboratory strains.

Human red blood cells

Human O+ erythrocytes were obtained from Interstate Blood Bank, Inc. (Memphis, TN). Red blood cells were subjected to four cycles of centrifugation at 1000xg with

resuspension in fresh PBS. Following the final wash step, the supernatant was clear and colorless. RBC concentration was determined using a standard hemocytometer.

Broth Dilution Assay

Antimicrobial peptides and conventional antibiotics were prepared at 5-times the final concentration needed in 0.025% acetic acid. The antibiotics were serially diluted by a factor of 2:3 horizontally across 96-well plates from Corning, 25 μl per well. One column was reserved for controls. For the assays performed in the presence of RBC, type O+ human RBCs at 0 or 2.5×10^9 cells/mL were added in 50 μl aliquots to all wells. Following a 30-minute incubation, 50 μl of TSB, inoculated with 5×10^5 CFU/mL, was added to all wells, and plates were incubated overnight at 37 °C. Following overnight incubation at 37° C, the OD600 was measured (values of less than 0.1 were considered sterilized). To assess bacterial growth in the assays with RBC, the OD600 was measured after a second day inoculation with 10 μl of solution from the original plate added to 100 μl of sterile TSB followed by overnight incubation.

Hemolysis **assay**

Peptide was serially diluted in PBS starting at a concentration of 100 μM. The final volume of peptide in each well was 50 μl. To each well, 50 μl of RBCs in PBS at 2×10^8 cells/mL was added. As a positive lysis control, 1% triton was used. The mixtures were incubated at 37°C for 1 hour, after which they were centrifuged at 1000g for 5 minutes. After centrifugation, 10 μl of supernatant was transferred to 90 μl of DI H_2O in a fresh 96-well plate. The absorbance of released hemoglobin at 410 nm was recorded and the fractional hemolysis was calculated based on the 100% and 0% lysis controls.

SYTOX Green cytotoxicity assay

Hela cells and WI-38 cells were grown to confluency in T-75 flasks in complete DMEM (10% FBS). The day before cytotoxicity experiments, the cells were plated in a 96-well tissue-culture plate as described in the Alamar Blue assay above. The next day, in a separate 96-well plate, peptides were serially diluted in complete DMEM or serum-free DMEM with 0.1% SYTOX Green starting at a concentration of 100 μM (1st), 50 μM (2nd), which was followed by serial dilutions by a factor of 2:3 horizontally across the plate. The final volume of the peptide in each well was 104 μl. To perform the cytotoxicity assay, media was removed from the wells and replaced with the peptide solutions. No peptide and 20 μM Melp5, a highly lytic peptide, were used as negative and positive controls, respectively. The plate was read for fluorescence every 5 minutes for an hour with an excitation wavelength of 504 nm and an emission wavelength of 523 nm. Cytotoxicity was calculated based on the 100% and 0% lysis controls.

Circular dichroism (CD)

Peptide samples were prepared in 10 mM sodium phosphate buffer (pH 7) and at 30 μM. CD was collected using a Jasco J-810 spectropolarimeter, flushed with N_2. Scans were at 20 nm/s, 3 accumulations, and samples were at room temperature. The quartz cuvette path length was 0.1 cm. The spectra for a given sample was calculated by first subtracting the no peptide sample values and then zeroing the spectra to the average θ value from 250 to 260 nm. The mean residue ellipticity (MRE) was then calculated by the equation MRE = ε (Cn), where ε is the ellipticity, C is the molar concentration of peptide, and n is the number of residues.

Wound infection model

All animal studies strictly adhered to protocol 131 which was approved by Tulane School of Medicine's *Murine* Institutional Animal Care and Use Committee. Female CD1 mice at 8-12 weeks of age were anesthetized via intraperitoneal injection of ketamine and xylazine at doses of 90 mg/kg and 10 mg/kg, respectively. Their dorsal surface was depilated using an electric razor and scrubbed with a chlorhexidine solution. A full thickness biopsy wound was generated using a 5 mm biopsy punch (Integra). To function as a splint for the wound, a silicone (Invitrogen) ring 0.5 mm thick with an outer diameter of 10mm and a hole with a 5mm diameter was placed over the wound and held to the skin with a surgical adhesive. The entire silicone ring was then covered with Tegaderm (3M), and further adhered using 4-0 braided silk interrupted sutures (Ethicon). Mice were given 0.05 mg/kg buprenorphine immediately following surgery as well as daily for the next two days to alleviate pain from the procedure. Wound beds were infected by penetrating the Tegaderm with an insulin syringe and injecting $1x10^4$ colony forming units (CFUs) of *P. aeruginosa* (PA01) and MRSA suspended in 10 µL sterile PBS directly onto the wound bed. All bacteria used were pelleted during early exponential growth phase prior to infection. Four hours after infection mice were topically treated with 2mM D-CONGA-Q7, or 0.025% acetic acid (vehicle control) in a 20µL volume, by penetrating the Tegaderm with an insulin syringe and injecting the treatment directly on the wound bed. Treatment was administered every 8 hours for the first 5 days of infection. Mice were imaged daily for two weeks using the *in vivo* imaging system (IVIS)-XMRS (PerkinElmer) and bioluminescence generated from the bacteria was quantified in values of radiance (photons/sec). Weight, activity, posture, coat condition and wound condition were monitored each day throughout the duration of the experiment to ensure the wellbeing of each mouse.

Scanning electron microscopy

Tegaderm dressings were removed from the wounds of each mice on Day 3 after surgery.

Tegaderm were washed with PBS and attached to hydroxyapatite discs placed

horizontally in 24-well microtiter plates. Following this, the Tegaderm was fixed by

placing the discs in 200 μl of 2.5% glutaraldehyde. The fixed samples were dehydrated

using increasing concentrations of ethanol and then desiccated with CO_2 critical point

drying. The samples were carbon coated and subjected to scanning electron microscopy

with a Hitachi S-4800 high-resolution microscope.

Results

Development of rational variants of the lead peptide D-CONGA

To study the roles of different residues of D-CONGA and possibly further

improve its antimicrobial abilities, we developed 13 rational variants of D-CONGA. We

further characterized them based on their antimicrobial activity against three bacterial

species and cytotoxicity in RBCs and WI-38 cells (figure 4-1 and figure 4-3). D-CONGA

has 13 residues with basic terminal cassettes of two arginines (RR). The nine-residue core

consists of hydrophobic residues at positions 3,4 and 7 to 11 and polar, cationic R at

position 5 and 6. To test if the central hydrophobic core, as it appears, is critical for D-

CONGA activity, the core was separated by inserting achiral glycine (G), beta alanine

(A), and polar glutamine (Q) after position 6 of D-CONGA to form three variants D-

CONGA-G7, D-CONGA-βA7, and D-CONGA-Q7. This group of variants was named

insertions (Figure 4-1 B). The core hydrophobicity was also reduced by deleting A in

positions 4 and 10 to form D-CONGA-ΔA4 and D-CONGA-ΔA10. The importance of

the basic terminal cassettes was tested by deleting the R at C terminus, which led to the

formation of D-CONGA-ΔR13. This group of variants obtained via removal of amino acid was named deletions.

To verify if the position of each hydrophobic core residue affects the activity of D-CONGA, amino acids at positions 7-11 (LAFAF) and positions 3-6 (WARR) were interchanged to form D-CONGA-FLIP. Furthermore, the effects of change in flexibility of D-CONGA on its activity was also tested by changing the residues R at position 5 and A at position 10 to L- amino acids, which formed D-CONGA-L (R5, A10). We have discussed in previous chapters that antimicrobial peptides in D-form, including D-CONGA, are more effective than their L-form counterparts. To test the theory that this is due to proteolysis, L-CONGA-D (R1, R13) with all L residues except the terminal D-R in positions 1 and 13 was constructed. The D residues at the ends of the peptide are expected to inhibit the initiation of proteolysis. Similarly, to determine the necessity of amphipathic R at positions 5 and 6 for the activity of D-CONGA, these residues were swapped for more polar homo-arginine, with a longer side chain, or less polar nor-arginine, with a shorter side chain, to get the two D-CONGA variants, D-CONGA-HomoR and D-CONGA-NorR. These five peptides formed by changing the positions of amino acids within the peptide sequence and by interchanging the amino acids into different forms of themselves, based on enantiomeric property and polarity, were grouped as swaps (figure 4-1 B). Next, the importance of the linear structure of the peptide was tested by cyclizing L-CONGA. The linear L-CONGA was converted to cyclized form using hydroxide (OH) at the C-terminal to form L-CONGA-OH cyclized. For another cyclized version, L-CONGA-E cyclized, a residue, glutamate (E), was added to the C terminus to facilitate the cyclization (figure 4-1 B). Prior to the characterization of the

138

variants for their bactericidal activity and cytotoxicity, we examined the secondary structure of the peptides using CD spectroscopy in buffer. The CD spectrum for D-CONGA and its variants exhibit a single minimum at ~200 nm (maximum for D-peptides), indicating a random coil secondary structure (figure 4-2).

 Characterization of D-CONGA Variants.

The variants were then characterized, and their bactericidal activity was compared with lead peptide D-CONGA (figure 4-3). Minimum inhibitory concentrations (MICs) of each peptide against gram-negatives, *E.coli* and *K.* pneumonia, and gram-positive, *S. aureus*, was assessed in the presence and absence of RBCs. Their cytotoxicity in RBCs and normal human fibroblast cells, WI-38, was also determined (figure 4-3).

In comparison to D-CONGA, D-CONGA-ΔA4, from the group deletions, had similar bactericidal activity. The decrease in the hydrophobicity in N terminal of D-CONGA did not affect its cytotoxicity either. D-CONGA-ΔA4 caused low hemolysis at 100μM, and its cytotoxicity in fibroblast cells was similar to that of the lead peptide. Surprisingly, D-CONGA-ΔA10, another variant from the group deletions with reduced hydrophobicity in C-terminal, showed no activity against *K. pneumonia* in RBCs and reduced activity than D-CONGA against *S. aureus* in the presence and absence of RBCs. D-CONGA-ΔA10 caused very low hemolysis and had reduced toxicity than D-CONGA against fibroblast cells, as demonstrated by a two-fold increase in the EC_{50}.

D-CONGA-FLIP, from the swaps group of variants, had very similar antibacterial characteristics as D-CONGA with a slight reduction in cytotoxicity against fibroblast cells. This demonstrates that as long as the net charge and thus, the residues are the same in the sequence of D-CONGA, their position does not affect the overall activity of the

peptide. Removal of the terminal R, which was selected in 8 out of 9 peptides in the screen of the second-generation library, caused loss of function. D-CONGA-ΔR13, from the group deletions, was not able to sterilize *S. aureus* in the presence of RBCs at the highest peptide concentration tested. D-CONGA-ΔR13 also had a substantial increase in the MIC against *S. aureus* in the absence of RBCs. Similarly, the attempt to change the flexibility of D-CONGA resulted in variant D-CONGA-L (R5, A10), from the group swaps, that had no activity against gram-positive *S. aureus*. However, D-CONGA-ΔR13 and D-CONGA-L (R5, A10) had low hemolysis and lowered cellular toxicity than D-CONGA. D-CONGA-L (R5, A10), especially had a very high EC_{50} at 2498 μM. Thus, these two peptides must be further investigated as potential broad-spectrum AMPs against gram-negative bacteria.

Next, we tested another swaps variant, L-CONGA-D (R1, R13). The conversion of terminal Rs at positions 1 and 13 into D-form did not prevent the proteolysis of L-CONGA, with the resulting peptide having higher MIC against *E. coli* and no activity against *S.aureus*. As a result, although this peptide had the lowest hemolysis at 100 uM among all the variants and had lower cytotoxicity against fibroblast than D-CONGA, L-CONGA-(R1, R13) was one of the worst antibacterial peptides out of the 13 variants. The cyclization of L-CONGA did not help its antibacterial activities either. Among the two variants from the cyclized group, L-CONGA-E cyclized had low hemolysis but was not very active against tested bacteria. L-CONGA-OH cyclized had high hemolysis of 7% at 100 uM and higher MIC against *E. coli* and *S.aureus* than most variants. Due to this, we decided not to pursue these cyclized versions of L-CONGA further. Hence their activity against *S.aureus* in the presence of RBCs and their cytotoxicity against fibroblast cells is

not yet determined. Changing the polar side chain of R at positions 5 and 6 to shorter and longer hydrocarbon chain to produce the last two swaps variants had contrasting effects. Both peptides had low hemolysis. D-CONGA-HomoR had similar bactericidal characteristics, with its cytotoxicity against fibroblast being slightly higher than D-CONGA. However, D-CONGA-NorR had higher MICs than D-CONGA against all three bacterial strains, especially against *K. pneumonia* and *S. aureus*. Shortening the sidechain of the D-CONGA also caused a significant increase in the cytotoxicity against fibroblast.

The most promising antimicrobial variants of D-CONGA were the peptides from the group insertions. The three peptides were synthesized by separating the hydrophobic core of D-CONGA with amino acids G, βA, and Q at position 7. D-CONGA-βA7 had low hemolysis and very high EC_{50} against the fibroblast cells, making it the least toxic peptide among all the variants. It was also active against gram-negative *E.Coli* and *K.pneumonia* with MICs less than 2 μM. Unfortunately, D-CONGA-βA7 did not have any activity against gram-positive *S. aureus*. Thus, D-CONGA-βA7 can be a great candidate for antimicrobial peptides against gram-negative bacteria but is not a broad-spectrum antibiotic. The other two insertion variants, D-CONGA-G7 and D-CONGA-Q7, showed the best activity among all the 13 D-CONGA variants tested. D-CONGA-G7 had low MICs against all three bacterial strains. It had low hemolysis and was less toxic than D-CONGA against fibroblast cells with almost twice the EC_{50}. D-CONGA-Q7 had MICs less than 2 μM against gram-negatives, *E. coli* and *K. pneumonia,* and less than 5 μM against gram-positive *S. aureus,* making it a superior antimicrobial peptide to even D-CONGA. With low hemolysis, D-CONGA-Q7 was also less toxic than D-CONGA with EC_{50} approximately four times higher. This demonstrates that splitting the hydrophobic

core of D-CONGA with a polar residue can make it more potent and less toxic. We will test this hypothesis in Chapter 5 as we synthesize the third-generation antimicrobial peptide library based on D-CONGA and its variants. D-CONGA-Q7 had lower toxicity than D-CONGA-G7. For this reason, we chose D-CONGA-Q7 for further characterization.

Comparison of antibacterial activities of AMPs, D-CONGA and D-CONGA-Q7, with conventional antibiotics.

The most promising D-CONGA variant, D-CONGA-Q7, was tested for antimicrobial activity, in comparison with D-CONGA and 8 conventional antibiotics, against 14 drug-resistant clinical isolates of bacteria (figure 4-4 and figure 4-5). Four bacterial isolates were resistant to all of the conventional antibiotics tested. Three of these isolates, KP-2146 NMD-1, KP ST258C2, and KP ST258C3, were *K. Pneumonia* strains, and one was pan drug-resistant (PDR) *A. baumannii*. Even D-CONGA had very high MICs against two of these three resistant *K. Pneumonia* strains, KP ST258C2 and KP ST258C3, while it was able to sterilize KP 2146 NMD-1 and (PDR) *A. baumannii* at lower concentrations. Amazingly, D-CONGA-Q7 sterilized all four isolates resistant to conventional antibiotics, including two that showed some resistance to D-CONGA, with excellent MICs. Against KP 2146 NMD-1 and (PDR) AB, the MICs of D-CONGA-Q7 was less than 2 μM. Against the more resistant strains, KP ST258C2 and KP ST258C3, the concentrations of D-CONGA-Q7 required for sterilization of the pathogens were less than 15 μM.

KP-6, another isolate of *K. pneumonia*, and MRSA were resistant to 5 out of 8 conventional antibiotics: Gentamicin, Ceftazidime, Ampicillin, Tobramycin, and

Ceftriaxone. Ciprofloxacin, Trimethoprim, and Meropenem were able to sterilize KP-6 and MRSA with low concentrations. D-CONGA and D-CONGA-Q7 also displayed high activity against these two isolates. KP-CRE was also resistant to 5 antibiotics: Ceftazidime, Ampicillin, Ciprofloxacin, Tobramycin and Trimethoprim. KP-CRE had high MICs of 49.8 µM and 91.4 µM for Ceftriaxone and Meropenem as well. Gentamicin was the only antibiotic tested that showed great activity against KP-CRE. Even D-CONGA had a higher than usual MIC of 23.4 µM against the isolate. D-CONGA-Q7 still maintained its superiority, compared to D-CONGA and antibiotics, with MIC against KP CRE at 2 µM.

Three isolates of *K. pneumonia*, KP-46, KP-396 and KP- Morici, as well as two isolates of *P. aeruginosa,* PA mucoid and PA non-mucoid, were all resistant to Ceftazidime and Ampicillin. All the other antibiotics and the two AMPs showed excellent activity against the first two *K. Pneumonia* isolates, KP-46 and KP-396. However, Trimethoprim had lower activity against KP-Morici and both isolates of *P. aeruginosa*. Gentamicin, Ciprofloxacin, Tobramycin, and Meropenem were able to sterilize KP-Morici and PA mucoid and non-mucoid strains at low concentrations. Among the three bacterial isolates, Ceftriaxone was potent against KP-Morici and PA non-mucoid but did not have much activity against PA mucoid demonstrated by its MIC at 124 µM. D-CONGA and D-CONGA-Q7 both had great bactericidal activity against all the 5 isolates. Lastly, KP- 398, a *K. pneumonia* isolate, was resistant towards only Ampicillin, although it had very high MIC for Ceftazidime. D-CONGA at MIC 31.6 µM also displayed lower than usual activity against KP-398. The remaining antibiotics and D-CONGA-Q7 were able to sterilize KP-398 in relevant concentrations.

Hence, among the conventional antibiotics and the two tested AMPs, only D-CONGA-Q7 and D-CONGA were able to sterilize 100 percent of the isolates, with D-CONGA-Q7 achieving sterilization at the lowest concentration (figure 4-6). Meropenem performed highest among antibiotics with 64% sterilization of the tested isolates. The least performing antibiotic was Ampicillin which failed to sterilize any of the isolates. With this experiment, we were able to show that our rational variant D-CONGA-Q7 outperform its predecessor D-CONGA, in both bactericidal activity and lack of toxicity, and is superior to most of the conventional antibiotics currently used to treat resistant bacterial infections in hospital settings.

Assessment of the AMP D-CONGA-Q7 against gram-positive and gram-negative bacterial infections in a murine wound model.

As described in chapter 3, Skin and soft tissue infections (SSTIs) are highly prevalent in humans. They cause more than 14 million ambulatory visits and more than 6 million emergency room visits in the United States annually[22,23]. The involvement of multi-drug resistant pathogens, such as *Pseudomonas aeruginosa* and methicillin-resistant *Staphylococcus aureus* (MRSA), further complicates SSTIs with increased hospitalization, health care costs, and overall mortality. The most optimal therapeutic treatment for these infections is topical antibiotics. However, with the emergence of rampant resistance against topical antibiotics that are often used to treat these infections, new treatment options for bacterial SSTIs are crucial. In chapter 3, we used our lead peptide, D-CONGA, on a full thickness excisional splinted wound model to evaluate its efficacy for treating SSTIs and chronic wounds. D-CONGA was an excellent AMP that was able to inhibit the bacterial burden by 2 to 3 logs against wounds infected with *P.*

aeruginosa and by 4 logs against wounds with MRSA. Earlier in this chapter, we have demonstrated that the rational variant D-CONGA-Q7 is a better antibiotic than D-CONGA against three laboratory strains and 14 multi-drug resistant clinical isolates of gram-positive and gram-negative bacteria. The EC_{50} of D-CONGA-Q7, the concentration required for the AMP to cause 50% WI-38 cell death, is four times higher than D-CONGA. Due to its great *in vitro* activity, we believe that D-CONGA-Q7 will surpass D-CONGA and have more significant effects on murine wound infections as well.

A complex wound environment similar to that described in chapter 3 was established in healthy adult CD1 mice. Briefly, a full thickness surgical punch wound was created on the dorsal surface of mice. A silicone ring was sutured around the wound to prevent healing through skin contraction, and Tegaderm dressing was placed over the ring to promote healing. The wounds were infected either with 10^4 CFUs of luminescent MRSA or 10^4 CFUs of luminescent *P. aeruginosa*, strain PA01. The first treatment was performed approximately 3 hours post-infection. Weak acetic acid, used as a solvent to dissolve the peptide, was used as the negative control. Whole animal imaging was performed to quantify bacterial burdens on the wound through bioluminescence.

75 μg of D-CONGA-Q7 in 20 μl of 0.025% acetic acid was administered every 8 hours for the first 5 days. The Tegaderm was removed on day 3 post-surgery and fixed in 2.5% glutaraldehyde for scanning electron microscopy (SEM). When wounds were infected with luminescent *MRSA*, and treated with vehicle only, they remained infected with high bacterial burdens to almost 5 subsequent days even after the Tegaderm was removed on Day 3. In contrast, the *MRSA* infected wounds treated with D-CONGA-Q7 had a dramatic 4 and half log decrease in luminescence in peak infection days 2 and 3.

This reduced bacterial burden, close to the background level, remained constant throughout the 14 days of the experiment. In fact, 4 out of 5 mice with wounds infected with MRSA and treated with D-CONGA-Q7 did not develop the infection even after the treatment was ceased in Day 5. Hence, D-CONGA-Q7 was able to completely sterilize the wound bed for these 4 mice (figure 4-8). For *P. aeruginosa infection*, the wound treated with vehicle displayed a dramatic increase in the bacterial burden for 3 days. After the removal of Tegaderm on day 3, the infection resolved. The treatments, every 8 hours with 75 µg of D-CONGA in 20 µl of 0.025% acetic acid, resulted in 2 to 3 logs of reduction in luminescence at the peak of infection. While the bacterial burden increased after the treatment with D-CONGA-Q7 stopped, it remained lower on peptide treated wounds throughout the experiment (figure 4-7). As described in chapter 3, the mice were monitored for weight, coat condition, wound condition, and overall health. These scores indicate that peptide-treated animals maintain similar health and wound pathology as the vehicle-treated mice (figure 4-12). In both cases, the silicone rings on mice fell off between days 6 to 13. Thus, D-CONGA-Q7 was successful at treating *MRSA* and *P.aeruginosa* infection in the mouse wound bed. It showed similar effects as D-CONGA against *P. aeruginosa*, but it was a superior antibiotic than D-CONGA against MRSA. D-CONGA-Q7 was also tested for its ability to inhibit bacterial colonization and biofilm formation on the Tegaderm dressing. Tegaderm dressings, fixed in 2.5% glutaraldehyde, were examined by SEM for bacteria and bacterial biofilms. Like D-CONGA, the Tegaderm from infected animals treated with the vehicle control has evidence of individual MRSA-like cocci or *Pseudomonas*-like rods. It also shows complex three-dimensional (3D) matrices containing bacteria, consistent with organized bacterial

biofilms. The Tegaderm films from animals treated with D-CONGA-Q7 illustrated marked inhibition in bacterial colonization and no indication of organized biofilms. All the Tegaderm dressing from wounds of mice infected with *P.aeruginosa* and *MRSA* and treated with vehicle showed bacterial cells and complex biofilm structure. In vehicle-treated *P.aeruginosa* Tegaderm, all 33 dressings had bacteria. In peptide-treated samples, bacteria was only observed in 8 out of 28 samples, and no biofilms were visible ($P < 0.0001$, for both, the proportion of positive samples and cell count) (figure 4-9). For MRSA-infected animals, *cocci*-like bacteria was observed in all 35 of the vehicle-treated samples, but only in 3 of the 35 peptide-treated samples ($P < 0.0001$, for both, the proportion of positive samples and cell count) (figure 4-10).

We also used one mouse each, with reduced D-CONGA-Q7 administrations, to look at the concentration-dependent effects of the peptide on the wound infection of *P. aeruginosa*. The peptide volume and concentration were the same, but the treatments were performed once or twice a day for five days. Hence, these two mice were getting 75 μg or 150 μg of peptide administrations per day for 5 days instead of 225 μg when the administrations are performed 3 times a day (figure 4-11 A). Even with the reduction in peptide administrations, D-CONGA-Q7 was able to slightly inhibit the growth of *P.aeruginosa* for the first few days of treatment. Still, the reduction in bacterial burden was not significant. The SEM performed on the Tegaderm taken from these mice showed rod-like *P. aeruginosa* and organized biofilms (figure 4-11 B). Hence, our regimen for peptide treatment is optimum to inhibit gram-positive and gram-negative bacterial infections on murine wound models. Anything less than 75 μg peptide treatment 3 times a day is not an effective regimen against bacterial infections in this wound model.

Discussion

The primary objective of this project was to synthesize variants of D-CONGA and study how different alterations in the sequence and structure of D-CONGA affect its activity. Through this process, we hoped to potentially characterize peptides that retain the activity of D-CONGA with improved bactericidal activity and reduced cytotoxicity. We synthesized and characterized 13 variants. 10 out of the 11 variants evaluated for cytotoxicity showed lower toxicity against WI-38 cells. 11 out of the 13 variants had minimum hemolysis of less than 1%. The experiments performed in the presence and absence of RBCs demonstrated that most variants had excellent activity against gram-negative bacteria, *K. Pneumonia,* and *E. coli*, but only 5 out of 13 variants could sterilize gram-positive *S. aureus* in concentrations less than 10 μM. The best peptides among the 13 variants based on minimum hemolysis and low toxicity were D-CONGA-G7, D-CONGA-Q7, and D-CONGA-βA7. Hence, the splitting of the hydrophobic core of the D-CONGA resulted in a decrease in cytotoxicity. Although D-CONGA-βA7 was the least toxic of the variants, it completely lost its activity against gram-positive *S. aureus*. The other two had similar antibacterial activity, but D-CONGA-Q7 had lesser toxicity which alludes to the significance of sequence composition in the function of AMP. D-CONGA-Q7 also had better activity against all the bacterial strains tested and lower cytotoxicity against human fibroblast cells, WI-38 cells, than even D-CONGA. In fact, EC_{50} of D-CONGA-Q7 for WI-38 cells is four times higher than that of D-CONGA. Thus, owing to the broad-spectrum activity, low cytotoxicity, and minimum hemolysis, D-CONGA-Q7, which varies from D-CONGA with only one amino acid at position 7 is selected for further characterization.

The clinical implementation of D-CONGA-Q7 could provide a new broad-spectrum treatment against resistant bacteria often encountered in hospital settings. To confirm the superior antimicrobial activity of D-CONGA-Q7, a head-to-head evaluation was performed where D-CONGA-Q7 was tested with D-CONGA and 8 conventional antibiotics against 14 clinical isolates of resistant bacterial strains. The 8 antibiotics belonged to five different classes of Penicillin (Ampicillin), Aminoglycoside (Gentamycin and Tobramycin), Cephalosporin (Ceftazidime and Ceftriaxone), Carbapenem (Meropenem), and Pyrimidine inhibitor (Trimethoprim), which are typically the therapeutic regimen for drug-resistant infections. The 14 resistant bacterial strains were obtained from clinical isolates, mainly from patients in Tulane Hospital, New Orleans. The clinical isolates consisted of 10 *K. pneumonia* strains, a MRSA strain, a PDR *A. baumannii* strain, and one strain each of mucous and non-mucous *P. aeruginosa* from patients of cystic fibrosis. D-CONGA-Q7 outperformed D-CONGA as well as major conventional antibiotics. Even the two *K. Pneumonia* strains resistant to all the antibiotics and had high MIC with D-CONGA were sterilized by D-CONGA-Q7 at a concentration less than 15 μM. D-CONGA-Q7 exhibited similar superior activity against bacterial infection and biofilms on an animal wound model. Given this excellent bactericidal activity of D-CONGA-Q7, we believe we successfully discovered a variant that outperforms the lead peptide itself. Taken collectively, our results demonstrate the potentials of D-CONGA-Q7, which as a drug candidate can sterilize the growth of 14 resistant bacterial strains. The present study describes and successfully tests the SME approach to discover new AMPs that can fill up the pipeline for promising drug candidates in the battle against antibiotic resistance.

Figure 4-1

A)

D-CONGA	rrwarr lafafrr
D-CONGA-G7	rrwarrglafafrr
D-CONGA-Q7	rrwarrqlafafrr
D-CONGA-β7	rrwarrβalafafrr
D-CONGA-ΔA4	rrwrr lafafrr
D-CONGA-ΔA10	rrwarr laffrr
D-CONGA-flip	rrlafa fwarrrr
D-CONGA-ΔR13	rrwarr lafafr
D-CONGA-R5A10	rrwaRr lafAfrr
L-CONGA-r1R13	rRWARR LAFAFRr
D-CONGA-E cycl.	RRWARR LAFAFRRE
D-CONGA-OH cycl.	RRWARR LAFAFRR-OH
D-CONGA- homoR	rrwahh lafafrr
D-CONGA- norR	rrwann lafafrr

B)

Insertions: rrwarr lafafrr

1. D-CONGA-G7   g
2. D-CONGA-Q7   q
3. D-CONGA-βA7   βa

Swaps: rrwarr lafafrr

7. D-CONGA-L(R5,A10)   R   A
8. L-CONGA-D(R1, R13) rRWARR LAFAFRr
9. D-CONGA-FLIP   warr ⟷ lafaf

                       rrwa r   r   lafafrr

10. D-CONGA-HomoR   rrwa hr   hr   lafafrr
11. D-CONGA-NorR   rrwa nr   nr   lafafrr

Deletions: rrwarr lafafrr

4. D-CONGA-ΔA4   X
5. D-CONGA-ΔA10   X
6. D-CONGA-ΔR13   X

Cyclized: rrwarr lafafrr
12. L-CONGA-E cycl.   RRWARR LAFAFRRE
13. L-CONGA-OH cycl. RRWARR LAFAFRR-OH

Figure 4-1. Design and Synthesis of D-CONGA Variants. 13 rational variants of D-CONGA were synthesized. **A)** The sequences of D-CONGA variants. **B)** The variants can be divided into four broad groups based on the modification in the sequence of D-CONGA. Insertions were made by adding an amino acid in to D-CONGA sequence. Deletions were synthesized by removing an amino acid from D-CONGA sequence. Swaps contain 5 variants with position and amino acid swaps within D-CONGA. Lastly, cyclized are two variants made by the cyclization of D-CONGA.
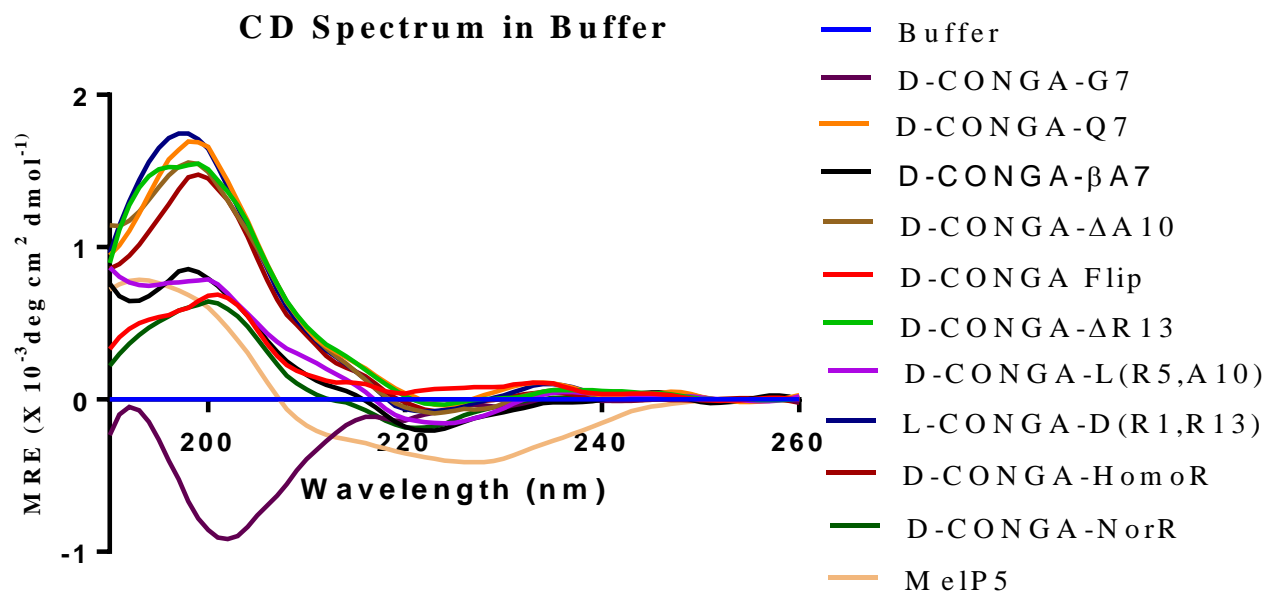
Figure 4-2

Figure 4-2. CD spectrum demonstrating the secondary structure of D-CONGA variants in buffer. Nominal peptide concentrations were 30 µM for all samples. Spectra were obtained in a 1 mm quartz cuvette at room temperature using a JASCO 810 CD spectrometer.

Figure 4-3

Peptides	Hemolysis at 100 µM	E. coli		K. Pneumoniae		S. Aureus		EC50, µM (WI-38)
		\-	+	\-	+	\-	+	
RBC (10⁹cells/ml RBC)	MIC in Broth Dilution, µM							
D-CONGA	0.06	1	0.8	4.4	3.8	5.7	6.3	110
D-CONGA-G7	0.07	1.3	1.4	1.7	4.4	6.4	6.9	235
D-CONGA-Q7	0.07	1	1.7	1.1	1.5	4.2	3.6	418.4
D-CONGA-βA7	0.02	1	1.3	1.4	1.5	30	30	6155
D-CONGA-ΔA4	0.02	1.6	2.8	4.5	6.2	3.2	2.3	142.9
D-CONGA-ΔA10	0.02	0.7	1.3	1.6	30	23.5	19	257
D-CONGA-FLIP	0.05	1	1.5	1.2	1.4	1.7	3.7	143.2
D-CONGA-ΔR13	0.03	0.9	0.6	2.1	2.1	27.1	30	300
D-CONGA-L(R5,A10)	0.04	1.4	1.4	2.3	2.2	30	30	2498
L-CONGA-(R1,R13)	0.01	20	26.2	5.1	9.3	30	30	134.3
L-CONGA-E cycl.	0.03	22.9	30	20	30	30	ND	ND
L-CONGA-OH cycl.	0.7	5.9	13.3	2.9	6	20	ND	ND
D-CONGA-HomoR	0.06	1.3	2.2	8	5.4	1.7	2.5	142.5
D-CONGA- NorR	0.03	1.9	2.4	13.3	11.8	7.6	17.2	66.02

Figure 4-3. Characterization of D-CONGA variants. MIC values are reported in μM peptide against gram-negative *E. coli* (EC), *P. aeruginosa* (PA), and gram-positive *S. aureus* (SA). The two columns under each organism are for assays performed in the absence (-) and presence (+) of 1×10^9 human RBCs/ml. MIC color codes are as follows: Yellow: Values for or similar to D-CONGA, Green: Value better than D-CONGA (lower MIC and hemolysis, higher EC_{50}), Red: Values worse than D-CONGA (higher MIC and hemolysis, lower EC_{50}). ">30" means that sterilization was not observed at 30 μM, the highest concentration tested. The column marked "hemolysis" is the fractional hemolysis of 1×10^8 human RBCs/ml at 100 μM peptide concentration determined from measurements of serially diluted peptide, starting from 100 μM. The column marked "EC_{50}" contains the concentration of peptide that kills 50% of WI-38 human fibroblast cells assayed by the entry of SYTOX Green DNA binding dye.

Figure 4-4

A)

Antimicrobial Agents	Classes
D-CONGA	AMP
D-Q7	AMP
Ampicillin	Penicillin
Gentamicin	Aminoglycoside
Tobramycin	Aminoglycoside
Ceftazidime	Cephalosporin
Ceftriaxone	Cephalosporin
Ciprofloxacin	Fluoroquinolone
Meropenem	Carbapenem
Trimethoprim	Pyrimidine Inhibitor of Dihydrofolate Reductase

B)

Clinical Isolates	References
KP (6)	Klebsiella pneumoniae
KP (46)	Klebsiella pneumoniae
KP 2146 (NDM-1)	Klebsiella pneumoniae
KP (396)	Klebsiella pneumoniae
KP (398)	Klebsiella pneumoniae
KP(St258 C2)	Klebsiella pneumoniae
KP (ST258C3)	Klebsiella pneumoniae
KP (ST258I2)	Klebsiella pneumoniae
KP (CRE)	Klebsiella pneumoniae
KP (Morici)	Klebsiella pneumoniae
MRSA	Methicillin-resistant Staphylococcus aureus
AB (PDR)	Acinetobacter baumannii
PA (CF mucoid)	Pseudomonas aeruginosa
PA (CF non-mucoid)	Pseudomonas aeruginosa

Figure 4-4. Conventional antibiotics and clinical isolates. A) The antimicrobial activity of D-CONGA and D-CONGA-Q7 was compared to eight conventional antibiotics from four different classes against **B)** 14 isolates of resistant bacterial strains obtained from hospitals. These isolates included gram-negative bacterial strains of *Klebsiella Pneumoniae, Pseudomonos aeruginosa* from patients with cystic fibrosis, and pan drug-resistant *Acinetobacter baumannii* as well as gram-positive methicillin-resistant *Staphylococcus aureus*.

Figure 4-5

Isolates	D-CONGA	D-CONGA-Q7	GEN	CAZ	AMP	CIPRO	TOB	TMP	CRO	MEM
					Antimicrobial Agents MIC, μM					
KP (6)	4.2	3.2	>150	>150	>150	9.4	>150	13.3	>150	0.2
KP (46)	4.4	2.2	1.6	>150	>150	0.2	3.5	1.3	1.9	0.4
KP 2146(NDM-1)	14.8	1.8	>150	>150	>150	>150	>150	>150	>150	>150
KP (ST396)	2	1.9	2	>150	>150	0.2	4.6	124	1.9	0.3
KP(St258 C2)	64.2	8.9	>150	>150	>150	>150	>150	>150	>150	>150
KP (ST258C3)	91.5	14	>150	>150	>150	>150	>150	>150	>150	>150
KP (ST258I2)	3.2	1.4	8.3	>150	>150	>150	>150	>150	>150	>150
KP (CRE)	23.4	2	5.2	>150	>150	>150	>150	>150	45	108.3
KP (Morici)	5	2.4	1.9	>150	>150	0.2	7.5	124	0.3	0.2
MRSA	2.6	1.5	>150	>150	>150	0.8	>150	3.2	>150	>150
AB (PDR)	2.4	1.1	>150	>150	>150	>150	>150	>150	>150	>150
PA(mucoid)	4.4	4.2	5.5	115.9	>150	4.2	4.2	74.7	137.2	13.3
PA(non-mucoid)	1.3	1.1	8.3	>150	>150	5.6	5.9	74.7	88.45	4
KP (398)	31.7	3.8	1.9	132.7	>150	0.2	6.9	17.6	0.2	0.2

Figure 4-5. Comparison of D-CONGA and D-CONGA-Q7 to conventional antibiotics. MIC values for D-CONGA and D-CONGA-Q7 along with eight conventional antibiotics, are reported in μM peptide concentrations against 14 clinical isolates of resistant bacterial strains. Color codes are as follows: Yellow: Values for activity similar to D-CONGA, Green: Value better than D-CONGA (lower MIC), Red: Values worse than D-CONGA (higher MIC) ">150" means that sterilization was not observed at 150 μM, the highest concentration tested, and the strains were resistant against the antibiotics used.
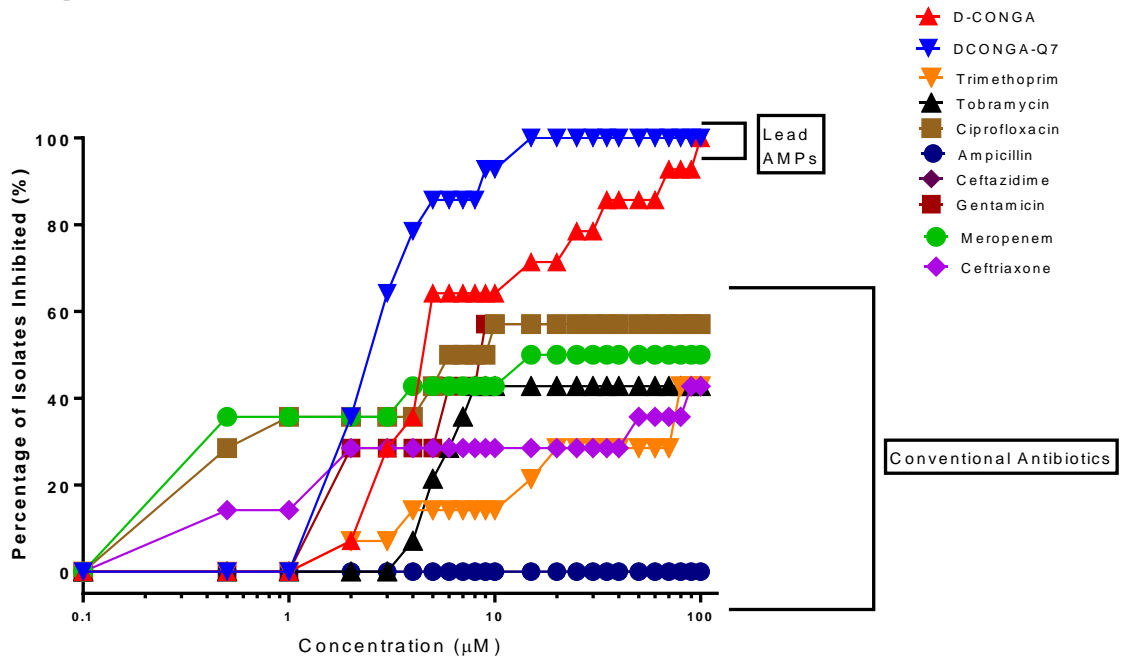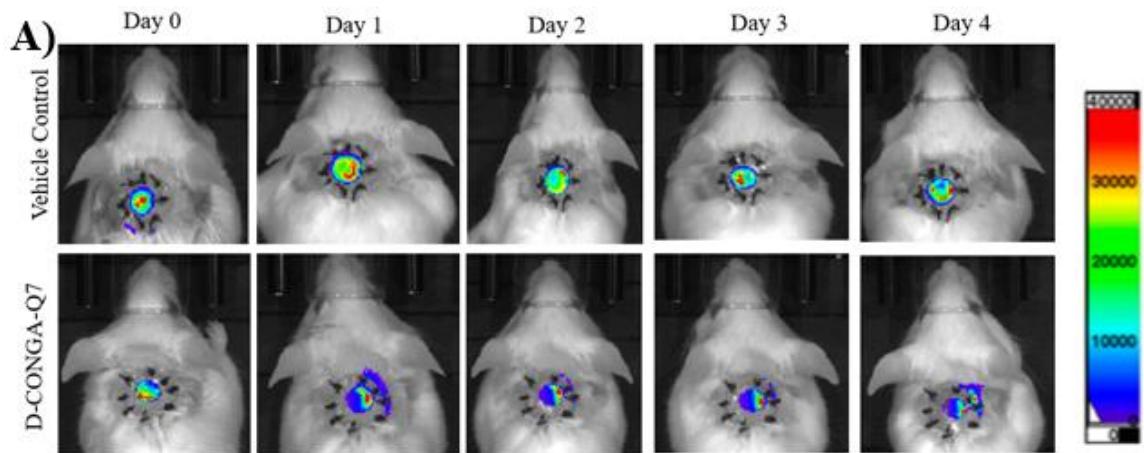
Figure 4-6

Figure 4-6. D-CONGA-Q7 is superior to D-CONGA and conventional antibiotics. Schematic representation of the percentage of resistant isolates sterilized by the AMPs and conventional antibiotics is described here. The x-axis represents the MIC in µM. The y-axis is the percentage of resistant isolates each antibiotic can eliminate in the given MIC. Different color labels for each antibiotic. The first two shown above are the AMPs, which are able to sterilize all the resistant isolates in the highest concentration tested.
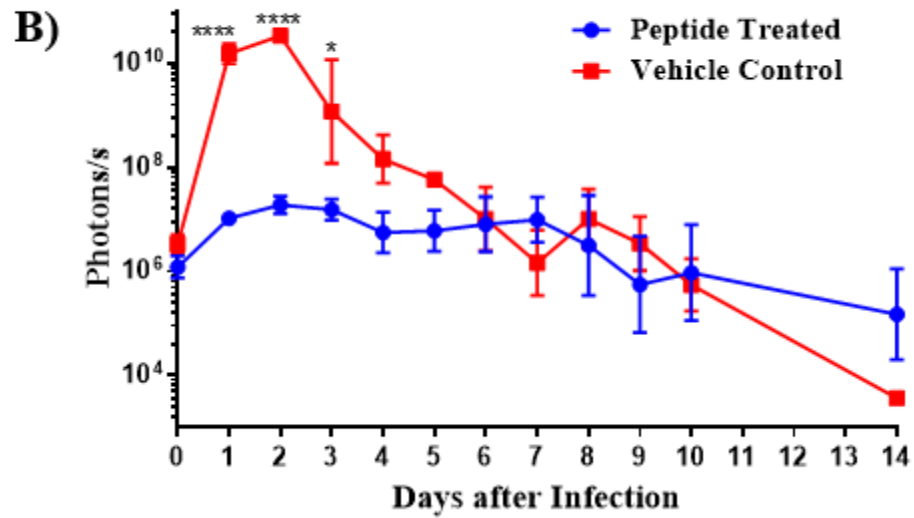
Figure 4-7

Figure 4-7. Animal model of deep surgery wound infection by *P.aeruginosa* treated with D-CONGA-Q7. Circular, dorsal puncture wounds were surgically created in healthy, adult CD1 mice, stabilized with a sutured silicone ring, and covered with Tegaderm dressing to better mimic infection and wound healing in humans. Wounds were infected with luminescent *P. aeruginosa* and were treated with D-CONGA-Q7 peptide or vehicle control every 8 hours until Day 4. An IVIS whole animal imager was used to measure luminescence in all animals once per day for 13 days after infection. **A)** Example of daily images of two mice infected with *P. aeruginosa* are shown. **B)** Total integrated radiance from the wound bed was measured daily in *P. aeruginosa.*
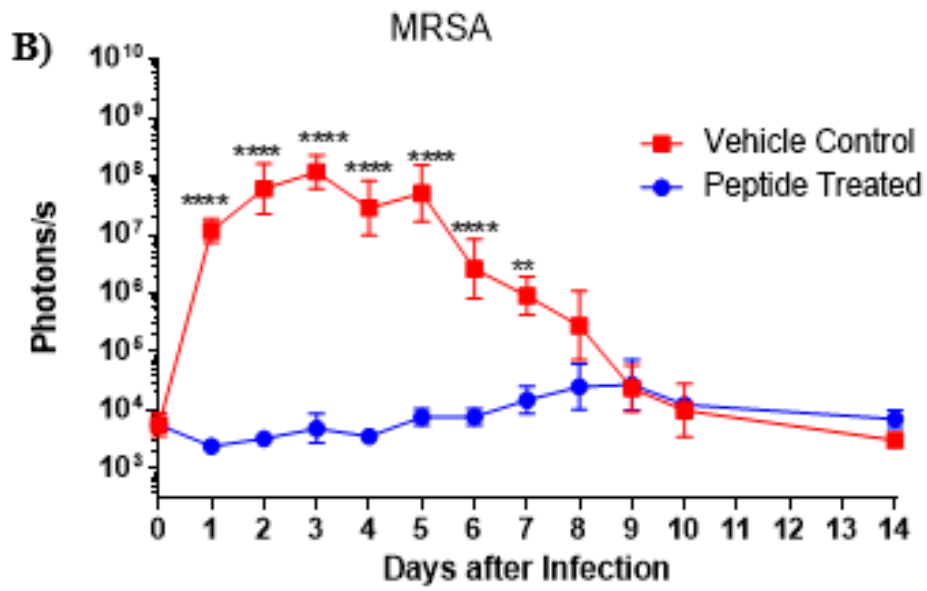
Figure 4-8

Figure 4-8. Animal model of deep surgery wound infection by MRSA treated with D-CONGA-Q7. The same surgical procedure was followed as described in figure 4-6. **A)** Example of daily images of two mice infected with *MRSA* are shown. **B)** Total integrated radiance from the wound bed was measured daily in *MRSA* infected mice. The pairwise d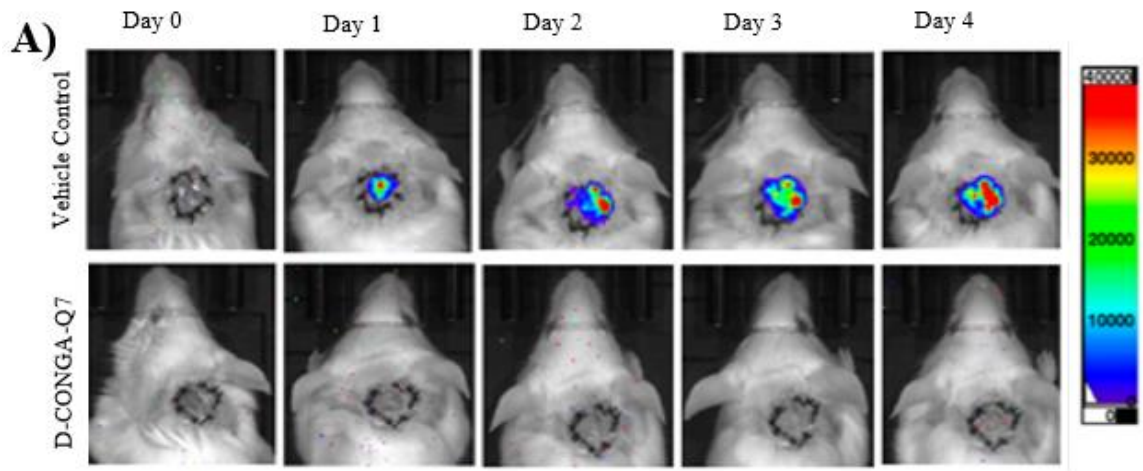ifferences are statistically significant, determined with a t-test on log values after applying the Bonferroni correction for multiple comparisons.

Figure 4-9

Pseudomonas aeruginosa

Figure 4-9. Representative scanning electron microscopy images of glutaraldehyde-fixed Tegaderm dressing from *P.aeruginosa* infected mice wound. The dressings removed from experimental animals on Day 3 is presented here in 1K and 10K magnifications. Scale bars are 50 μm for 1K magnifications and 5 μm for 10K magnifications. The top two images show vehicle controls with abundant biofilms and rod-like *P.aeruginosa* in all samples. The bottom two images point on the Tegaderm of wound treated 3 times a day with D-CONGA-Q7. They have few individual bacteria. No biofilm is observed, and only the Tegaderm adhesive is visible.
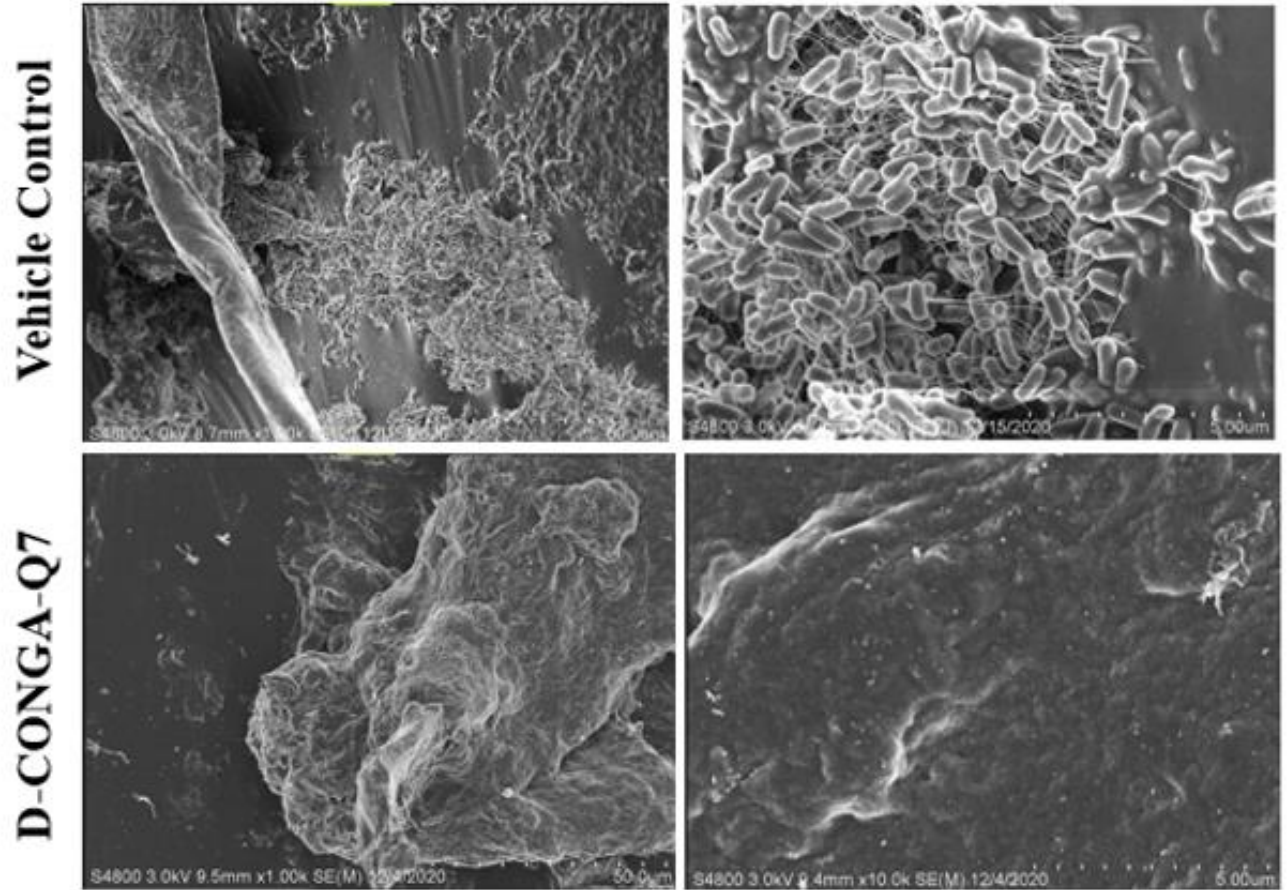
Figure 4-10

Figure 4-10. Representative scanning electron microscopy images of glutaraldehyde fixed Tegaderm dressing from MRSA infected mice wound. The dressings removed from experimental animals on Day 3 is presented here in 1K and 10K magnifications. Scale bars are 50 μm for 1K magnifications and 5 μm for 10K magnifications. The top two images show vehicle controls with abundant biofilms and cocci-like MRSA in all samples. The bottom two images point on the Tegaderm of wound treated 3 times a day with D-CONGA-Q7. They have few individual bacteria. No biofilm is observed, and only the Tegaderm adhesive is visible.
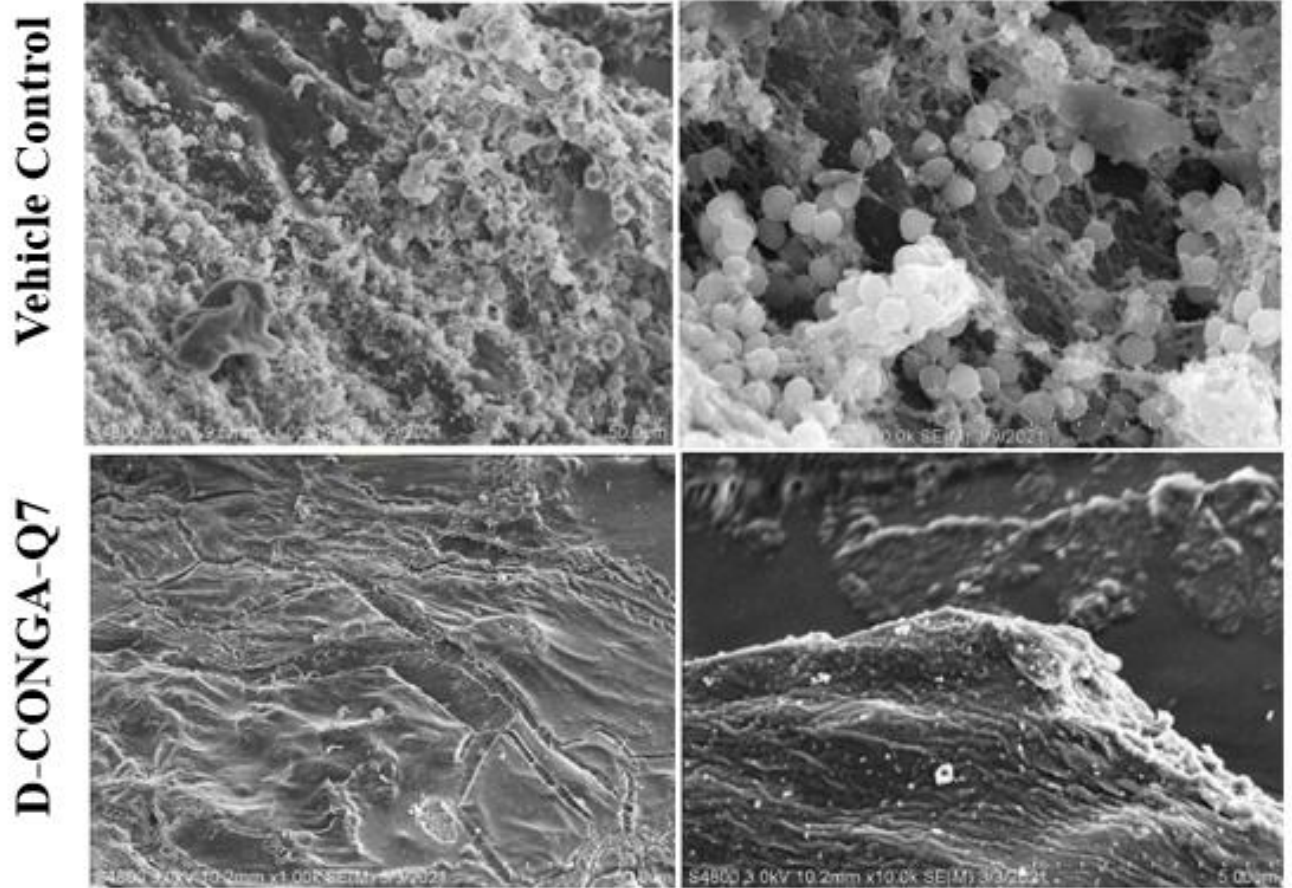
Figure 4-11

Pseudomonas aeruginosa

A)

Pseudomonas aeruginosa

B)

Figure 4-11. Animal model of deep surgery wound infection by *P.aeruginosa* treated with D-CONGA-Q7 once and twice a day. A) Total integrated radiance from the wound bed was measured daily in *P.aeruginosa* infected mice treated with vehicle. **B)** The SEM of the dressings removed from experimental animals on Day 3 is presented here in 1K and 10K magnifications. Scale bars are 50 μm for 1K magnifications and 5 μm for 10K magnifications. The top two images are the Tegaderm dressings from mice infected with *P.aeruginosa* and treated once a day with D-CONGA-Q7. The bottom two images point on the Tegaderm of wound infected with *P.aeruginosa* and treated 2 times a day with D-CONGA-Q7. They both have few individual bacteria. Biofilm is observed in both Tegaderm dressings.
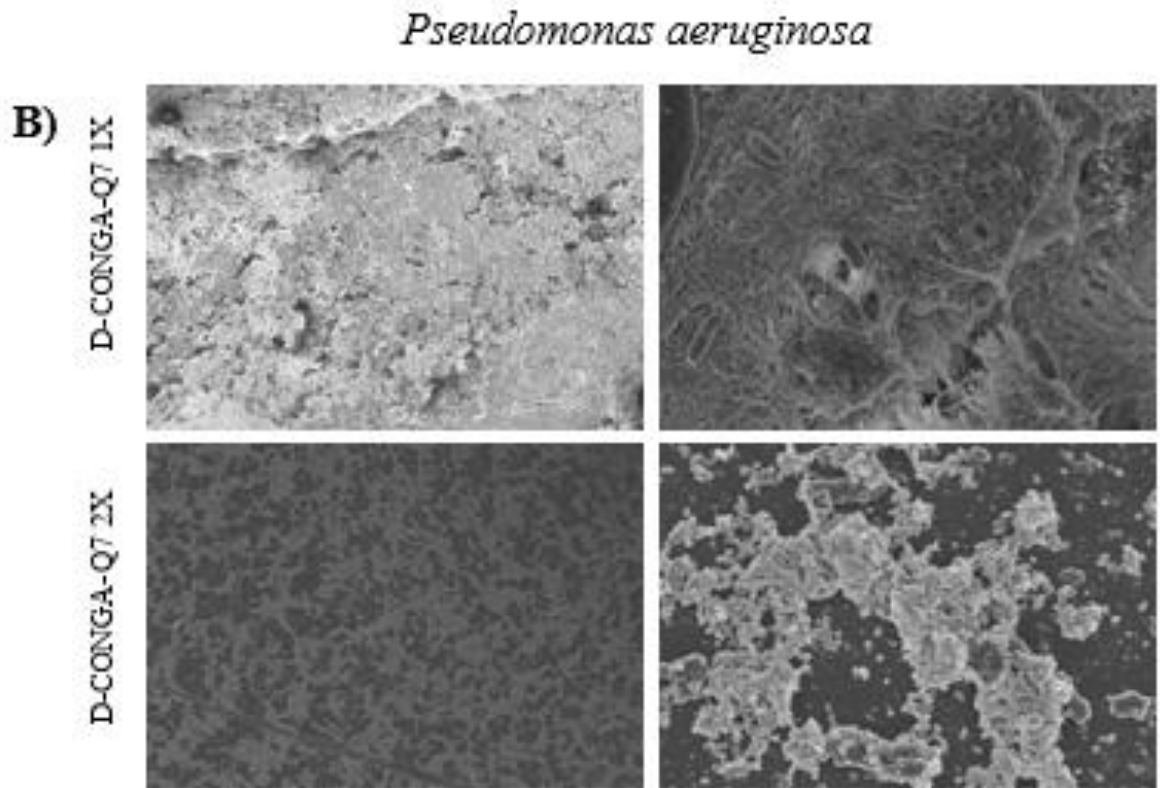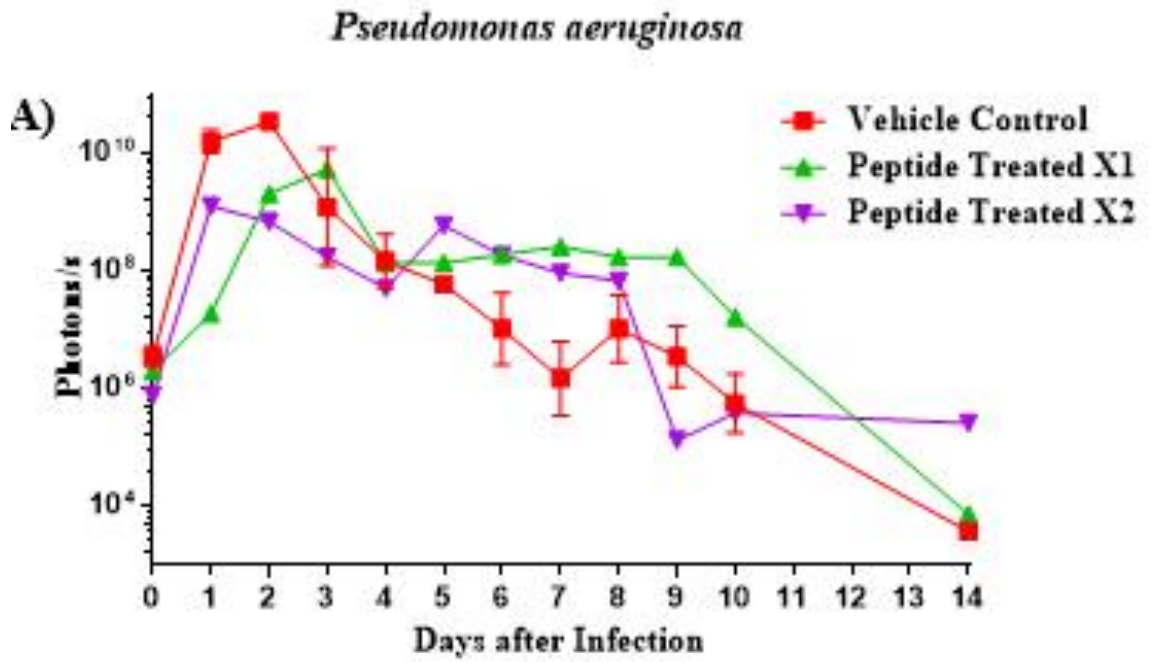
Figure 4-12
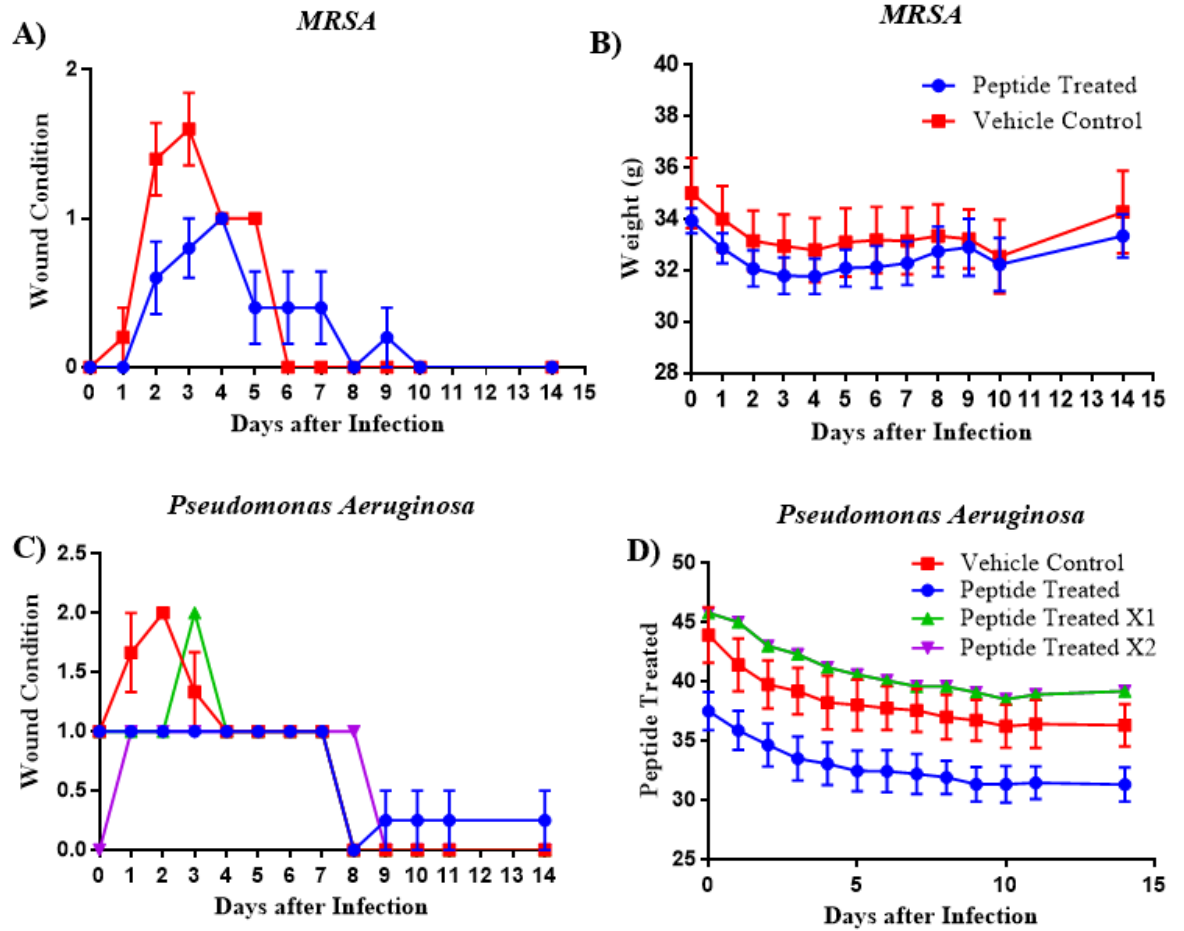
Figure 4-12. Post-surgery mouse monitoring data for wound infections treated with D-CONGA-Q7. A and C) The weights and **B and D)** wound condition of each mice was monitored every day for the 14 days of the experiment. The mice did not demonstrate any weight loss based on different bacterial infections or solvent treatments. There was no significant difference in the wound condition of mice treated with peptide versus the mice treated with vehicle control in *P.aeruginosa.* and *MRSA* infected mice.

CHAPTER 5: High-throughput screening of a combinatorial peptide library based on superior antimicrobial peptides D-CONGA-Q7

Introduction

As described in previous chapters, our laboratory has developed and extensively used an approach that we call synthetic molecular evolution (SME) to identify peptide drugs[1–4]. The approach involves the synthesis and screening of small, iterative peptide libraries under experimental conditions relevant to the physiological environment. This allows for the discovery of AMPs without impediments to activity *in vivo*. We approach these clinically pertinent conditions in a stepwise manner. First, a library is synthesized based on the characterization of natural peptides or peptides selected from a previous library. ARVA and NATT are broad-spectrum antimicrobial peptides selected from a *de novo* designed first-generation library. They were chosen via vesicle-based and multi organism-based screenings[5–7]. Further characterization of the two peptides demonstrated that these potent antibiotics lose their bactericidal activity in the presence of RBCs[8,9]. A second-generation library was designed and synthesized based on ARVA and NATT and was screened against multiple organisms in the presence of RBCs. This screen designed to identify peptides with antimicrobial activity in the physiologically relevant conditions, where eukaryotic cells are present, produced DBS peptides, which retained the potent antibiotic effects of ARVA and NATT in RBCs[2].

In this work so far, we have characterized the peptides obtained from screening the second-generation peptide library based on their bactericidal activity against ESKAPE pathogens, their hemolysis in RBCs, and their cytotoxicity in HeLa and WI-38 cells. Next, we used these peptide sequences that displayed some desired characteristics

and systemically modified them to identify antimicrobial peptides with higher

antimicrobial activity and lower toxicity. This process, often referred to as rational

sequence engineering, was utilized to design D-CONGA. D-CONGA was able to sterilize

all the ESKAPE pathogens in the presence and absence of RBCs and serum. It had very

low hemolysis. It did not develop resistance against *P.aeruginosa* for 10 generations. In

comparison, conventional antibiotics, and template peptide, ARVA, showed complete or

partial resistance within the 10 bacterial passages.

D-CONGA was also able to inhibit biofilm formation from gram-negative

Pseudomonas aeruginosa and gram-positive *Streptococcus mutans*. The EC_{50} of D-

CONGA for WI-38 was over 100 times higher than its MICs against all the pathogens

tested. Thus, we demonstrated that D-CONGA is suitable for *in vivo* experiments. We

investigated the efficacy of D-CONGA against *P.aeruginosa* and *MRSA* in a relevant

murine wound infection model. D-CONGA treatment resulted in 2 to 3 logs decrease in

bacterial burden for *P. aeruginosa* and 4 logs reduction in *MRSA* infection in the wound

model. However, systemic use of D-CONGA demonstrated toxicity in mice. The toxic

reaction that occurred immediately after peptide injection resulted in moribund mice with

intermittent seizure-like behavior, which was indistinguishable from anaphylaxis

symptoms and could be the result of a robust immune response called pseudoallergy.

As the next step in SME, we engineered 13 rational variants of D-CONGA. D-

CONGA-Q7, formed by the insertion of glutamine (Q) after the sixth position of D-

CONGA, had better antimicrobial activity than even D-CONGA. It was able to sterilize 3

laboratory strains and 14 drug-resistant clinical isolates of gram-positive and gram-

negative bacteria at low concentrations. It demonstrated better antibiotic effects than D-

CONGA and 8 conventional antibiotics, used as primary therapeutic regimens against multi-drug resistant bacterial infections. It had low hemolysis in RBCs, and the EC_{50} of D-CONGA-Q7 for toxicity in WI-38 was four times higher than that of D-CONGA. In a murine wound infection model, D-CONGA-Q7 was able to inhibit bacterial infection of *P.aeruginosa* and MRSA by reducing the bacterial burden in the wound in logs higher than that by D-CONGA. While the cytotoxicity in nucleated cells is lower with D-CONGA-Q7, the EC_{50} of the peptide may not be low enough for it to be considered as a potential therapeutic against systemic bacterial infections. In the next generation, we hope to select peptides with antimicrobial activity of D-CONGA-Q7 but reduced cytotoxicity.

Rational sequence engineering that led to the discovery of D-CONGA and D-CONGA-Q7 is beneficial but only allows for the exploration of small sequence spaces, which does not give us the freedom to study the contributions and interactions of different amino acids within a sequence. A better approach to successfully engineer a more selective antimicrobial peptide is the employment of high-throughput screening. Rational sequence engineering can be utilized again in the later stages to fine-tune the activity of the selected peptides after their sequence-activity relationships are more firmly investigated and understood. After two rounds of synthesis and characterization of rational variants based on the peptides selected from the second-generation library, we decided to design and synthesize a fresh third-generation peptide library (figure 5-1). This library, with 6912 unique members, used D-CONGA and D-CONGA-Q7 as the parent templates. The library screening gives us the advantage of exploring a much larger sequence space and increasing the potential of discovering antimicrobial peptides that

satisfy our desired criterion, which is the maintenance of antibacterial activity with low cytotoxicity.

High throughput screening of a large library can result in the selection of higher number of peptides that might appear to have the characteristics we desire. To justify the return on investment per selected peptide, a balance must be maintained between peptide throughput and the quality of the data recovered. Since the number of natural amino acid is limited to 20, the size of any peptide library is naturally constrained. The maximum number of possible sequence variants can be described by 20^x where x is the length of the sequence. To further limit the size of the peptide library and prevent it from growing exponentially, we have used combinatorial peptide library synthesis templated by D-CONGA and D-CONGA-Q7 in which we allow limited variation in a subset of positions in the sequence.

As with the previous libraries, we utilized solid-phase peptide synthesis (SPPS) method developed by Merrifield in 1963 to synthesize the third-generation combinatorial peptide library[10]. Combinatorial libraries can be broadly divided into two categories: indexed and non-indexed. The sequence identity of each member of an indexed library is readily available following synthesis[11–13]. While post-screening analysis is more straightforward, this method of library synthesis is only possible when libraries are small (~10^2-10^3 members). In contrast, a non-indexed library does not allow for the immediate identification of member peptides. It allows for a large library, but constant sequence deconvolution entails multiple synthesis cycles that require more time and resources[14]. Here, we have employed a combinatorial synthesis method called "one bead, one sequence". This technique can be considered "semi-indexed". It employs an approach

known as "split and recombine" (figure 5-2). The resulting library does not have members with readily known sequences, but individual sequences are physically separated on distinct beads and can be determined post-screen using Edman degradation or peptide LC-MS/MS[15,16]. Our laboratory has previously used this technique successfully in the synthesis of the first-generation and second-generation libraries that led to the discovery of ARVA and D-CONGA, respectively.

After the library synthesis, different solvents and techniques were used to cleave and extract individual peptide from each bead. We were able to extract less than 8 μM peptide consistently from each bead of the library. We adapted and optimized the broth dilution assay mentioned in earlier chapters to a high-throughput format such that each library member was assessed in a single well of a 96-well plate. The peptides were screened for activity against gram-positive *Staphylococcus aureus* in the absence of RBCs and gram-negative *Klebsiella pneumonia* in the presence of RBCs. The hemolysis for each selected peptide was also measured. Since the concentration of the extracted library member was usually less than 8 μM, any selected peptide that is able to sterilize *S. aureus* and *K. pneumonia* has very high broad-spectrum antimicrobial potency. The concentrations of peptides that were extracted from each bead were too low to screen for cytotoxicity against nucleated cells. However, when the MICs are low, reduced concentrations of selected peptides will be used for treatments against the wound and systemic infections. Low concentrations of peptides indicate lower cytotoxicity. Hence, by screening for peptides that can sterilize multiple pathogens in possibly sub micromolar concentrations, we are also selecting peptides that are functional without toxicity to nucleated cells. Lastly, in ongoing experiments, we are using Edman degradation and

LC-MS/MS to obtain sequence data for the screen positives. The sequenced peptides will be synthesized for post-screen validation.

Methods and Materials

Library Synthesis

The combinatorial peptide library was synthesized on TentaGel mega beads from Rapp Polymere (Tuebindin, Germany). 10 g of beads was hydrated prior to library synthesis. The loading capacity of the resin was amplified 3 times. First a lysine with two different N terminal protecting groups, FMOC and BOC, was conjugated to the resin. Glycine was added after removing FMOC, and another lysine with two of the same protecting groups, FMOC, was conjugated after removing BOC. The sidechains were also removed during the process. Beta-alanine was added to the two available positions on lysine. Prior to addition of amino acids, a UV-sensitive photo-labile linker was added to allow the peptides to be cleaved from the resin by exposure to UV-light. The library was synthesized using the "split and recombine" strategy for different combinatorial sites. Residues were added using standard solid-phase peptide synthesis (SPPS) principles for FMOC protected amino acids. Briefly, for each amino acid, FMOC is removed from the N-terminus of the growing peptide by treatment with 30% piperidine in DMF. Next residue is dissolved in HBTU/HOBt in DIPEA/DMF for activation and added to beads. When synthesis is complete, the sidechains are deprotected with incubation in Reagent B, which is a mixture of trifluoroacetic acid (88%), phenol (5%), water (5%), and triisopropylsilane (2%).

Peptide Extraction

A small amount of resin beads with library members were taken and affixed in a petri dish by adding dichloromethane (DCM) and allowing it to evaporate completely. The beads were then "pre-cleaved" by exposing the petri dish to UV light for five hours on each side. Prior to use in an antimicrobial assay(s), 150 µl of 100% ethanol was added to each well of a 96-well plate. Individual beads were picked from the petri dish using forceps and placed in a well (one bead per well). The plate was then incubated under UV-light with shaking for around 4 hours until the solvent evaporated. Next, 40 µl of 0.0025% acetic acid was added to all wells, and the plates were placed in room temperature for two hours. Prior to a screening assay, the peptide solutions were transferred to a fresh 96-well plate to separate peptide solution from synthesis resin, and the extraction plates were stored for indexing. The average concentration of extracted peptide was less than 6 µM.

Bacterial Strains and Growth Conditions

S. aureus ATCC 25923, and *K.Pneumonia* ATCC 13883 were used in this study. Overnight culture was prepared by adding a colony of bacteria into 5 ml fresh tryptic soy broth (TSB) and incubating it overnight in 37 °C. Subcultures were prepared the next day by inoculating 25 mL of TSB with 200 µl of the overnight culture. After the secondary culture was grown to log phase (OD600 = 0.3−0.6), cell counts were determined by measuring the OD600 (1.0 = 1.5x108 CFU/mL for *S. aureus* and 4x108 CFU/mL for *K. pneumoniae*). Bacterial cells were diluted to appropriate concentrations in TSB.

Broth Dilution Screen

The 40 µl of the peptide dissolved in 0.025% acetic acid was split into 3 aliquots. To each well in the 96 well plate with 8 µl of the aliquot, 21 µl of RBCs/ml at $2.4X10^9$ cells/ml

was added. This mixture was allowed to incubate for 30 minutes at room temperature. A *K. pneumonia* suspension at $2X10^5$ cells/ml was prepared in fresh TSB. 21 μl of this suspension was added to the RBC/peptide solution. The mixture was incubated overnight. To the second plate with 20 μl of the aliquot, 30 μl of *S. aureus* in suspension at a concentration of 1.7 $X10^5$ cells/ml was added. Both the plates were incubated at 37°C overnight. Because of the presence of dense RBCs, inhibition of bacterial growth was initially detected by the change in RBC coloration. The following day, 10 μls of the solution from the wells with *K. pneumonia* that appeared sterilized in the presence of RBCs and corresponding wells in the plate with *S. aureus* was plated onto TSB plates. These plates were incubated at 37 °C to verify the presence/absence of microbes. The samples which showed a complete absence of microbes were selected as the library member that was able to sterilize both pathogens. The third aliquot of the library member was left in the extraction plate and stored in 4°C for sequencing.

Human erythrocytes

Human O+ erythrocytes were obtained from Interstate Blood Bank, Inc. (Memphis, TN). RBCs were subjected to four cycles of centrifugation at 1000xg with resuspension in fresh PBS. Following the final wash step, the supernatant was clear and colorless. RBC concentration was determined using a standard hemocytometer.

Hemolysis

On the second day of the broth dilution screen described above, the wells with library peptides that were suspected to have sterilized *K.pneumonia* in the presence of RBCs was transferred to a microcentrifuge tube. The concentration of RBCs was diluted to $1X10^8$ cells/ml from $1X10^9$ cells/ml used to perform the broth dilution screen. The diluted

solutions of all the expected positive peptides were placed in 96 well plates. 1% triton and RBCs only were used for positive and negative controls, respectively. The plate was centrifuged at 1000xg for 5 minutes. After centrifugation, 10 μl of supernatant was transferred to 90 μl of DI H2O in a fresh 96-well plate. The absorbance of released hemoglobin at 410 nm was recorded, and the fractional hemolysis was calculated based on the 100% and 0% lysis controls. 1% triton with RBCs were further diluted 10 times to avoid overflow readings.

Results

Library Design and Synthesis

A combinatorial library was designed based on the sequence template of D-CONGA and D-CONGA-Q7. The library consisted of 6,912 unique members varying in length between 11 and 16 residues. There were 9 combinatorial sites with at least 43% sequence similarity to D-CONGA and D-CONGA-Q7. The terminal cassettes made by two arginines (RR) present in all potent peptides selected from the second-generation library were kept constant in this library. D-CONGA, characterized in chapter 2, was formed by removing invariant glycine from the N-terminal and C-terminal ends of the consensus sequence of the selected peptides from the second-generation library. While glycine was selected in the screen, the removal increased the activity of resultant peptides. Hence, we designed this library so that glycine was optional in the third and the eleventh position of the library members. Many aspects of the third-generation library design were based on the characterization of the 13 variants of D-CONGA as described in chapter 4. The hydrophobicity properties of the members of the library were varied in different ways. The alanine in fourth and tenth positions was present or absent in the

library members. The central core of the template sequence, which expands from positions 4-13, were altered with residues having different hydrophobic and electrostatic properties. Substitutions with different aromatic residues was also explored. Based on the success of D-CONGA-Q7, the hydrophobic central core was also split by addition of residues in the seventh position of the sequence. A representation of the library design principle is described in figure 5-1.

The library was synthesized using FMOC-based solid-state peptide synthesis (SPPS) reactions using the "split and recombine" method for combinatorial library generation. "Split and recombine" refers to a repetitive process, where for each position of the sequence in the library template, the synthesis resin is divided into several parts equal to the number of amino acid variations at that position. After the addition of unique residue into each of the resin parts, the resin beads are recombined, ensuring that every possible combination of residues occurs in the library (figure 5-2). The synthesis is performed on solid supports, in our case, TentaGel mega beads. The resins are usually FMOC-protected and should be deprotected before the incorporation of the first residue. Also, before the start of library synthesis, the resin was modified with branches using lysine as an attempt to increase the molar loading capacity of the beads by a factor of three. The library was synthesized in a linear fashion from the C -terminus to the N-terminus by repetitive cycles of NH_2 deprotection and amino acid coupling reactions. For some bulky C-terminal amino acids, double or even triple coupling may be required. Kaiser test is used to verify the deprotection of NH_2 group[17]. The same test also allows for the confirmation that complete coupling of the amino acid residue has occurred. Measurement of the absorbance of active NH_2 at 585 nm also permits for the

quantification of the peptide on the bead. Another way to measure the concentration of the peptide on the resin is through quantification of FMOC group released during deprotection of each residue[18]. Using these methods, the peptide on each resin was found to be approximately 6 nanomoles per bead, on average.

Post library synthesis, the small quantity of resins was affixed on a glass petri dish using DCM. The library members were then cleaved off from each resin bead by application of UV-light on both sides of the glass dish. The photolabile linker that connects the library members with the support bead is readily cleaved by UV-light, but the peptide remains attached to the bead. Hexafluoroisopropanol (HFIP) was used to extract peptide from individual beads during the second-generation library synthesis. However, for the third-generation library, the peptide concentration obtained after incubation of individual resin in HFIP under UV-light was much lower than expected. Hence, we used a series of different chemical compounds, including dimethylformamide (DMF), acetonitrile (MeCN), acetonitrile and water, 100% glacier acetic acid (AcOH), 0.025% glacier acetic acid, and ethanol (EtOH), in an effort to extract maximum concentration of peptide per bead. A variety of techniques was also used to amplify the removal of the peptide from the bead. Shake, sonication, heat, and UV-light secondary cleavage was all tested. Although still lower than what we had expected to extract from each bead, the comparison of known concentration of D-CONGA-Q7 with extracted peptide via HPLC showed that the maximum concentration of peptide could be extracted when the bead is incubated in 100% ethanol under UV-light until the solvent evaporates completely. 0.025% AcOH was then used to dissolve the peptide for screening.

Screening of the third-generation peptide library

Before initiating a large-scale screen, we wanted to verify the presence of peptides with antimicrobial activity. At the same time, we also needed to optimize the conditions for screen that will allow us to select for peptides that will have the desired characteristics. In this library, we want to screen for peptides with great bactericidal activity and low cytotoxicity in nucleated cells. Despite extensive attempts with different solvents and techniques, we could only extract peptides at concentrations of approximately 6 μM. Initially, we attempted to incorporate cytotoxicity assays in nucleated cells into our screening process. Even when all the extracted peptide was used, no quantitative cytotoxicity could be measured in Hela Cells. However, we were only able to use a fraction of extracted peptide for the assay as we require the rest for investigation of bactericidal activity against multi pathogens and sequencing purposes. When the cytotoxicity was measured, the signal from Alamar Blue assay and SYTOX Green assay was very close to the background level. From chapter 3, we know that D-CONGA and other peptides selected from the second-generation library are not very toxic up to 10 μM. Hence, this cytotoxicity signals from the library members is expected. Therefore, due to reduced extraction of library peptides, we could not incorporate cytotoxicity assay in this screen. However, we could use the small concentration of peptide to screen for sterilization against gram-positive and gram-negative bacteria. The selected peptides will be broad-spectrum antibiotics that are functional in low concentrations. Therefore, while the peptides cannot be selected based on their cytotoxicity, selecting peptides with very low MICs against multiple pathogens will automatically eliminate the need to use these peptides in higher concentrations that might be cytotoxic.

We designed a screen where we can select for peptides in stringent broth dilution assays. We know that the members from the previous library, including D-CONGA, retained their activity in RBCs. We expect the members of the third-generation library to behave similarly. However, we also wanted to select the peptides that had low hemolysis in RBCs. So, we performed the broth dilution screen in two different conditions (figure 5-3). Against *S.aureus*, we selected peptides in the absence of RBCs, while against *K.pneumonia*, the screen was conducted in the presence of RBCs. The hemolysis was measured for selected peptides from the plates that were incubated overnight in 37 °C with *K.pneumonia*. This approach of screen allows us to measure hemolysis while confirming the bactericidal activity of our selected peptides in the presence of RBCs (figure 5-4). Around 8000 beads were screened for activity against *S.aureus* and *K.pneumonia*. 63 of these peptides were able to sterilize *S.aureus,* and 105 were able to prevent *K.pneumonia* growth. 46 peptides, which is approximately 0.6% of the total tested, were able to sterilize both the pathogens (figure 5-5). 8 out of the 46 peptides showed hemolysis of less than 1%. 44 of these peptides had hemolysis of less than 10% (figure 5-6). Hence, we accomplished our goal with this screen and selected for broad-spectrum peptides that retain antimicrobial activity in very low concentrations. We are currently in the process of determining the sequences of the selected peptides via Edman degradation and LC-MS/MS.

Discussion

In principle, library-based peptide discovery follows a particular paradigm (1) creation of a pooled peptide library, (2) screening of the library under certain conditions for the isolation of selected peptides (3) peptide identification. In this chapter, we have

created a peptide library using SPPS, screened it for highly potent antibacterial activity, and isolated 46 peptides with desired characteristics. The next step will use sequencing techniques, such as LC-MS/MS and Edman degradation, to identify these hits. SPPS involves the consecutive addition of amino acids to a growing peptide chain. If every reaction of deprotection and coupling goes to completion, a pure full-length peptide is produced. However, the risk of side reactions and incomplete reactions always remains. Hence, each extracted peptide is not necessarily a full-length peptide library member. We compared the HPLC traces of extracted peptides with very similar D-CONGA-Q7. Most peptides had one distinct peak around the same retention time as D-CONGA-Q7. However, as compared to known concentrations of D-CONGA-Q7, the extracted peptides were low in quantity. This is not consistent with the measurements for total loaded peptide that we obtained from the quantification of the active NH_2 group and released FMOC during the library synthesis. We tried extensive methods to isolate the peptides from the beads. However, due to factors such as inadequate beads, ineffective photolabile linkers, inappropriate elution solvents, or some combination of them, complete cleavage, and extraction of peptides from the beads was not possible. We used the solvent and technique that consistently extracted a comparatively higher concentration of peptides from library beads.

Before the screen, we measure the concentration of some of the library members extracted from the beads. All 19 extracted peptides, tested by HPLC, had concentrations less than 9 μM. Among them, the majority, 12 out of 19 of the peptides, had concentrations of less than 6 μM. Hence, when split into aliquots, approximately 3 μM was used for the screen against *S.aureus*, 1.2 μM was used against *K.pneumonia* in the

presence of RBCs and 1.5 μM was stored for sequencing. In reaction plates with bacterial cells, the concentrations of extracted peptides were lower, most likely in sub micromolar concentrations.

At these sub micromolar concentrations, we had difficulty selecting for peptides that could sterilize *S. aureus* in the presence of RBCs. Characterization of members from the previous library has shown that our antimicrobial peptides usually are active in higher concentrations against *S.aureus* than most other pathogens. Additionally, these AMPs are not sensitive to the presence of RBCs. To fulfill our criterion that selects for peptides that sterilize the two pathogens in low concentrations and in the presence of eukaryotic cells, we designed a screen that includes RBCs for the screen against *K.pneumonia* but is performed without it against *S. aureus*. The RBCs from the sterilized cells in plates screened for *K.pneumonia* were diluted from $1X10^9$ cells/ml to $1X10^8$ cells/ml for quantification of peptide-induced fractional hemolysis. Out of the 7912 peptides screen, 46 peptides (0.6%) showed complete inhibition of both the pathogens. Thus, in this chapter, despite difficulties in cleaving and extracting library members from the beads of the third-generation library, we were still able to select many antimicrobial peptides with superior bactericidal activity.

Hence, the work presented in the chapter have brought us a full circle. We screened and selected peptides from second-generation library. We rationally optimized the first-generation hits, and then used the information obtained from the characterization of the selected peptides and their variants to design and synthesize the third-generation library. We screened the library and selected 46 superior peptides. Once again, we have

successfully used synthetic molecular evolution (SME) to isolate potent peptides that function in desired physiologically relevant conditions.

Future Direction

The next step in this process is sequencing of selected peptides for identification and further validation. We hope to have selected antimicrobial peptides that retain the activity of D-CONGA-Q7 with diminished cytotoxicity. The techniques we are using for sequencing include Edman degradation and liquid chromatography with tandem mass spectrometry (LC-MS/MS). Edman degradation was first identified by Pehr Edman, which labels and cleaves peptides from N-terminal without disrupting the bonds between other amino acids. Edman and Beggs further automated it in 1967, which is now used widely for peptide and protein sequence[19]. Concurrently, within the last two decades, a method for peptide and protein sequence determination by repeated mass spectrometry (MS/MS) has been developed and further refined mainly by the improvements of LC techniques combined with electrospray ionization (ESI). MS/MS technique is faster, more sensitive, and easily applicable to complex peptide[20–22]. This has resulted in gradual replacement of Edman degradation by LC-MS/MS. Consequently, MS-based proteomics has emerged as a new method of choice for the identification of proteins via database-supported interpretation of MS data.

We are also investigating different avenues to find alternative formulations and delivery systems for systemically and topically applied antimicrobial peptides. Our objective is to develop a system that delivers antimicrobial peptides in a sustained manner for an extended period of time. In this work, we have used 2 mM antimicrobial peptides 3 times a day for efficient inhibition of gram-positive and gram-negative

bacterial infection in a relevant murine wound infection model. Administration of the antimicrobial peptide one or two times a day was not an effective treatment against the infection. The use of a different delivery system and formulation could reduce the frequency of administrations and improve the bioavailability of antimicrobial peptides. Similarly, systemic intraperitoneal injection of our peptides produced rapid anaphylaxis-like conditions in mice. Slow release of the antimicrobial peptide could also help us circumvent this problem. Exposure to a smaller concentration of peptide at a given time could decrease the probability of immediate and severe reaction in mice.

The work described in this dissertation shows that one can use synthetic molecular evolution and rational variation to identify superior host cell- and tissue-compatible AMPs with lower cytotoxicity. The results demonstrate that the stringent selection conditions can lead to the identification of peptides that retain activity in the presence of concentrated RBCs and serum, do not cause hemolysis, and have little cytotoxicity in nucleated cells. These peptides are active in the very challenging environment of purulent wounds infected with drug-resistant bacteria and can treat infections and prevent biofilm formation under the same conditions. Here, we have discovered new improved peptides with each generation by applying SME. DBS peptides with activity in the presence of RBCs were selected through screening of peptide library based on ARVA and NATT. Rational variation of DBS peptides led to the discovery D-CONGA which in turn was used to design D-CONGA-Q7. Lastly, a new peptide library was synthesized based on D-CONGA and D-CONGA-Q7 that gave rise to peptides that are active in sub micromolar concentrations.

As discussed in previous chapters, antimicrobial resistance is a major public health crisis that causes worldwide morbidity and mortality. Unfortunately, the rise in antibiotic resistance is also accompanied by a decline in antibacterial drug research and development. Between 1940 and 1962, more than 20 new classes of antibiotics were marketed. Since then, only two new classes have reached the market. Two reports released by World Health Organization (WHO) in 2020 describes the weak development pipeline for antibiotic agents. The 60 products in development bring little benefit over existing treatments, and very few target the most critical resistant bacteria. Through the work we have presented here, we are aiming to tackle the dwindling antibiotics development pipeline by establishing SME as a reliable approach to produce efficient AMPs. The antimicrobial peptides discovered through this approach are expected to have a greater probability of success in the clinic in protecting and treating wounds against drug-resistant bacterial infections than other AMPs described in the primary literature. We believe that identifying these effective AMPs will increase the population of potentially viable AMP therapeutics that might successfully proceed into clinical trials. Eventually, as more AMPs fill up the development pipeline, our hope is one, or more, will succeed in becoming novel broad-spectrum antibiotics against multi-drug resistant bacterial strains.

Figure 5-1

"D-CONGA-Q7" template sequence

| R | R | X | W | A | R | R | X | L | A | F | A | F | X | R | R |

D-CONGA-Q7 based iterative combinatorial library

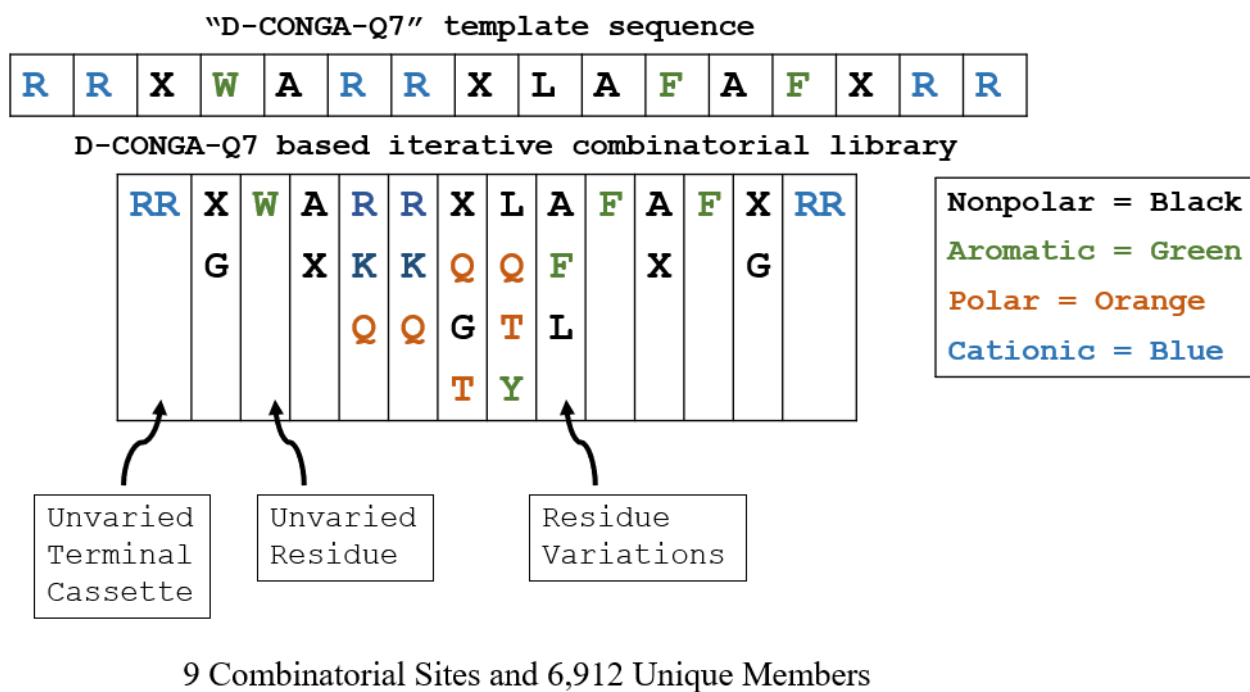9 Combinatorial Sites and 6,912 Unique Members

Figure 5-1. Design of the D-CONGA and D-CONGA-Q7 derived combinatorial library. A unique combinatorial library based on the antimicrobial peptides D-CONGA and D-CONGA-Q7 was synthesized. The library has 9 potential combinatorial sites yielding a total of 6,912 unique members. It was synthesized using solid-phase peptide synthesis (SPPS) principles for FMOC-protected amino acids. A macro-sized solid support resin, TentaGel bead, was used to enable easy separation of individual peptides post synthesis. The major concepts of the library design were based on the characterization of the variants of D-CONGA. The changes made in the hydrophobicity and electrostatic properties of the peptides are described in the figure using different colors.
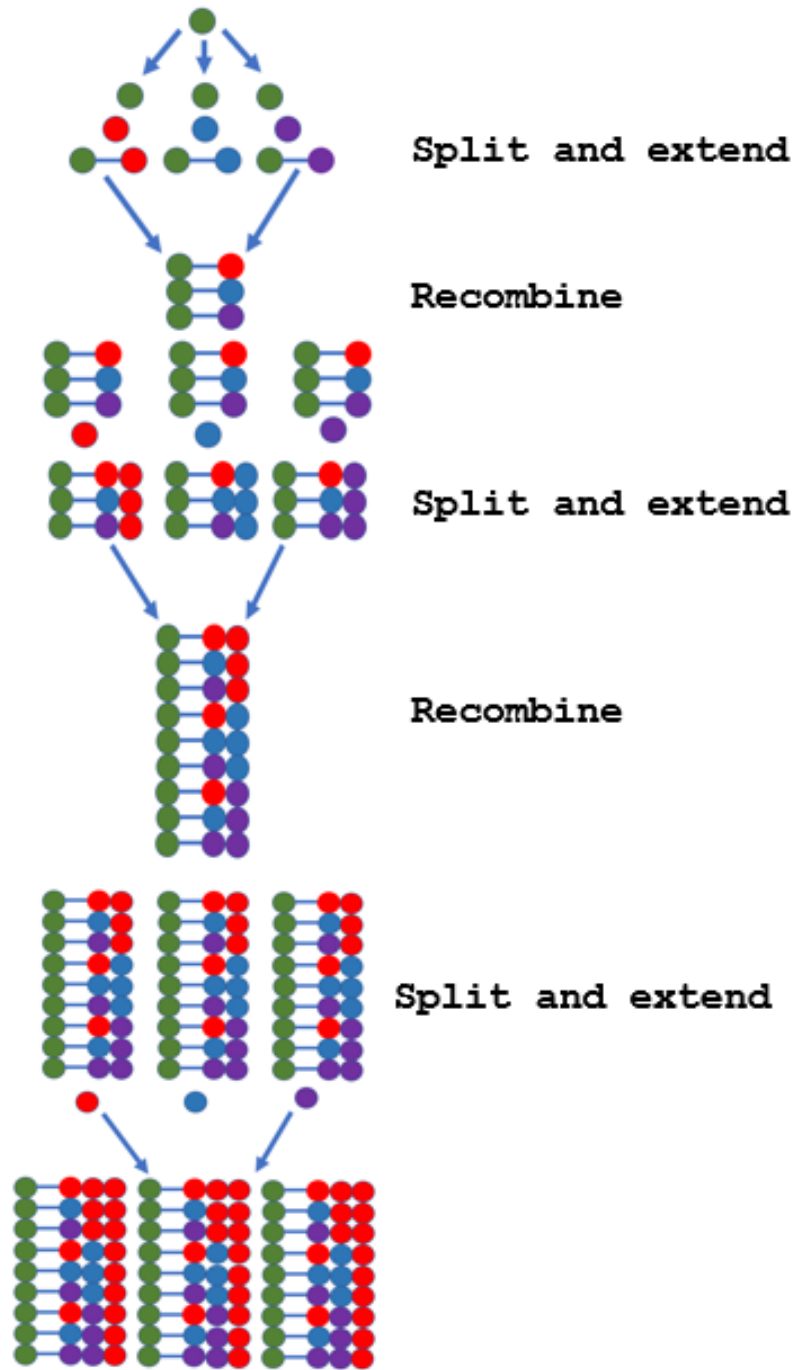
Figure 5-2

Split and extend

Recombine

Split and extend

Recombine

Split and extend

Figure 5-2. The "split and recombine" technique for combinatorial library synthesis. The library was synthesized by using the "split and recombine" approach, which starts with a quantity of beads. With the addition of each residue, the beads are divided into parts equal to the number of variable residues at that site. After which, the parts are recombined into a single unit. In this example, we follow synthesis through three rounds with three variable residues at each site. The end result is a small library with 27 (3x3x3) peptides.

Figure 5-3

20 µl of solvent → 30 µl of *S.aureus* cells

100,000 bacterial cells/ well
1×10^9 RBCs/well

8 µl of solvent → 21 µl of *K.Pneumonia*
21 µl of RBCs

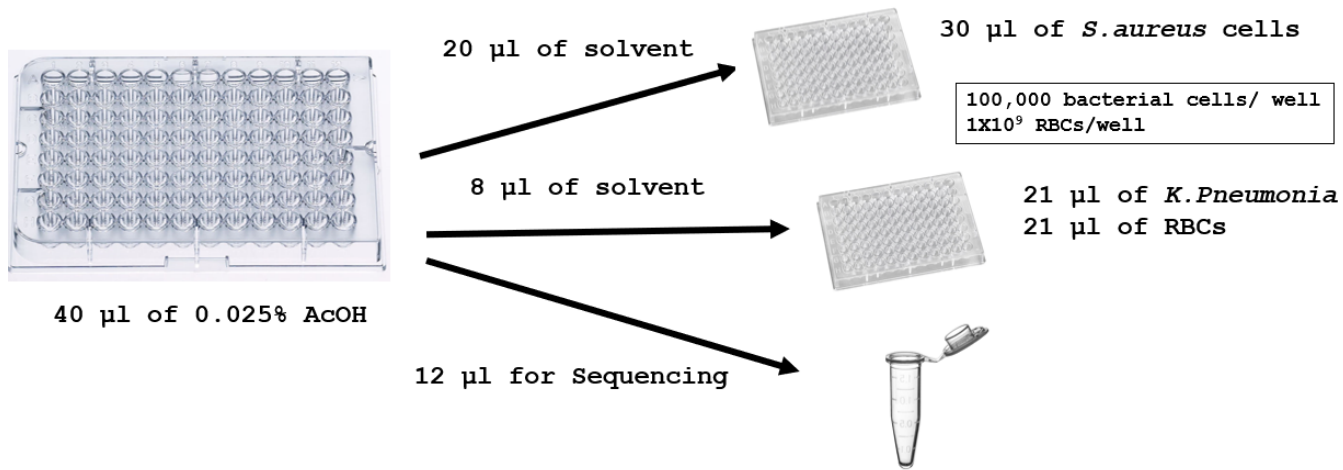40 µl of 0.025% AcOH

12 µl for Sequencing

Figure 5-3. Antimicrobial peptide library screen using broth dilution assay. After cleavage under UV-light, an individual bead with a single library member was placed in each well of a 96 well plate. Ethanol incubation in the UV-light was used to extract the peptide from the beads. Post extraction, 0.025% acetic acid was used to dissolve the peptides. 20 µl of the extracted peptide was transferred to a plate used to screen for activity against *S. aureus*. 8 µl of the extracted peptide was transported to another plate and was screened for activity against *K.pneumonia* in the presence of RBCs. The remaining 12 µl was stored for sequencing.
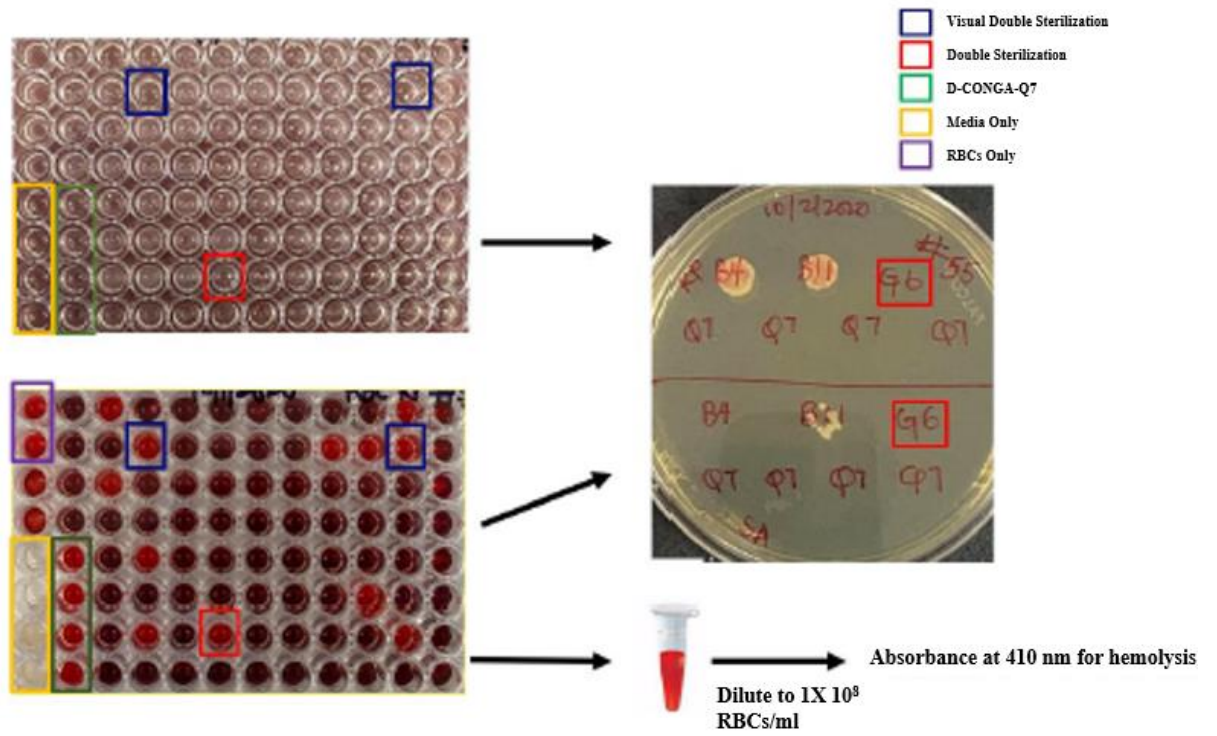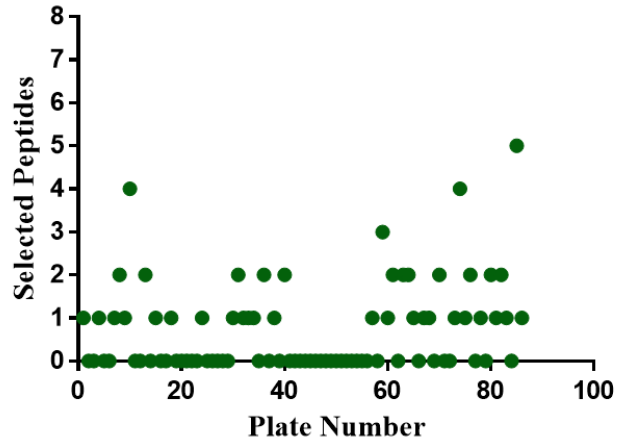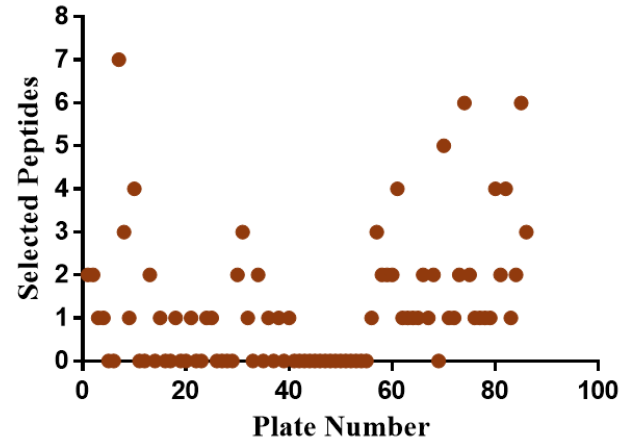
Figure 5-4

Figure 5-4. Schematic representation of the selection process of peptides from the screen of the library. The screen was a combination of broth dilution assays performed in two conditions. *S.aureus* was screened in the absence of RBCs. *K.pneumonia* was screened in the presence of RBCs. 10 µl of the sample from the wells in the plate with *K. pneumonia* that was suspected to be sterilized was used to plate on TSB. 10µl of corresponding well in the plate with *S. aureus* was also plated on the same media. D-CONGA-Q7 was used as positive control that can sterilize both gram-positive and gram-negative bacteria. The rest of the sample from the selected wells of plate with *K.pneumonia* was used for hemolysis. Only the samples that showed no microbial growth on the plate for both *S.aureus* and *K.pneumonia* were selected for sequencing.

Figure 5-5

A) *Staphylococcus aureus* Sterilization

B) *Klebsiella pneumoniae* Sterilization

C) Double Sterilization of *Staphylococcus aureus* and *Klebsiella Pneumonia*
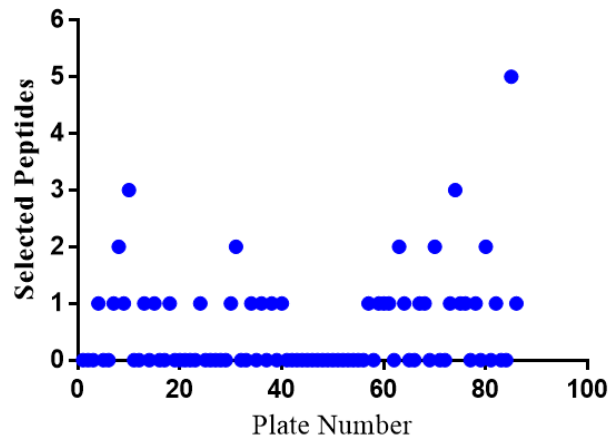
Figure 5-5. Selection of broad-spectrum peptides from the screen of the third-generation peptide library. 85 plates were used to screen 7912 peptides from the library. **A)** 63 of the antimicrobial peptides were able to sterilize *S. aureus*. **B)** This number was lower than 103 peptides that were able to completely inhibit growth of *K.pneumonia*. **C)** Out of these peptides, only 46 library members were able to double sterilize *S. aureus* and *K. pneumoniae.*

Figure 5-6

Hemolysis of Selected Peptides
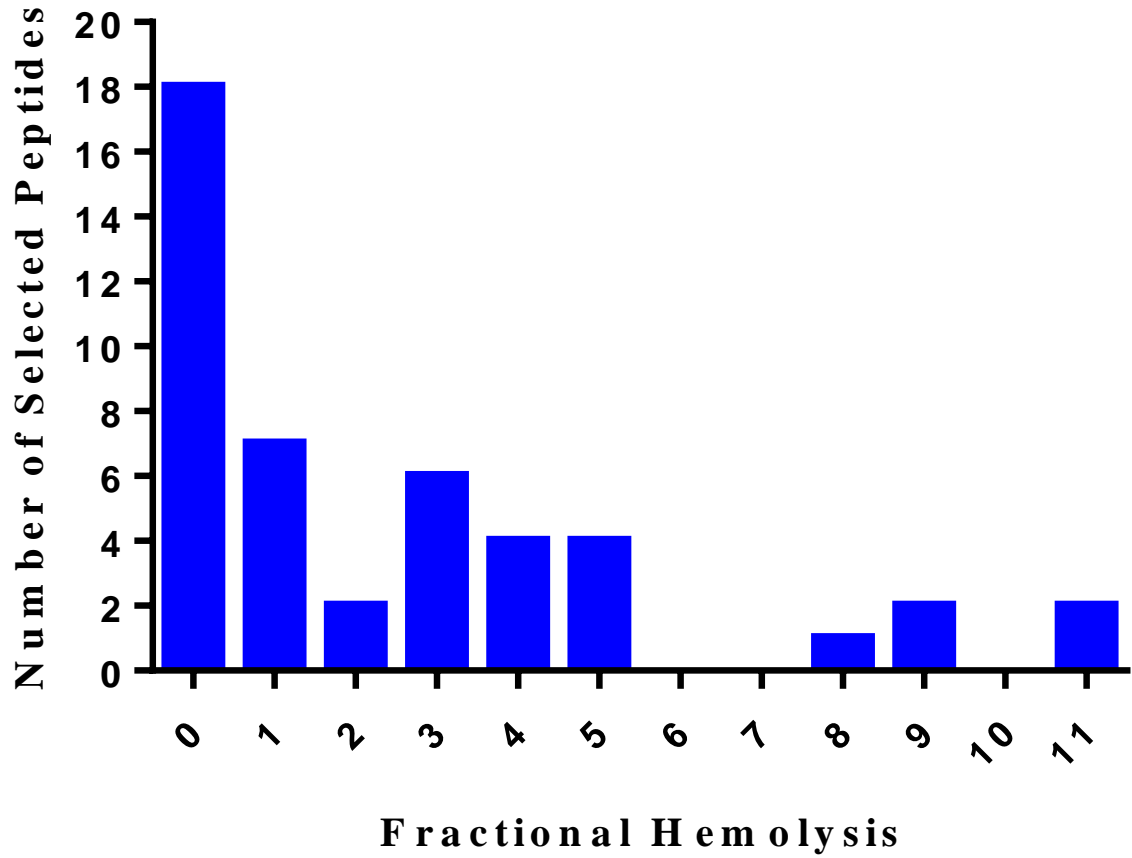
Figure 5-6. Hemolysis in RBCs shown by the selected peptide. The plates used for the screening of peptide library against *K.pneumonia* was also used for measurement of fractional hemolysis caused by library members. The selected samples from plates used to screen *K.pneumonia* was taken and the RBCs was diluted to $1X10^8$ cells/well. After centrifugation, 10 µl of each sample was used to calculate fractional hemolysis. 1% triton and RBCs only were used for positive and negative control. All the selected peptides had hemolysis of less than or approximately 10%. As shown in the figure, majority of these peptides caused hemolysis between 0% to 5%.

List of References

(1) Dykhuizen, D. Species Numbers in Bacteria. *Proc. Calif. Acad. Sci.* **2005**, *56*, 62–71.

(2) Louca, S.; Mazel, F.; Doebeli, M.; Parfrey, L. W. A Census-Based Estimate of Earth's Bacterial and Archaeal Diversity. *PLoS Biol.* **2019**, *17*, 1–30.

(3) Lovitt, R. W.; Wright, C. J. *Bacteria: The Bacterial Cell*, Second Edi.; Elsevier, 2014; Vol. 1.

(4) Coico, R. Gram Staining BASIC PROTOCOL Commonly Used Techniques. *Curr. Protoc. Microbiol.* **2005**, 3–4.

(5) Raetz, C. R. H.; Whitfield, C. Lipopolysaccharide Endotoxins. *Annu. Rev. Biochem.* **2002**, *71*, 635–700.

(6) Wanger, A.; Chavez, V.; Huang, R. S. P.; Wahed, A.; Actor, J. K.; Dasgupta, A. Biochemical Tests and Staining Techniques for Microbial Identification. *Microbiol. Mol. Diagnosis Pathol.* **2017**, 61–73.

(7) Alderwick, L. J.; Harrison, J.; Lloyd, G. S.; Birch, H. L. The Mycobacterial Cell Wall—Peptidoglycan and Arabinogalactan. *Cold Spring Harb. Perspect. Med.* **2015**, *5*, 1–16.

(8) Sa, M.; Sleytr, U. S-Layer Proteins. *J. Bacteriol.* **2000**, *182*, 859–868.

(9) WAKSMAN, S. A. What Is an Antibiotic or an Antibiotic Substance? *Mycologia* **1947**, *39*, 565–569.

(10) Woodward, R. B.; Doering, W. E. The Total Synthesis of Quinine. *J. Am. Chem. Soc.* **1945**, *67*, 860–874.

(11)   Gosio, B. Contributo All'etiologia Della Pellagra; Ricerche Chimiche e Batteriologiche Sulle Alterazioni Del Mais. *G. R. Accad. Med. Torino* **1893**, *61*, 484–487.

(12)   Gosio, B. Ricerdre Batteriologische Chirmide Sulle Alterazioni Del Mais. *Riv. d'Ingienne e Sanita Publica* **1896**, *7*, :825–868.

(13)   Ehrlich, P.; Bertheim, A. Über Das Salzsaure 3.3′-Diamino-4.4′-dioxy-arsenobenzol Und Seine Nächsten Verwandten. *Berichte der Dtsch. Chem. Gesellschaft* **1912**, *45*, 756–766.

(14)   Ehrlich, P.; Hata, S. Die Experimentelle Chemotherapie Der Spirillosen. *Die Exp. Chemother. der Spirillosen* **1910**.

(15)   Domagk, G. Ein Beitrag Zur Chemotherapie Der Bakteriellen Infektionen. *Dtsch. Medizinische Wochenschrift* **1935**, *61*, 250–253.

(16)   Fleming, A. On the Antibacterial Action of Cultures of a Penicillium, with Special Reference to Their Use in the Isolation of B. Influenzae. *Br. J. Exp. Pathol.* **1929**, *10*, 226–236.

(17)   Chain, E.; Florey, H. W.; Adelaide, M. B.; Gardner, A. D.; Oxfd, D. M.; Heatley, N. G.; Jennings, M. A.; Orr-Ewing, J.; Sanders, A. G. Penicillin As a Chemotherapeutic Agent. *Lancet* **1940**, *236*, 226–228.

(18)   Robert Gaynes. The Discovery of Penicillin—New Insights After More Than 75 Years of Clinical Use. *Emerg. Infect. Dis.* **2017**, *23*, 849–853.

(19)   Mohr, K. I. History of Antibiotics Research. *Curr. Top. Microbiol. Immunol.* **2016**,

398, 237–272.

(20) BREWER, G. A.; JOHNSON, M. J. Activity and Properties of Para-Aminobenzyl Penicillin. *Appl. Microbiol.* **1953**, *1*, 163–166.

(21) Newton, G. G. F.; Abraham, E. P. Cephalosporin C, a New Antibiotic Containing Sulphur and D-α-Aminoadipic Acid [1]. *Nature* **1955**, *175*, 548.

(22) Kahan, J. S.; Kahan, F. M.; Goegelman, R.; Currie, S. A.; Jackson, M.; Stapley, E. O.; Miller, T. W.; Miller, A. K.; Hendlin, D.; Woodruff, H. B.; et al. Thienamycin, a New β-Lactam Antibiotic i. Discovery, Taxonomy, Isolation and Physical Properties. *J. Antibiot. (Tokyo).* **1979**, *32*, 1–12.

(23) Papp-Wallace, K. M.; Endimiani, A.; Taracila, M. A.; Bonomo, R. A. Carbapenems: Past, Present, and Future. *Antimicrob. Agents Chemother.* **2011**, *55*, 4943–4960.

(24) Miyadera, T.; Sugimura, Y.; Hashimoto, T.; Tanaka, T.; Iino, K.; Shibata, T.; Sugawara, S. Synthesis and in Vitro Activity of a New Carbapenem, RS-533. *J. Antibiot. (Tokyo).* **1983**, *36*, 1034–1039.

(25) DUBOS, R. J.; HOTCHKISS, R. D. Origin, Nature and Properties of Gramicidin and Tyrocidine. *Trans. Stud. Coll. Physicians Philadelphia* **1942**, *10*, 11–19.

(26) Dubos, R. J.; Hotchkiss, R. D.; Coburn, A. F. The Effect of Gramicidin and Tyrocidine on Bacterial Metabolism. *J. Biol. Chem.* **1942**, *146*, 421–426.

(27) Hotchkiss, R. D.; Dubos, R. J. Fractionation of the Bactericidal Agent From Cultures of a Soil Bacillus. *J. Biol. Chem.* **1940**, *132*, 791–792.

(28)   Hotchkiss, R. D.; Dubos, R. J. Chemical Properties of Bactericidal Substances Isolated From Cultures of a Soil Bacillus. *J. Biol. Chem.* **1940**, *132*, 793–794.

(29)   Gause, G. F.; Brazhnikova, M. G. Gramicidin S and Its Use in the Treatment of Infected Wounds [3]. *Nature* **1944**, *154*, 703.

(30)   Aminov, R. I. A Brief History of the Antibiotic Era: Lessons Learned and Challenges for the Future. *Front. Microbiol.* **2010**, *1*, 1–7.

(31)   Waksman, S. A.; Woodruff, H. B. Bacteriostatic and Bactericidal Substances Produced by a Soil Actinomyces. *Proc. Soc. Exp. Biol. Med.* **1940**, *45*, 609–614.

(32)   Waksman, S. A.; Woodruff, H. B. Actinomyces Antibioticus, a New Soil Organism Antagonistic to Pathogenic and Non-Pathogenic Bacteria 1. *J. Bacteriol.* **1941**, *42*, 231–249.

(33)   Hollstein, U. Actinomycin. Chemistry and Mechanism of Action. *Chem. Rev.* **1974**, *74*, 625–652.

(34)   Johnson, B. A.; Anker, H.; Meleney, F. L. Bacitracin: A New Antibiotic Produced by a Member of the B. Subtilis Group. *Science (80-.).* **1945**, *102*, 376–377.

(35)   Schatz, A.; Bugle, E.; Waksman, S. A. Streptomycin, a Substance Exhibiting Antibiotic Activity Against Gram-Positive and Gram-Negative Bacteria. *Proc. Soc. Exp. Biol. Med.* **1944**, *55*, 66–69.

(36)   Mingeot-Leclercq, M. P.; Glupczynski, Y.; Tulkens, P. M. Aminoglycosides: Activity and Resistance. *Antimicrob. Agents Chemother.* **1999**, *43*, 727–737.

(37)   WAKSMAN, S. A.; LECHEVALIER, H. A.; HARRIS, D. A. Neomycin;

Production and Antibiotic Properties. *J. Clin. Invest.* **1949**, *28*, 934–939.

(38)   TAKEUCHI, T.; HIKIJI, T.; NITTA, K.; YAMAZAKI, S.; ABE, S.; TAKAYAMA, H.; UMEZAWA, H. Biological Studies on Kanamycin. *J. Antibiot. (Tokyo).* **1957**, *10*, 107–114.

(39)   Listed, N. authors. Gentamicin. *Br. Med. J.* **1967**, *1*, 158–159.

(40)   Ehrlich, J.; Bartz, Q. R.; Smith, R. M.; Joslyn, D. A.; Burkholder, P. R. Chloromycetin, a New Antibiotic from a Soil Actinomycete. *Science (80-.).* **1885**, *106*, 417.

(41)   EHRLICH, J.; GOTTLIEB, D. Streptomyces Venezuelae, n. Sp., the Source of Chloromycetin. *J. Bacteriol.* **1948**, *56*, 467–477.

(42)   SMITH, R. M.; JOSLYN, D. A. Chloromycetin; Biological Studies. *J. Bacteriol.* **1948**, *55*, 425–448.

(43)   GOTTLIEB, D.; BHATTACHARYYA, P. K. Some Properties of an Antibiotic Obtained from a Species Of. *J. Bacteriol.* **1948**, *55*, 409–417.

(44)   Duggar, B. M. Aureomycin: A Product of the Continuing Search for New Antibiotics. *Ann. N. Y. Acad. Sci.* **1948**, *51*, 177–181.

(45)   del VILLAR MADRID, R. [Terramycin, a New Antibiotic]. *Bol. Sanid. Mil.* **1950**, *3*, 333–336.

(46)   Nelson, M. L.; Park, B. H.; Andrews, J. S.; Georgian, V. A.; Thomas, R. C.; Levy, S. B. Inhibition of the Tetracycline Efflux Antiport Protein by 13-Thio-Substituted 5-Hydroxy-6-Deoxytetracyclines. *J. Med. Chem.* **1993**, *36*, 370–377.

(47) Nelson, M. L.; Levy, S. B. Reversal of Tetracycline Resistance Mediated by Different Bacterial Tetracycline Resistance Determinants by an Inhibitor of the Tet(B) Antiport Protein. *Antimicrob. Agents Chemother.* **1999**, *43*, 1719–1724.

(48) Mitscher, L. A.; Rosenbrook, W.; Andres, W. W.; Egan, R. S.; Schenck, J.; Juvarkar, J. V. Structure of Chelocardin, a Novel Tetracycline Antibiotic. *Antimicrob. Agents Chemother.* **1970**, *10*, 38–41.

(49) Oliva, B.; Gordon, G.; McNicholas, P.; Ellestad, G.; Chopra, I. Evidence That Tetracycline Analogs Whose Primary Target Is Not the Bacterial Ribosome Cause Lysis of Escherichia Coli. *Antimicrob. Agents Chemother.* **1992**, *36*, 913–919.

(50) Lešnik, U.; Lukežič, T.; Podgoršek, A.; Horvat, J.; Polak, T.; Šala, M.; Jenko, B.; Harmrolfs, K.; Ocampo-Sosa, A.; Martínez-Martínez, L.; et al. Construction of a New Class of Tetracycline Lead Structures with Potent Antibacterial Activity through Biosynthetic Engineering. *Angew. Chemie* **2015**, *127*, 4009–4012.

(51) McGUIRE, J. M.; BUNCH, R. L.; ANDERSON, R. C.; BOAZ, H. E.; FLYNN, E. H.; POWELL, H. M.; SMITH, J. W. Ilotycin, a New Antibiotic. *Antibiot. Chemother.* **1952**, *2*, 281–283.

(52) Chellat, M. F.; Raguž, L.; Riedl, R. Antibiotikaresistenzen Gezielt Überwinden. *Angew. Chemie* **2016**, *128*, 6710–6738.

(53) G.G., Z.; M., W.; A., N.; L.M., V.; A., W.; J.M., E.; A.S., G.; S., D.; D.J., H. The Ketolides: A Critical Review. *Drugs* **2002**, *62*, 1771–1804.

(54) Griesgraber, G.; Or, Y. S.; Chu, D. T. W.; Nilius, A. M.; Johnson, P. M.; Flamm,

R. K.; Henry, R. F.; Plattner, J. J. 3-Keto-11,12-Carbazate Derivatives of 6-O-Methylerythromycin A Synthesis and in Vitro Activity. *J. Antibiot. (Tokyo).* **1996**, *49*, 465–477.

(55)   MCCORMICK, M. H.; MCGUIRE, J. M.; PITTENGER, G. E.; PITTENGER, R. C.; STARK, W. M. Vancomycin, a New Antibiotic. I. Chemical and Biologic Properties. *Antibiot. Annu.* **1955**, *3*, 606–611.

(56)   Jovetic, S.; Zhu, Y.; Marcone, G. L.; Marinelli, F.; Tramper, J. β-Lactam and Glycopeptide Antibiotics: First and Last Line of Defense? *Trends Biotechnol.* **2010**, *28*, 596–604.

(57)   Somma, S.; Gastaldo, L.; Corti, A. Teicoplanin, a New Antibiotic from Actinoplanes Teichomyceticus Nov. Sp. *Antimicrob. Agents Chemother.* **1984**, *26*, 917–923.

(58)   GRUNDY, W. E.; SINCLAIR, A. C.; THERIAULT, R. J.; GOLDSTEIN, A. W.; RICKHER, C. J.; WARREN, H. B.; OLIVER, T. J.; SYLVESTER, J. C. Ristocetin, Microbiologic Properties. *Antibiot. Annu.* **1956**, 687–692.

(59)   T., H. Antibiotics Clinical Development and Pipeline. *Curr. Top. Microbiol. Immunol.* **2016**, *398*, 447–474.

(60)   CHARNEY, J.; FISHER, W. P.; CURRAN, C.; MACHLOWITZ, R. A.; TYTELL, A. A. Streptogramin, a New Antibiotic. *Antibiot. Chemother.* **1953**, *3*, 1283–1286.

(61)   Khosla, R.; Verma, D. D.; Kapur, A.; Aruna, R. V.; Khanna, N. Streptogramins: A

New Class of Antibiotics. *Indian J. Med. Sci.* **1999**, *53*, 111–119.

(62) Giambattista, M. Di; Chinali, G.; Cocito, C. The Molecular Basis of the Inhibitory Activities of Type A and Type B Synergimycins and Related Antibiotics on Ribosomes. *J. Antimicrob. Chemother.* **1989**, *24*, 485–507.

(63) D.J. Mason, A. Dietz, C. D. Lincomycin, a New Antibiotic. I. Discovery and Biological Properties. *Antimicrob. Agents Chemother.* **1963**, *184*, 554–559.

(64) Lewis, C.; Clapp, H. W.; Grady, J. E. In Vitro and In Vivo Evaluation of Lincomycin, A New Antibiotic. *Antimicrob. Agents Chemother.* **1963**, 570–582.

(65) Leclercq, R. Mechanisms of Resistance to Macrolides and Lincosamides: Nature of the Resistance Elements and Their Clinical Implications. *Clin. Infect. Dis.* **2002**, *34*, 482–492.

(66) Meyers, B. R.; Kaplan, K.; Weinstein, L. Microbiological and Pharmacological Behavior of 7-Chlorolincomycin. *Appl. Microbiol.* **1969**, *17*, 653–657.

(67) SENSI, P.; GRECO, A. M.; BALLOTTA, R. Rifomycin. I. Isolation and Properties of Rifomycin B and Rifomycin Complex. *Antibiot. Annu.* **1959**, *7*, 262–270.

(68) Nielsen, E.; Hamilton, P.; David Rosi, D.; Peruzzotti, G. Microbiological Oxidation of 7-Methyl-1, 8-Naphthyridines to 7-Hydroxymethyl-1, 8-Naphthyridines. *US 3317401 A Sterl. Drug Inc* **1963**.

(69) Grohe, K.; Heitzer, H. Cycloaracylierung von Enaminen, I. Synthese von 4-Chinolon-3-carbonsäuren. *Liebigs Ann. der Chemie* **1987**, *1987*, 29–37.

(70)   Stahlmann, R.; Riecke, K. Die Infektiologie. In *Die Infektiologie*; Adam, D., Doerr, H., Link, H., Lode, H. (Hrsg. ., Eds.; Springer, 2004.

(71)   Pandit, N.; Singla, R. K.; Shrivastava, B. Current Updates on Oxazolidinone and Its Significance. *Int. J. Med. Chem.* **2012**, *2012*, 1–24.

(72)   Browne, K.; Chakraborty, S.; Chen, R.; Willcox, M. D. P.; Black, D. S.; Walsh, W. R.; Kumar, N. A New Era of Antibiotics: The Clinical Potential of Antimicrobial Peptides. *Int. J. Mol. Sci.* **2020**, *21*, 1–23.

(73)   Zhang, L. J.; Gallo, R. L. Antimicrobial Peptides. *Curr. Biol.* **2016**, *26*, R14–R19.

(74)   Diamond, G.; Beckloff, N.; Weinberg, A.; Kisich, K. The Roles of Antimicrobial Peptides in Innate Host Defense. *Curr. Pharm. Des.* **2009**, *15*, 2377–2392.

(75)   Steiner, H.; Hultmark, D.; Engström, Å.; Bennich, H.; Boman, H. G. Sequence and Specificity of Two Antibacterial Proteins Involved in Insect Immunity. *Nature* **1981**, *292*, 246–248.

(76)   Zasloff, M. Magainins, a Class of Antimicrobial Peptides from Xenopus Skin: Isolation, Characterization of Two Active Forms, and Partial CDNA Sequence of a Precursor. *Proc. Natl. Acad. Sci. U. S. A.* **1987**, *84*, 5449–5453.

(77)   Lehrer, R. I.; Ganz, T.; Selsted, M. E. Defensins: Endogenous Antibiotic Peptides of Animal Cells. *Cell* **1991**, *64*, 229–230.

(78)   Tedesco, K. L.; Rybak, M. J. Daptomycin. *Pharmacotherapy* **2004**, *24*, 41–57.

(79)   Cha, R.; Grucz, R. G.; Rybak, M. J. Daptomycin Dose-Effect Relationship against Resistant Gram-Positive Organisms. *Antimicrob. Agents Chemother.* **2003**, *47*,

1598–1603.

(80)   Tally, F. P.; DeBruin, M. F. Development of Daptomycin for Gram-Positive Infections. *J. Antimicrob. Chemother.* **2000**, *46*, 523–526.

(81)   STANSLY, P. G.; SHEPHERD, R. G.; WHITE, H. J. Polymyxin: A New Chemotherapeutic Agent. *Bull. Johns Hopkins Hosp.* **1947**, *81*, 43–54.

(82)   BENEDICT, R. G.; LANGLYKKE, A. F. Antibiotic Activity of Bacillus Polymyxa. *J. Bacteriol.* **1947**, *54*, 24.

(83)   Komura, S.; Kurahashi, K. Partial Purification and Properties of L-2, 4-Diaminobutyric Acid Activating Enzyme from a Polymyxin e Producing Organism. *J. Biochem.* **1979**, *86*, 1013–1021.

(84)   Koyama Y; Kurosasa A; Tsuchiya A; Takakuta K. A New Antibiotic "Colistin" Produced by Spore-Forming Soil Bacteria. *J Antibiot* **1950**, *3*, 457–458.

(85)   ROSS, S.; PUIG, J. R.; ZAREMBA, E. A. Colistin: Some Preliminary Laboratory and Clinical Observations in Specific Gastroenteritis in Infants and Children. *Antibiot. Annu.* **1959**, *7*, 89–100.

(86)   Suzuki, T.; Hayashi, K.; Fujikawa, K.; Tsukamoto, K. The Chemical Structure of Polymyxin E: The Identities of Polymyxin E1 with Colistin A and of Polymyxin E2 with Colistin B. *J. Biochem.* **1965**, *57*, 226–227.

(87)   Walkty, A.; DeCorby, M.; Nichol, K.; Karlowsky, J. A.; Hoban, D. J.; Zhanel, G. G. In Vitro Activity of Colistin (Polymyxin E) against 3,480 Isolates of Gram-Negative Bacilli Obtained from Patients in Canadian Hospitals in the CANWARD

Study, 2007-2008. *Antimicrob. Agents Chemother.* **2009**, *53*, 4924–4926.

(88)   Landman, D.; Georgescu, C.; Martin, D. A.; Quale, J. Polymyxins Revisited. *Clin. Microbiol. Rev.* **2008**, *21*, 449–465.

(89)   Casadevall, A. The Case for Pathogen-Specific Therapy. *Expert Opin. Pharmacother.* **2009**, *10*, 1699–1703.

(90)   Brown, E. D.; Wright, G. D. Antibacterial Drug Discovery in the Resistance Era. *Nature* **2016**, *529*, 336–343.

(91)   Petchiappan, A.; Chatterji, D. Antibiotic Resistance: Current Perspectives. *ACS Omega* **2017**, *2*, 7400–7409.

(92)   Smith, T.; Wolff, K. A.; Nguyen, L. Molecular Biology of Drug Resistance in Mycobacterium Tuberculosis. *Curr. Top. Microbiol. Immunol.* **2013**, *374*, 53–80.

(93)   Blair, J. M. A.; Webber, M. A.; Baylay, A. J.; Ogbolu, D. O.; Piddock, L. J. V. Molecular Mechanisms of Antibiotic Resistance. *Nat. Rev. Microbiol.* **2015**, *13*, 42–51.

(94)   Katayama, Y.; Ito, T.; Hiramatsu, K. A New Class of Genetic Element, Staphylococcus Cassette Chromosome Mec, Encodes Methicillin Resistance in Staphylococcus Aureus. *Antimicrob. Agents Chemother.* **2000**, *44*, 1549–1555.

(95)   Smith, A.; Bazan, J. F.; Strop, P.; McKay, D.; Weis, B.; Bushnell, D.; Hegde, S. S.; Vetting, M. W.; Roderick, S. L.; Mitchenall, L. A.; et al. A Fluoroquinolone Resistance Protein from Mycobacterium Tuberculosis That Mimics DNA. *Proc. Natl. Acad. Sci. U.S.A* **1988**, *240*, 6228.

(96)   Bigger, J. W. Treatment of Staphylococcal Infections With Penicillin By
         Intermittent Sterilisation. *Lancet* **1944**, *244*, 497–500.

(97)   Balaban, N. Q.; Merrin, J.; Chait, R.; Kowalik, L.; Leibler, S. Bacterial Persistence
         as a Phenotypic Switch. *Science (80-.).* **2004**, *305*, 1622–1625.

(98)   Fisher, R. A.; Gollan, B.; Helaine, S. Persistent Bacterial Infections and Persister
         Cells. *Nat. Rev. Microbiol.* **2017**, *15*, 453–464.

(99)   Gonçalves-Pereira, J.; Póvoa, P. Antibiotics in Critically Ill Patients: A Systematic
         Review of the Pharmacokinetics of β-Lactams. *Crit. Care* **2011**, *15*.

(100)   Kardas, P. Patient Compliance with Antibiotic Treatment for Respiratory Tract
         Infections. *J. Antimicrob. Chemother.* **2002**, *49*, 897–903.

(101)   Services, U. . D. of H. and H. Antibiotic Resistance Threats in the United States.
         Centers Dis. Control Prev. **2019**, 1–113.

(102)   The Review on Antimicrobial Resistance (Chaired by Jim O'Neill). Tackling
         Drug-Resistant Infections Globally: Final Report and Recommendations. **2016**,
         No. May, 1–80.

(103)   Snitkin, E. S.; Zelazny, A. M.; Thomas, P. J.; Stock, F.; Henderson, D. K.;
         Palmore, T. N.; Segre, J. A. Tracking a Hospital Outbreak of Carbapenem-
         Resistant Klebsiella Pneumoniae with Whole-Genome Sequencing. *Sci. Transl.
         Med.* **2012**, *4*.

(104)   Chaib, F.; Kieny, M.-P.; Helen, B.; Magrini, N.; Deborah, M.; Oelrich, C.;
         Tacconelli, E.; Gonzalo, V.; Dasilva, C. P.; Mcneil, D. Antibiotic-Resistant

Priority Pathogens List. *Oms* **2017**, No. February, 11.

(105) World Health Organization. 2019 Antibacterial Agents in Clinical Development: An Analysis of the Antibacterial Clinical Development Pipeline. **2019**, 48.

(106) Beyer, P.; Paulin, S. Priority Pathogens and the Antibiotic Pipeline: An Update. *Bull. World Health Organ.* **2020**, *98*, 151.

(107) Dheman, N.; Mahoney, N.; Cox, E. M.; Farley, J. J.; Amini, T.; Lanthier, M. L. An Analysis of Antibacterial Drug Development Trends in the United States, 1980–2019. *Clin. Infect. Dis.* **2020**.

(108) Michael, C. A.; Dominey-Howes, D.; Labbate, M. The Antimicrobial Resistance Crisis: Causes, Consequences, and Management. *Front. Public Heal.* **2014**, *2*.

(109) Mah, M. W.; Memish, Z. A. Antibiotic Resistance: An Impending Crisis. *Saudi Med. J.* **2000**, *21*, 1125–1129.

(110) French, G. L. The Continuing Crisis in Antibiotic Resistance. *Int. J. Antimicrob. Agents* **2010**, *36*.

(111) Aslam, B.; Wang, W.; Arshad, M. I.; Khurshid, M.; Muzammil, S.; Rasool, M. H.; Nisar, M. A.; Alvi, R. F.; Aslam, M. A.; Qamar, M. U.; et al. Antibiotic Resistance: A Rundown of a Global Crisis. *Infect. Drug Resist.* **2018**, *11*, 1645–1658.

(112) Gordon, Y. J.; Romanowski, E. G. A Review of Antimicrobial Peptides and Their Therapeutic Potential as Anti-Infective Drugs. *Curr. Eye Res* **2010**, *48*, 1–6.

(113) Hancock, R. E. W.; Sahl, H. G. Antimicrobial and Host-Defense Peptides as New

Anti-Infective Therapeutic Strategies. *Nat. Biotechnol.* **2006**, *24*, 1551–1557.

(114) Peschel, A.; Sahl, H. G. The Co-Evolution of Host Cationic Antimicrobial Peptides and Microbial Resistance. *Nat. Rev. Microbiol.* **2006**, *4*, 529–536.

(115) Fjell, C. D.; Hiss, J. A.; Hancock, R. E. W.; Schneider, G. Designing Antimicrobial Peptides: Form Follows Function. *Nat. Rev. Drug Discov.* **2012**, *11*, 37–51.

(116) Seo, M. D.; Won, H. S.; Kim, J. H.; Mishig-Ochir, T.; Lee, B. J. Antimicrobial Peptides for Therapeutic Applications: A Review. *Molecules* **2012**, *17*, 12276– 12286.

(117) Starr, C. G.; Wimley, W. C. Antimicrobial Peptides Are Degraded by the Cytosolic Proteases of Human Erythrocytes. *Biochim. Biophys. Acta - Biomembr.* **2017**, *1859*, 2319–2326.

(118) Starr, C.; He, J.; Wimley, W. Host Cell Interactions Are a Significant Barrier to the Clinical Utility of Peptide Antibiotics. *ACS Chem. Biol.* **2016**, *11*, 3391–3399.

(119) Haney, E. F.; Brito-Sánchez, Y.; Trimble, M. J.; Mansour, S. C.; Cherkasov, A.; Hancock, R. E. W. Computer-Aided Discovery of Peptides That Specifically Attack Bacterial Biofilms. *Sci. Rep.* **2018**, *8*.

(120) Porto, W. F.; Irazazabal, L.; Alves, E. S. F.; Ribeiro, S. M.; Matos, C. O.; Pires, Á. S.; Fensterseifer, I. C. M.; Miranda, V. J.; Haney, E. F.; Humblot, V.; et al. In Silico Optimization of a Guava Antimicrobial Peptide Enables Combinatorial Exploration for Peptide Design. *Nat. Commun.* **2018**, *9*.

(121) Starr, C. G.; Ghimire, J.; Guha, S.; Hoffmann, J. P.; Wang, Y.; Sun, L.; Landreneau, B. N.; Kolansky, Z. D.; Kilanowski-Doroh, I. M.; Sammarco, M. C.; et al. Synthetic Molecular Evolution of Host Cell-Compatible, Antimicrobial Peptides Effective against Drug-Resistant, Biofilm-Forming Bacteria. *Proc. Natl. Acad. Sci. U. S. A.* **2020**, *117*, 8437–8448.

(122) Hoffmann, J. P.; Friedman, J. K.; Wang, Y.; McLachlan, J. B.; Sammarco, M. C.; Morici, L. A.; Roy, C. J. In Situ Treatment With Novel Microbiocide Inhibits Methicillin Resistant Staphylococcus Aureus in a Murine Wound Infection Model. *Front. Microbiol.* **2020**, *10*.

(123) Dunn, L.; Prosser, H. C. G.; Tan, J. T. M.; Vanags, L. Z.; Ng, M. K. C.; Bursill, C. A. Murine Model of Wound Healing. *J. Vis. Exp.* **2013**, *2013*, 1–6.

(124) Andersson, D. I.; Hughes, D.; Kubicek-Sutherland, J. Z. Mechanisms and Consequences of Bacterial Resistance to Antimicrobial Peptides. *Drug Resist. Updat.* **2016**, *26*, 43–57.

(125) Zhang, L. J.; Gallo, R. L. Albumin Binding of Short Cationic Antimicrobial Micropeptides and Its Influence on the in Vitro Bactericidal Effect. *J. Med. Chem.* **2007**, *50*, 3334–3339.

(126) Travkova, O. G.; Moehwald, H.; Brezesinski, G. The Interaction of Antimicrobial Peptides with Membranes. *Adv. Colloid Interface Sci.* **2017**, *247*, 521–532.

(127) Papo, N.; Shai, Y. Can We Predict Biological Activity of Antimicrobial Peptides from Their Interactions with Model Phospholipid Membranes? *Peptides* **2003**, *24*, 1693–1703.

(128) Shai, Y. Mechanism of the Binding, Insertion and Destabilization of Phospholipid Bilayer Membranes by α-Helical Antimicrobial and Cell Non-Selective Membrane-Lytic Peptides. *Biochim. Biophys. Acta - Biomembr.* **1999**, *1462*, 55–70.

(129) OREN, Z.; LERMAN, J. C.; GUDMUNDSSON, G. H.; AGERBERTH, B.; SHAI, Y. Structure and Organization of the Human Antimicrobial Peptide LL-37 in Phospholipid Membranes: Relevance to the Molecular Basis for Its Non-Cell-Selective Activity. *Biochem. J.* **1999**, *341*, 501–513.

(130) E, G.; A, B.; HG, B.; Y., S. Interaction of the Mammalian Antibacterial Peptide Cecropin P1 with Phospholipid Vesicles. *Biochemistry* **1995**, *34*, 11479–11488.

(131) Wimley, W. C.; Selsted, M. E.; White, S. H. Interactions between Human Defensins and Lipid Bilayers: Evidence for Formation of Multimeric Pores. *Protein Sci.* **1994**, *3*, 1362–1373.

(132) Shai, Y. Mode of Action of Membrane Active Antimicrobial Peptides. *Biopolym. - Pept. Sci. Sect.* **2002**, *66*, 236–248.

(133) Yeaman, M. R.; Yount, N. Y. Mechanisms of Antimicrobial Peptide Action and Resistance. *Pharmacol. Rev.* **2003**, *55*, 27–55.

(134) V., T.; M.J., F.; M., B. Role of Lipids in the Interaction of Antimicrobial Peptides with Membranes. *Prog. Lipid Res.* **2012**, *51*, 149–177.

(135) Torcato, I. M.; Huang, Y. H.; Franquelim, H. G.; Gaspar, D. D.; Craik, D. J.; Castanho, M. A. R. B.; Henriques, S. T. The Antimicrobial Activity of Sub3 Is

Dependent on Membrane Binding and Cell-Penetrating Ability. *ChemBioChem* **2013**, *14*, 2013–2022.

(136) Hong, K.; Hubbell, W. L. Preparation and Properties of Phospholipid Bilayers Containing Rhodopsin. *Proc. Natl. Acad. Sci. U. S. A.* **1972**, *69*, 2617–2621.

(137) Varki, A. Glycan-Based Interactions Involving Vertebrate Sialic-Acid-Recognizing Proteins. *Nature* **2007**, *446*, 1023–1029.

(138) Lee, H. S.; Park, C. B.; Kim, J. M.; Jang, S. A.; Park, I. Y.; Kim, M. S.; Cho, J. H.; Kim, S. C. Mechanism of Anticancer Activity of Buforin IIb, a Histone H2A-Derived Peptide. *Cancer Lett.* **2008**, *271*, 47–55.

(139) Af, C.; Bs, C. Invasion of Red Blood Cells by Malaria Parasites. *Cell* **2006**.

(140) Kato, G. J.; Gladwin, M. T.; Steinberg, M. H. Deconstructing Sickle Cell Disease: Reappraisal of the Role of Hemolysis in the Development of Clinical Subphenotypes. *Blood Rev.* **2007**, *21*, 37–47.

(141) Servick, K. A Powerful New Weapon against Drug-Resistant Bacteria Was Inspired by the Human Body. *Science (80-.).* **2018**.

(142) De Breij, A.; Riool, M.; Kwakman, P. H. S.; De Boer, L.; Cordfunke, R. A.; Drijfhout, J. W.; Cohen, O.; Emanuel, N.; Zaat, S. A. J.; Nibbering, P. H.; et al. Prevention of Staphylococcus Aureus Biomaterial-Associated Infections Using a Polymer-Lipid Coating Containing the Antimicrobial Peptide OP-145. *J. Control. Release* **2016**, *222*, 1–8.

(143) De Breij, A.; Riool, M.; Cordfunke, R. A.; Malanovic, N.; De Boer, L.; Koning, R.

I.; Ravensbergen, E.; Franken, M.; Van Der Heijde, T.; Boekema, B. K.; et al. The Antimicrobial Peptide SAAP-148 Combats Drug-Resistant Bacteria and Biofilms. *Sci. Transl. Med.* **2018**, *10*.

(144) Starr, C. G.; He, J.; Wimley, W. C. Host Cell Interactions Are a Significant Barrier to the Clinical Utility of Peptide Antibiotics. *ACS Chem. Biol.* **2016**, *11*, 3391–3399.

(145) Matsuzaki, K. Control of Cell Selectivity of Antimicrobial Peptides. *Biochim. Biophys. Acta - Biomembr.* **2009**, *1788*, 1687–1692.

(146) Matsuzaki, K.; Sugishita, K. I.; Fujii, N.; Miyajima, K. Molecular Basis for Membrane Selectivity of an Antimicrobial Peptide, Magainin 2. *Biochemistry* **1995**, *34*, 3423–3429.

(147) Tytler, E. M.; Anantharamaiah, G. M.; Walker, D. E.; Mishra, V. K.; Palgunachari, M. N.; Segrest, J. P. Molecular Basis for Prokaryotic Specificity of Magainin-Induced Lysis. *Biochemistry* **1995**, *34*, 4393–4401.

(148) Gorter, E.; Grendel, F. On Bimolecular Layers of Lipoids on the Chromocytes of the Blood. *J. Exp. Med.* **1925**, *41*, 439–444.

(149) Cooper, G. M.; Hausman, R. E. The Cell: A Molecular Approach 2nd Edition. *Sinauer Assoc.* **2000**.

(150) Maher, S.; McClean, S. Investigation of the Cytotoxicity of Eukaryotic and Prokaryotic Antimicrobial Peptides in Intestinal Epithelial Cells in Vitro. *Biochem. Pharmacol.* **2006**, *71*, 1289–1298.

(151) Rozman, K. K.; Doull, J.; Hayes, W. J. Dose and Time Determining, and Other Factors Influencing, Toxicity. *Hayes' Handb. Pestic. Toxicol.* **2010**, 3–101.

(152) Munshi, S.; Twining, R. C.; Dahl, R. Alamar Blue Reagent Interacts with Cell-Culture Media Giving Different Fluorescence over Time: Potential for False Positives. *J. Pharmacol. Toxicol. Methods* **2014**, *70*, 195–198.

(153) Goegan, P.; Johnson, G.; Vincent, R. Effects of Serum Protein and Colloid on the AlamarBlue Assay in Cell Cultures. *Toxicol. Vitr.* **1995**, *9*, 257–266.

(154) Riedl, S.; Zweytick, D.; Lohner, K. Membrane-Active Host Defense Peptides - Challenges and Perspectives for the Development of Novel Anticancer Drugs. *Chem. Phys. Lipids* **2011**, *164*, 766–781.

(155) Bevers, E. M.; Comfurius, P.; Zwaal, R. F. A. Regulatory Mechanisms in Maintenance and Modulation of Transmembrane Lipid Asymmetry: Pathophysiological Implications. *Lupus* **1996**, *5*, 480–487.

(156) Kufe, D. W. Mucins in Cancer: Function, Prognosis and Therapy. *Nat. Rev. Cancer* **2009**, *9*, 874–885.

(157) Carraway, K. L.; Price-Schiavi, S. A.; Zhu, X.; Komatsu, M. Membrane Mucins and Breast Cancer. *Cancer Control* **1999**, *6*, 613–614.

(158) Bafna, S.; Kaur, S.; Batra, S. K. Membrane-Bound Mucins: The Mechanistic Basis for Alterations in the Growth and Survival of Cancer Cells. *Oncogene* **2010**, *29*, 2893–2904.

(159) Ki, V.; Rotstein, C. Bacterial Skin and Soft Tissue Infections in Adults: A Review

of Their Epidemiology, Pathogenesis, Diagnosis, Treatment and Site of Care. *Can. J. Infect. Dis. Med. Microbiol.* **2008**, *19*, 173–184.

(160) Esposito, S.; Bassetti, M.; Concia, E.; De Simone, G.; De Rosa, F. G.; Grossi, P.; Novelli, A.; Menichetti, F.; Petrosillo, N.; Tinelli, M.; et al. Diagnosis and Management of Skin and Soft-Tissue Infections (SSTI). A Literature Review and Consensus Statement: An Update. *J. Chemother.* **2017**, *29*, 197–214.

(161) J.B., L.; C.L., C.; G.B., P. Lung Infections Associated with Cystic Fibrosis. *Clin. Microbiol. Rev.* **2002**, *15*, 194–222.

(162) Hubert, D.; Réglier-Poupet, H.; Sermet-Gaudelus, I.; Ferroni, A.; Le Bourgeois, M.; Burgel, P. R.; Serreau, R.; Dusser, D.; Poyart, C.; Coste, J. Association between Staphylococcus Aureus Alone or Combined with Pseudomonas Aeruginosa and the Clinical Condition of Patients with Cystic Fibrosis. *J. Cyst. Fibros.* **2013**, *12*, 497–503.

(163) Yadav, M. K.; Chae, S. W.; Go, Y. Y.; Im, G. J.; Song, J. J. In Vitro Multi-Species Biofilms of Methicillin-Resistant Staphylococcus Aureus and Pseudomonas Aeruginosa and Their Host Interaction during in Vivo Colonization of an Otitis Media Rat Model. *Front. Cell. Infect. Microbiol.* **2017**, *7*.

(164) Gjødsbøl, K.; Christensen, J. J.; Karlsmark, T.; Jørgensen, B.; Klein, B. M.; Krogfelt, K. A. Multiple Bacterial Species Reside in Chronic Wounds: A Longitudinal Study. *Int. Wound J.* **2006**, *3*, 225–231.

(165) Fazli, M.; Bjarnsholt, T.; Kirketerp-Møller, K.; Jørgensen, B.; Andersen, A. S.; Krogfelt, K. A.; Givskov, M.; Tolker-Nielsen, T. Nonrandom Distribution of

Pseudomonas Aeruginosa and Staphylococcus Aureus in Chronic Wounds. *J. Clin. Microbiol.* **2009**, *47*, 4084–4089.

(166) Chopra, S.; Harjai, K.; Chhibber, S. Antibiotic Susceptibility of Ica-Positive and Ica-Negative MRSA in Different Phases of Biofilm Growth. *J. Antibiot. (Tokyo).* **2015**, *68*, 15–22.

(167) Jung, H.; Lee, S. K.; Cha, S. H.; Byun, J. Y.; Park, M. S.; Yeo, S. G. Current Bacteriology of Chronic Otitis Media with Effusion: High Rate of Nosocomial Infection and Decreased Antibiotic Sensitivity. *J. Infect.* **2009**, *59*, 308–316.

(168) Kim, S. H. oo.; Kim, M. G. u.; Kim, S. S. o.; Cha, S. H. o.; Yeo, S. G. eu. Change in Detection Rate of Methicillin-Resistant Staphylococcus Aureus and Pseudomonas Aeruginosa and Their Antibiotic Sensitivities in Patients with Chronic Suppurative Otitis Media. *J. Int. Adv. Otol.* **2015**, *11*, 151–156.

(169) U.S. Department of Health and Human Services. Antibiotic Resistance Threats in the United States. *Centers Dis. Control Prev.* **2019**, 1–113.

(170) Garau, J.; Bouza, E.; Chastre, J.; Gudiol, F.; Harbarth, S. Management of Methicillin-Resistant Staphylococcus Aureus Infections. *Clin. Microbiol. Infect.* **2009**, *15*, 125–136.

(171) McConeghy, K. W.; Mikolich, D. J.; Laplante, K. L. Agents for the Decolonization of Methicillin-Resistant Staphylococcus Aureus. *Pharmacotherapy* **2009**, *29*, 263–280.

(172) Lentino, J. R.; Narita, M.; Yu, V. L. New Antimicrobial Agents as Therapy for

Resistant Gram-Positive Cocci. *Eur. J. Clin. Microbiol. Infect. Dis.* **2008**, *27*, 3–15.

(173) B.A., L.; C., H. Topical Antimicrobial Therapy for Treating Chronic Wounds. *Clin. Infect. Dis.* **2009**, *49*, 1541–1549.

(174) Lio, P. A.; Kaye, E. T. Topical Antibacterial Agents. *Infect. Dis. Clin. North Am.* **2004**, *18*, 717–733.

(175) Neely, A. N.; Gardner, J.; Durkee, P.; Warden, G. D.; Greenhalgh, D. G.; Gallagher, J. J.; Herndon, D. N.; Tompkins, R. G.; Kagan, R. J. Are Topical Antimicrobials Effective against Bacteria That Are Highly Resistant to Systemic Antibiotics? *J. Burn Care Res.* **2009**, *30*, 19–29.

(176) Kugelberg, E.; Norström, T.; Petersen, T. K.; Duvold, T.; Andersson, D. I.; Hughes, D. Establishment of a Superficial Skin Infection Model in Mice by Using Staphylococcus Aureus and Streptococcus Pyogenes. *Antimicrob. Agents Chemother.* **2005**, *49*, 3435–3441.

(177) Lu, C. W.; Lin, T. Y.; Shieh, J. S.; Wang, M. J.; Chiu, K. M. Antimicrobial Effect of Continuous Lidocaine Infusion in a Staphylococcus Aureus-Induced Wound Infection in a Mouse Model. *Ann. Plast. Surg.* **2014**, *73*, 598–601.

(178) Liu, Y.; Zhou, Q.; Wang, Y.; Liu, Z.; Dong, M.; Wang, Y.; Li, X.; Hu, D. Negative Pressure Wound Therapy Decreases Mortality in a Murine Model of Burn-Wound Sepsis Involving Pseudomonas Aeruginosa Infection. *PLoS One* **2014**, *9*.

(179) Chhibber, S.; Kaur, J.; Kaur, S. Liposome Entrapment of Bacteriophages Improves Wound Healing in a Diabetic Mouse MRSA Infection. *Front. Microbiol.* **2018**, *9*.

(180) Galiano, R. D.; Michaels V, J.; Dobryansky, M.; Levine, J. P.; Gurtner, G. C. Quantitative and Reproducible Murine Model of Excisional Wound Healing. *Wound Repair Regen.* **2004**, *12*, 485–492.

(181) Wang, X.; Ge, J.; Tredget, E. E.; Wu, Y. The Mouse Excisional Wound Splinting Model, Including Applications for Stem Cell Transplantation. *Nat. Protoc.* **2013**, *8*, 302–309.

(182) Du, P.; Suhaeri, M.; Ha, S. S.; Oh, S. J.; Kim, S. H.; Park, K. Human Lung Fibroblast-Derived Matrix Facilitates Vascular Morphogenesis in 3D Environment and Enhances Skin Wound Healing. *Acta Biomater.* **2017**, *54*, 333–344.

(183) Schierle, C. F.; De La Garza, M.; Mustoe, T. A.; Galiano, R. D. Staphylococcal Biofilms Impair Wound Healing by Delaying Reepithelialization in a Murine Cutaneous Wound Model. *Wound Repair Regen.* **2009**, *17*, 354–359.

(184) Brandenburg, K. S.; Calderon, D. F.; Kierski, P. R.; Brown, A. L.; Shah, N. M.; Abbott, N. L.; Schurr, M. J.; Murphy, C. J.; McAnulty, J. F.; Czuprynski, C. J. Inhibition of Pseudomonas Aeruginosa Biofilm Formation on Wound Dressings. *Wound Repair Regen.* **2015**, *23*, 842–854.

(185) Kim, W. R.; Flamm, S. L.; Di Bisceglie, A. M.; Bodenheimer, H. C. Serum Activity of Alanine Aminotransferase (ALT) as an Indicator of Health and Disease. *Hepatology* **2008**, *47*, 1363–1370.

(186) Webb, C. Engineering Fundamentals of Biotechnology. *Compr. Biotechnol.* **2011**, 1–3.

(187) Dias, C.; Nylandsted, J. Plasma Membrane Integrity in Health and Disease: Significance and Therapeutic Potential. *Cell Discov.* **2021**, *7*.

(188) Williamson, D. A.; Carter, G. P.; Howden, B. P. Current and Emerging Topical Antibacterials and Antiseptics: Agents, Action, and Resistance Patterns. *Clin. Microbiol. Rev.* **2017**, *30*, 827–860.

(189) Upton, A.; Lang, S.; Heffernan, H. Mupirocin and Staphylococcus Aureus: A Recent Paradigm of Emerging Antibiotic Resistance. *J. Antimicrob. Chemother.* **2003**, *51*, 613–617.

(190) D.A., W.; S.R., R.; E., B.; A., U.; A., L.; A., S. A Bug in the Ointment: Topical Antimicrobial Usage and Resistance in New Zealand. *N. Z. Med. J.* **2015**, *128*, 103–109.

(191) Mahlapuu, M.; Håkansson, J.; Ringstad, L.; Björn, C. Antimicrobial Peptides: An Emerging Category of Therapeutic Agents. *Front. Cell. Infect. Microbiol.* **2016**, *6*.

(192) Zhao, X.; Wu, H.; Lu, H.; Li, G.; Huang, Q. LAMP: A Database Linking Antimicrobial Peptides. *PLoS One* **2013**, *8*.

(193) Fan, L.; Sun, J.; Zhou, M.; Zhou, J.; Lao, X.; Zheng, H.; Xu, H. DRAMP: A Comprehensive Data Repository of Antimicrobial Peptides. *Sci. Rep.* **2016**, *6*.

(194) Fosgerau, K.; Hoffmann, T. Peptide Therapeutics: Current Status and Future Directions. *Drug Discov. Today* **2015**, *20*, 122–128.

(195) Fox, J. L. Antimicrobial Peptides Stage a Comeback. *Nat. Biotechnol.* **2013**, *31*, 379–382.

(196) Matsuzaki, K.; Sugishita, K. I.; Harada, M.; Fujii, N.; Miyajima, K. Interactions of an Antimicrobial Peptide, Magainin 2, with Outer and Inner Membranes of Gram-Negative Bacteria. *Biochim. Biophys. Acta - Biomembr.* **1997**, *1327*, 119–130.

(197) Thakur, S.; Cattoni, D. I.; Nöllmann, M. The Fluorescence Properties and Binding Mechanism of SYTOX Green, a Bright, Low Photo-Damage DNA Intercalating Agent. *Eur. Biophys. J.* **2015**, *44*, 337–348.

(198) Hoskin, D. W.; Ramamoorthy, A. Studies on Anticancer Activities of Antimicrobial Peptides. *Biochim. Biophys. Acta - Biomembr.* **2008**, *1778*, 357–375.

(199) Zomer, H. D.; Trentin, A. G. Skin Wound Healing in Humans and Mice: Challenges in Translational Research. *J. Dermatol. Sci.* **2018**, *90*, 3–12.

(200) Finlay, B. B.; McFadden, G. Anti-Immunology: Evasion of the Host Immune System by Bacterial and Viral Pathogens. *Cell* **2006**, *124*, 767–782.

(201) Zhang, B.; Li, Q.; Shi, C.; Zhang, X. Drug-Induced Pseudoallergy: A Review of the Causes and Mechanisms. *Pharmacology* **2017**, *101*, 104–110.

(202) Drug Allergy: An Updated Practice Parameter. *Ann. Allergy, Asthma Immunol.* **2010**, *105*.

(203) Liu, Z.; Qiu, S.; Liu, Z.; Hou, L.; Li, Y.; Wang, J.; Wang, H.; Du, W.; Wang, W.; Qin, Y. Complement Activation Associated with Polysorbate 80 in Beagle Dogs.

Int. Immunopharmacol. **2013**, *15*, 144–149.

(204) He, S. H.; Zhang, H. Y.; Zeng, X. N.; Chen, D.; Yang, P. C. Mast Cells and Basophils Are Essential for Allergies: Mechanisms of Allergic Inflammation and a Proposed Procedure for Diagnosis. *Acta Pharmacol. Sin.* **2013**, *34*, 1270–1283.

(205) Cutting, G. R. Modifier Genetics: Cystic Fibrosis. *Annu. Rev. Genomics Hum. Genet.* **2005**, *6*, 237–260.

(206) Schrijver, I.; Pique, L.; Graham, S.; Pearl, M.; Cherry, A.; Kharrazi, M. The Spectrum of CFTR Variants in Nonwhite Cystic Fibrosis Patients: Implications for Molecular Diagnostic Testing. *J. Mol. Diagnostics* **2016**, *18*, 39–50.

(207) Hamosh, A.; FitzSimmons, S. C.; Macek M., J.; Knowles, M. R.; Rosenstein, B. J.; Cutting, G. R. Comparison of the Clinical Manifestations of Cystic Fibrosis in Black and White Patients. *J. Pediatr.* **1998**, *132*, 255–259.

(208) Palomaki, G. E.; FitzSimmons, S. C.; Haddow, J. E. Clinical Sensitivity of Prenatal Screening for Cystic Fibrosis via CFTR Carrier Testing in a United States Panethnic Population. *Genet. Med.* **2004**, *6*, 405–414.

(209) O'Toole, G. A. Cystic Fibrosis Airway Microbiome: Overturning the Old, Opening the Way for the New. *J. Bacteriol.* **2018**, *200*.

(210) Pedersen, S. S.; Hoiby, N.; Espersen, F.; Koch, C. Role of Alginate in Infection with Mucoid Pseudomonas Aeruginosa in Cystic Fibrosis. *Thorax* **1992**, *47*, 6–13.

(211) Limoli, D. H.; Yang, J.; Khansaheb, M. K.; Helfman, B.; Peng, L.; Stecenko, A. A.; Goldberg, J. B. Staphylococcus Aureus and Pseudomonas Aeruginosa Co-

Infection Is Associated with Cystic Fibrosis-Related Diabetes and Poor Clinical Outcomes. *Eur. J. Clin. Microbiol. Infect. Dis.* **2016**, *35*, 947–953.

(212) Marshall, B.; Faro, A.; Elbert, A.; Fink, A.; Sewall, A. Cystic Fibrosis Foundation Patient Registry 2018 Annual Data Report. **2018**, 92.

(213) Dasenbrook, E. C.; Checkley, W.; Merlo, C. A.; Konstan, M. W.; Lechtzin, N.; Boyle, M. P. Association between Respiratory Tract Methicillin-Resistant Staphylococcus Aureus and Survival in Cystic Fibrosis. *JAMA - J. Am. Med. Assoc.* **2010**, *303*, 2386–2393.

(214) Phang, S. H.; Greysson-Wong, J.; Somayaji, R.; Storey, D. G.; Rabin, H. R.; Surette, M. G.; Parkins, M. Incidence, Impact and Natural History of Klebsiella Species Infections in Cystic Fibrosis: A Longitudinal Single Center Study. *Can. J. Respir. Crit. Care, Sleep Med.* **2019**, *3*, 148–154.

(215) Sharifi, M. N.; Kianifar, H. R.; Bagheri, S.; Sayedi, S. J. Microbiology of Upper Respiratory Tract Pathogens in Cystic Fibrosis Patients. *Acta Med. Iran.* **2018**, *56*, 450–456.

(216) Mubareka, S.; Rubinstein, E. Aerosolized Colistin for the Treatment of Nosocomial Pneumonia Due to Multidrug-Resistant Gram-Negative Bacteria in Patients without Cystic Fibrosis. *Crit. Care* **2005**, *9*, 29–30.

(217) Rocha, G. A.; Lima, D. F.; Rodrigues, E. R.; Leão, R. S.; Folescu, T. W.; Firmida, M. C.; Cohen, R. W. F.; Albano, R. M.; Marques, E. A. Species Distribution, Sequence Types and Antimicrobial Resistance of Acinetobacter Spp. from Cystic Fibrosis Patients. *Epidemiol. Infect.* **2018**, *146*, 524–530.

(218) Kiedrowski, M. R.; Gaston, J. R.; Kocak, B. R.; Coburn, S. L.; Lee, S.; Pilewski, J. M.; Myerburg, M. M.; Bomberger, J. M. Staphylococcus Aureus Biofilm Growth on Cystic Fibrosis Airway Epithelial Cells Is Enhanced during Respiratory Syncytial Virus Coinfection . *mSphere* **2018**, *3*.

(219) Høiby, N. Understanding Bacterial Biofilms in Patients with Cystic Fibrosis: Current and Innovative Approaches to Potential Therapies. *J. Cyst. Fibros.* **2002**, *1*, 249–254.

(220) Costerton, J. W. Cystic Fibrosis Pathogenesis and the Role of Biofilms in Persistent Infection. *Trends Microbiol.* **2001**, *9*, 50–52.

(221) Ciofu, O.; Rojo-Molinero, E.; Macià, M. D.; Oliver, A. Antibiotic Treatment of Biofilm Infections. *Apmis* **2017**, *125*, 304–319.

(222) Smith, D. J.; Ramsay, K. A.; Yerkovich, S. T.; Reid, D. W.; Wainwright, C. E.; Grimwood, K.; Bell, S. C.; Kidd, T. J. Pseudomonas Aeruginosa Antibiotic Resistance in Australian Cystic Fibrosis Centres. *Respirology* **2016**, *21*, 329–337.

(223) Martin, L. W.; Robson, C. L.; Watts, A. M.; Gray, A. R.; Wainwright, C. E.; Bell, S. C.; Ramsay, K. A.; Kidd, T. J.; Reid, D. W.; Brockway, B.; et al. Expression of Pseudomonas Aeruginosa Antibiotic Resistance Genes Varies Greatly during Infections in Cystic Fibrosis Patients. *Antimicrob. Agents Chemother.* **2018**, *62*.

(224) Remmington, T.; Jahnke, N.; Harkensee, C. Oral Anti-Pseudomonal Antibiotics for Cystic Fibrosis. *Cochrane Database Syst. Rev.* **2005**.

(225) Breyre, A.; Frazee, B. W. Skin and Soft Tissue Infections in the Emergency

Department. *Emerg. Med. Clin. North Am.* **2018**, *36*, 723–750.

(226) Houghland, J. E. National Trends in Ambulatory Visits and Antibiotic Prescribing for Skin and Soft-Tissue Infections. *J. Emerg. Med.* **2009**, *36*, 98.

(227) Kauffman, W. B.; Guha, S.; Wimley, W. C. Synthetic Molecular Evolution of Hybrid Cell Penetrating Peptides. *Nat. Commun.* **2018**, *9*, 2568.

(228) Krauson, A. J.; He, J.; Wimley, A. W.; Hoffmann, A. R.; Wimley, W. C. Synthetic Molecular Evolution of Pore-Forming Peptides by Iterative Combinatorial Library Screening. *ACS Chem. Biol.* **2013**, *8*, 823–831.

(229) Wimley, W. C. Application of Synthetic Molecular Evolution to the Discovery of Antimicrobial Peptides. *Adv. Exp. Med. Biol.* **2019**, *1117*, 241–255.

(230) Rathinakumar, R.; Wimley, W. C. High-throughput Discovery of Broad-spectrum Peptide Antibiotics. *FASEB J.* **2010**, *24*, 3232–3238.

(231) Rathinakumar, R.; Wimley, W. C. Biomolecular Engineering by Combinatorial Design and High-Throughput Screening: Small, Soluble Peptides That Permeabilize Membranes. *J. Am. Chem. Soc.* **2008**, *130*, 9849–9858.

(232) Rathinakumar, R.; Walkenhorst, W. F.; Wimley, W. C. Broad-Spectrum Antimicrobial Peptides by Rational Combinatorial Design and High-Throughput Screening: The Importance of Interfacial Activity. *J. Am. Chem. Soc.* **2009**, *131*, 7609–7617.

(233) B., M. Solid Phase Peptide Synthesis. I. The Synthesis Of. *J. Am. Chem. Soc.* **1963**, *85*, 2149–2154.

(234) Brenner, S.; Lerner, R. A. Encoded Combinatorial Chemistry. *Proc. Natl. Acad. Sci. U. S. A.* **1992**, *89*, 5381–5383.

(235) Frank, R. The SPOT-Synthesis Technique: Synthetic Peptide Arrays on Membrane Supports - Principles and Applications. *J. Immunol. Methods* **2002**, *267*, 13–26.

(236) Geysen, H. M.; Meloen, R. H.; Barteling, S. J. Use of Peptide Synthesis to Probe Viral Antigens for Epitopes to a Resolution of a Single Amino Acid. *Proc. Natl. Acad. Sci. U. S. A.* **1984**, *81*, 3998–4002.

(237) Houghten, R. A.; Pinilla, C.; Blondelle, S. E.; Appel, J. R.; Dooley, C. T.; Cuervo, J. H. Generation and Use of Synthetic Peptide Combinatorial Libraries for Basic Research and Drug Discovery. *Nature* **1991**, *354*, 84–86.

(238) Lam, K. S.; Salmon, S. E.; Hersh, E. M.; Hruby, V. J.; Kazmierskit, W. M.; Knappt, R. J. A New Type of Synthetic Peptide Library for Identifying Ligand-Binding Activity. *Nature* **1991**, *354*, 82–84.

(239) Lam, K. S.; Lebl, M.; Krchňák, V. The "One-Bead-One-Compound" Combinatorial Library Method. *Chem. Rev.* **1997**, *97*, 411–448.

(240) Coin, I.; Beyermann, M.; Bienert, M. Monitoring Solid Phase Peptide Synthesis. *Protoc. Exch.* **2007**.

(241) Eissler, S.; Kley, M.; Bächle, D.; Loidl, G.; Meier, T.; Samson, D. Substitution Determination of Fmoc-Substituted Resins at Different Wavelengths. *J. Pept. Sci.* **2017**, *23*, 757–762.

(242) Edman, P.; Begg, G. A Protein Sequenator. *Eur. J. Biochem.* **1967**, *1*, 80–91.

(243) Cox, J.; Mann, M. Is Proteomics the New Genomics? *Cell* **2007**, *130*, 395–398.

(244) Aebersold, R.; Mann, M. Mass Spectrometry-Based Proteomics. *Nature* **2003**, *422*, 198–207.

(245) Fenn, J. B.; Mann, M.; Meng, C. K.; Wong, S. F.; Whitehouse, C. M. Electrospray Ionization for Mass Spectrometry of Large Biomolecules. *Science (80-.).* **1989**, *246*, 64–71.

Biography

Jenisha Ghimire was born on November 20, 1988, in Kathmandu, Nepal, the youngest daughter of Bishnu Bibhu Ghimire and Sodha Koirala Ghimire. She received her secondary and high school education from GEMS and Xavier Academy, both located in Kathmandu valley. She moved to New Orleans, LA in the fall of 2008 for college. As a junior at the University of New Orleans, she was selected to work in a yeast molecular genetics lab through the UNO College of Sciences Undergraduate Research Program (COSURP). It was during this time that she first developed an interest in research. After completing the Bachelor of Science in biology with magna cum laude and departmental honors in May of 2012, she received the prestigious Privateer Graduate Scholarship Award from the University of New Orleans and began her Master of Sciences in her alma mater. She obtained her MSc. in spring of 2015. Following that, with further desire and drive to improve her scientific perspective, she joined the Ph.D. program in Biomedical Sciences at Tulane Medical School in August of 2015.